Non-unitary Yang-Lee fusion category in a matrix product operator description of topological order

Laurens Lootens

Promoter: Prof. Dr. Frank Verstraete
Supervisor: Prof. Dr. Jutho Haegeman

Master thesis submitted in partial fulfilment of the requirements for the degree of Master of Science in Physics and Astronomy

Department of Theoretical
and Mathematical Physics
Faculty of Sciences
Academic year 2017-2018

Acknowledgements

I would like to take the time to thank a few people without whom this thesis would not be what it is.

First of all, I would like to express my gratitude to my promoter Frank, for presenting this problem to me, as well as the countless valuable insights, fruitful discussions, opportunities and conveying a genuine passion for physics.

Jutho, for being extraordinarily helpful in every aspect of this thesis, but in particular for your clear explanations and incredibly helpful notes on the extensive amount of preliminaries required for this thesis.

Everyone from the office but in particular Robijn, for helping me put all this into a computer, the many discussions and explanations, and proofreading most of this document. Benoît, for proofreading parts of this work with extraordinary care.

My parents for their continued support in my academic journey and providing me the incredible luxury of studying theoretical physics.

Marine, for some of what is in this thesis, and everything that is not.

Nederlandstalige samenvatting

In deze thesis onderzoeken we het projector matrix product operator (PMPO) formalisme, een tensor netwerk beschrijving van topologische orde. Dit formalisme is gebaseerd op symmetrieën van een 2 dimensionale projected entangled pair state (PEPS) die zich uiten als matrix product operators (MPOs) op het virtuele niveau die vrij door het rooster kunnen bewegen. Deze MPOs vormen een algebra die overeenkomt met een fusie-categorie, die we de input fusie-categorie noemen. Het is geweten dat deze constructie geldig is voor unitaire fusie-categorieën, en in deze thesis breiden we dit resultaat uit naar niet-unitaire fusie-categorieën aan de hand van het eenvoudigste gekende voorbeeld: de Yang-Lee fusie-categorie.

We beginnen met een zeer korte inleiding tot tensor netwerken in hoofdstuk 1 om de verscheidene concepten gebruikt doorheen deze thesis te introduceren. Meer specifiek behandelen we matrix product states (MPS), projected entangled pair states (PEPS) en matrix product operators (MPOs).

In hoofdstuk 2 geven we een standaard introductie tot conforme veldentheorie, dewelke nodig is om de resultaten van hoofdstuk 5 te begrijpen. We geven enkele verwijzingen naar het minder gekende domein van niet-unitaire of logaritmische conforme veldentheorie, waarvan de Yang-Lee edge singularity het simpelste gekende voorbeeld is. Zoals de naam impliceert, is deze niet-unitaire conforme veldentheorie sterk gerelateerd aan de Yang-Lee fusie-categorie, een connectie die we verder onderzoeken in hoofdstuk 5.

Hoofdstuk 3 behandelt de bulk van de theoretische achtergrond vereist voor deze thesis. We starten met een korte introductie tot topologische orde, niet door te doelen op een fundamenteel wiskundige opbouw maar door de belangrijkste eigenschappen ervan te illustreren aan de hand van het simpelste voorbeeld, de toric code. Vervolgens geven we een gedetailleerde uiteenzetting van het PMPO formalisme voor de beschrijving van topologische orde met tensor netwerken, en we illustreren de belangrijke eigenschappen door het formalisme toe te passen op de eenvoudige Fibonacci unitaire fusie-categorie.

De Fibonacci unitaire fusie-categorie heeft een sterk gerelateerde niet-unitaire fusie-categorie; via een proces bekend als Galois toevoeging bekomen we de Yang-Lee fusie categorie. In hoofdstuk 4 proberen we het PMPO formalisme toe te passen op deze Yang-Lee niet-unitaire fusie categorie, en we zien dat in de huidige vorm het formalisme deze categorieën niet correct kan beschrijven. Gebaseerd op de sterke gelijkenissen tussen de Fibonacci en Yang-Lee categorieën stellen we aanpassingen tot het PMPO for-

malisme voor en we tonen aan dat deze de correcte resultaten geven voor de Yang-Lee categorie. Verder gebruiken we de inzichten verwonnen door de beschrijving van een unitaire categorie en zijn niet-unitaire tegenhanger om verdere resultaten binnen het PMPO formalisme af te leiden, met name met betrekking tot de verscheidene factoren van kwantum dimensies die doorheen de theorie verschijnen.

Het laatste hoofdstuk gaat over de "strange correlator" methode om topologische veldentheorieën op conforme veldentheorieën af te beelden, toegepast op de Yang-Lee categorie. We breiden de resultaten voor de Fibonacci categorie uit en tonen aan dat de bijhorende conforme veldentheorie de Yang-Lee edge singularity is. De eenvoud van deze conforme veldentheorie laat toe om deze strange correlator afbeelding beter te begrijpen, met name het verband tussen topologische sectoren en conforme defecten. In de laatste sectie van dit hoofdstuk behandelen we het "hard square" model, een niet-integreerbaar statistisch model dat een kritisch punt in de Yang-Lee universitaliteitsklasse bezit. We gebruiken de strange correlator afbeelding tussen de topologische Yang-Lee PEPS en dit statistisch mechanisch model door de overlap te nemen met een gepaste product state, die we zodanig proberen kiezen dat we de hard square partitie functie bekomen. Dit is grotendeels niet succesvol, maar verder onderzoek in deze richting kan een interpretatie voor integreerbaarheid in statistische mechanica opleveren in termen van tensor netwerken.

Het belangrijkste resultaat uit deze thesis is de afbeelding van tensor netwerken naar niet-unitaire conforme veldentheorieën. Deze laatste zijn interessant aangezien ze verscheidene kritische statistische modellen beschrijven. Een van de meest prominente hiervan is het probleem van percolatie, het gedrag van geconnecteerde clusters in een willekeurige graaf. Dit probleem duikt op in verschillende vakgebieden en de theoretische studie ervan heeft reeds tot nieuwe inzichten en technieken geleid. Deze thesis opent de deur naar de studie van dit probleem met tensor netwerken, en we hopen dat deze hun nut nogmaals kunnen bewijzen om voortgang te maken op de openstaande vragen binnen dit onderwerp.

Contents

Introduction

The quantum many-body problem has been a steady source of new physics ever since the conception of quantum mechanics. The whole seems to be much more than the sum of its parts, and the collective behaviour of many quantum degrees of freedom can lead to interesting and surprising features. One such feature is topological order, in which a quantum many-body system that one would a priori expect to behave in a very uncontrolled and noisy way seems to exhibit quantised behaviour for many of the macroscopic quantities that is robust under local perturbations. These systems can not be studied using exact methods and one has to resort to approximate techniques such as mean field theory, perturbative expansions or effective descriptions based on renormalisation arguments. In the last decades one particularly promising description by the name of tensor networks has arised based on the local entanglement structure of these quantum many-body systems, and it has been immensely successful in understanding and simulating the behaviour of these systems.

In this thesis, we investigate the projector matrix product operator (PMPO) formalism, a tensor network description of topological order. This formalism is based on symmetries of a 2 dimensional projected entangled pair state (PEPS) that manifest themselves as matrix product operators (MPOs) on the virtual level that can be freely moved through the lattice. These MPOs can be shown to form an algebra that corresponds to a fusion category, called the input fusion category. It is known that this construction is valid for unitary fusion categories, and in this thesis we extend this result to non-unitary fusion categories by considering the simplest known example: the Yang-Lee fusion category.

We begin by giving a very short introduction to tensor networks in chapter 1 to introduce various concepts used throughout this thesis. More specifically, we discuss matrix product states, projected entangled pair states and matrix product operators.

In chapter 2 we provide a fairly standard introduction to conformal field theory, which is required to understand the results of chapter 5. We include a few points on the lesser

known domain of non-unitary or logarithmic conformal field theory, of which the Yang-Lee edge singularity is the simplest known example. As the name implies, this non-unitary CFT will turn out to be closely connected to the Yang-Lee fusion category, a connection we explore in chapter 5.

Chapter 3 deals with the bulk of the theoretical background required for this thesis. We start by briefly introducing topological order, not by aiming for mathematical rigour but rather give an idea of its main features through example by considering the toric code, the simplest model in which topological order occurs. This is followed by the detailed exposition of the PMPO formalism for describing topological order using tensor networks, and we apply it to the simple Fibonacci unitary fusion category to illustrate the important features.

The Fibonacci unitary fusion category turns out to have a very closely related non-unitary fusion category; more specifically, through a process known as Galois conjugation we arrive at the Yang-Lee fusion category. In chapter 4 we try to apply the PMPO formalism to this non-unitary category and we see that in its current form it fails to correctly incorporate these categories. Based on the similarity between the Fibonacci and Yang-Lee categories we propose modifications to the PMPO formalism and we show that these give the correct results for the Yang-Lee category. We further use the insights gained by describing both a unitary category and its non-unitary counterpart to derive further results considering the PMPO formalism, in particular dealing with the factors of quantum dimensions appearing throughout the theory.

The final chapter concerns the strange correlator method for mapping topological to conformal field theories (CFT), applied to the Yang-Lee category. We extend the results obtained for the Fibonacci theory and show that the corresponding CFT is the aforementioned Yang-Lee edge singularity. The simplicity of this CFT allows us to better understand this strange correlator mapping and in particular the relation between topological sectors and conformal defects. In the last section of this chapter we consider the hard square model, a non-integrable statistical mechanics model that has been shown to contain a critical point in the Yang-Lee edge singularity universality class. We use the strange correlator mapping to map the topological Yang-Lee PEPS to this statistical mechanics model by taking the overlap with an appropriate product state, which we try to tune in such a way that we obtain the hard square partition function. This is largely unsuccessful, but further investigations in this direction could provide an interpretation for integrability of statistical mechanics models in terms of tensor networks.

Chapter 1

Tensor Networks

In this chapter we present a very brief overview of tensor networks [1,2], a field which has enjoyed success among many disciplines of physics over the last few years. While this is especially true for quantum many-body systems on both the theoretical and numerical side, it has also provided a handle on the holographic principle and the AdS/CFT correspondence in quantum gravity [3,4]. We give a short motivation for tensor networks, followed by an introduction to matrix product states (MPS), its higher dimensional generalisation known as projected entangled pair states (PEPS) and perhaps most importantly for this thesis, matrix product operators (MPO). There exist a plethora of numerical methods to simulate quantum many-body systems in the tensor network formalism, but our interest is mainly in the conceptual insights provided by tensor networks and therefore we will not discuss them here.

1.1 Quantum many-body Hilbert space

Consider a system of N spin 1/2 particles. The dimension of the associated Hilbert space is 2^N, exponential in the number of particles. This means that representing a quantum state of this system just by giving its coefficients of the wave function in a local basis is extremely costly, and already computationally intractable for relatively low N. Fortunately, not all states in the Hilbert space are equal, and some are more relevant than others. More specifically, many important Hamiltonians in Nature are such that the interactions between different particles are local (e.g. nearest neighbour interactions on a lattice), and have an energy gap between the ground state and the first excited state. For these gapped Hamiltonians with local interactions, one can prove that the low-energy eigenstates obey an area-law for the entanglement entropy. More specifically, if we consider a system $\mathcal{H}_A + \mathcal{H}_B$, the Von Neumann entropy associated to the reduced

density matrix

$$\rho_A = \mathrm{Tr}_B(\rho), \tag{1.1}$$

where Tr_B denotes the partial trace over subsystem $\mathcal{H}_B$, is defined as

$$S(A) = -\mathrm{Tr}(\rho_A \log(\rho_A)) \tag{1.2}$$

For states that satisfy the area-law, this entanglement entropy satisfies

$$S(A) \sim \partial A. \tag{1.3}$$

The space of states that satisfy the area-law is an exponentially small subspace of the full Hilbert space. It is clear that a description that treats all states in the full Hilbert space equally is horribly inefficient for describing these area-law states. Additionally, given some initial state, the manifold that can be reached in polynomial time by evolving this state is also exponentially small. In this sense, the immensity of the Hilbert space is really an illusion, since we will never see most of it. If we aim to study states within this exponentially small space, we better choose a description that directly targets these states. This description is precisely the tensor network formalism, which can be shown to efficiently represent states obeying an area-law for the entanglement entropy.

The main focus of this thesis are systems that exhibit *topological order*, with ground states that can not be distinguished from each other with local order parameters. This long range interaction can be shown to introduce a correction to the area law [5],

$$S(A) \sim \partial A + \gamma, \tag{1.4}$$

where γ is called the *topological entanglement entropy*. It was demonstrated in [6] that systems exhibiting this topological order can also be described using tensor networks, which is the formalism with which we will treat it in this thesis.

1.2 Matrix product states

We will start by considering a general quantum many-body wave function of N qudits (d-dimensional quantum systems) in 1 space dimension:

$$|\psi\rangle = \sum_{j_1, j_2, \ldots j_N}^{d} C^{j_1 j_2 \ldots j_N} |j_1\rangle |j_2\rangle \ldots |j_N\rangle . \tag{1.5}$$

This wave function is specified entirely by the N-index tensor C with N *physical* indices j, which we pictorially depict as

$|\psi\rangle =$ 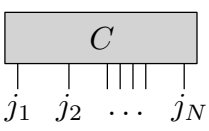

(1.6)

By splitting out the first index j_1 and grouping the rest, we can interpret this tensor as a $d \times d^{N-1}$ matrix, and perform a singular value decomposition to obtain the Schmidt decomposition

$$|\psi\rangle = \sum_{i}^{D} \lambda_i \sum_{j_1}^{d} A_i^{j_1} |j_1\rangle \sum_{j_2,\dots j_N}^{d} C_i^{j_2 \dots j_N} |j_2\rangle \dots |j_N\rangle \tag{1.7}$$

$$= \sum_{i}^{D} \sum_{j_1}^{d} A_i^{j_1} |j_1\rangle \sum_{j_2,\dots j_N}^{d} C_i^{j_2 \dots j_N} |j_2\rangle \dots |j_N\rangle \tag{1.8}$$

where λ_i are the Schmidt weights which we absorbed into A^j. The notation quickly becomes cumbersome, but graphically we can simply depict this as

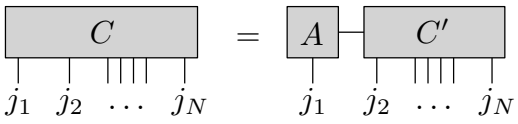

(1.9)

where the leg connecting the A and C' tensor implies a sum over the internal or *virtual* indices $i = 1, \dots, D$ and D is called the *bond dimension*. Performing this procedure $N-2$ more times, we arrive at

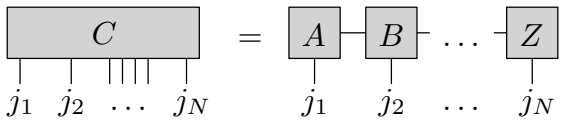

(1.10)

For simplicity, we now impose translation invariance and periodic boundary conditions, so this becomes

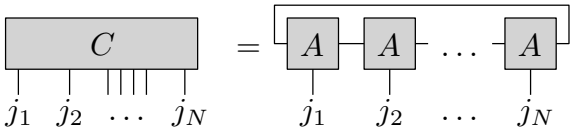

(1.11)

which can be written in terms of the $D \times D$ matrices A^j as

$$|\psi\rangle = \sum_{j_1, j_2, \dots j_N}^{d} \mathrm{Tr}(A^{j_1} A^{j_2} \dots A^{j_N}) |j_1\rangle |j_2\rangle \dots |j_N\rangle , \tag{1.12}$$

which is an example of a *matrix product state* or MPS. We haven't really done anything, since we showed that by repeated Schmidt decompositions any wave function can be written in this way, generally with the bond dimension growing exponentially in the system size. We note however that the Schmidt weights and in particular the number of non-zero Schmidt weights determine the Von Neumann entanglement entropy between two subsystems. The condition that a state has to obey an area law for its entanglement entropy then translates in an upper bound on D, such that these states can be faithfully represented for relatively low values of D [7], which in turn means that we have exponentially reduced the number of parameters used to describe the wave function.

1.3 Projected Entangled Pair States

There is a different way of constructing MPS, which both provides more physical insight and a way of generalising to higher dimensions. We consider again a translation invariant system with periodic boundary conditions. At each physical d-dimensional degree of freedom j, we place two D dimensional quantum degrees of freedom, such that at every site we have a $\mathbb{C}^D \otimes \mathbb{C}^D$ dimensional Hilbert space:

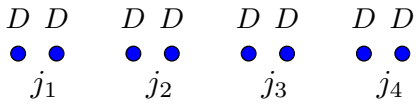

(1.13)

We now maximally entangle all the pairs of qudits on neighbouring sites by projecting onto the maximally entangled state

$$|\alpha\rangle = \sum_{i=1}^{D} |i\rangle\,|i\rangle \tag{1.14}$$

which we depict as

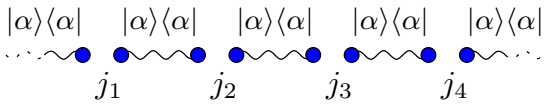

(1.15)

where the dotted lines indicate periodic boundary conditions. Finally, we act on the pairs of qudits associated to one physical degree of freedom j with a linear map $\mathbb{C}^D \otimes \mathbb{C}^D \to \mathbb{C}^d$, i.e. we map the virtual degrees of freedom to the physical degrees of freedom:

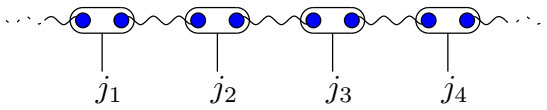

(1.16)

This is called a projected entangled pair state, or PEPS for short. The entanglement entropy between any two subsystems is given by $2\log(D)$, and if D is subexponential in the system size we have constructed a state that satisfies the area-law. The advantage of this picture is that it has a straightforward generalisation to higher dimensions; in particular, Figure 1.1a shows a depiction of a PEPS in 2 dimensions, which is usually what the terminology PEPS is reserved for. We can easily imagine more general PEPS, with different tensors for every physical degree of freedom, such a tensor network is depicted in Figure 1.1b. It has been shown that many interesting systems admit such a PEPS description for their low-energy states with a bond dimension D that is subexponential in the system size, [8] indicating that we have really identified the correct description of this low-energy manifold. It is obvious that this construction is not limited to square lattice configurations, and we will employ a hexagonal and a truncated square lattice in chapter 5.

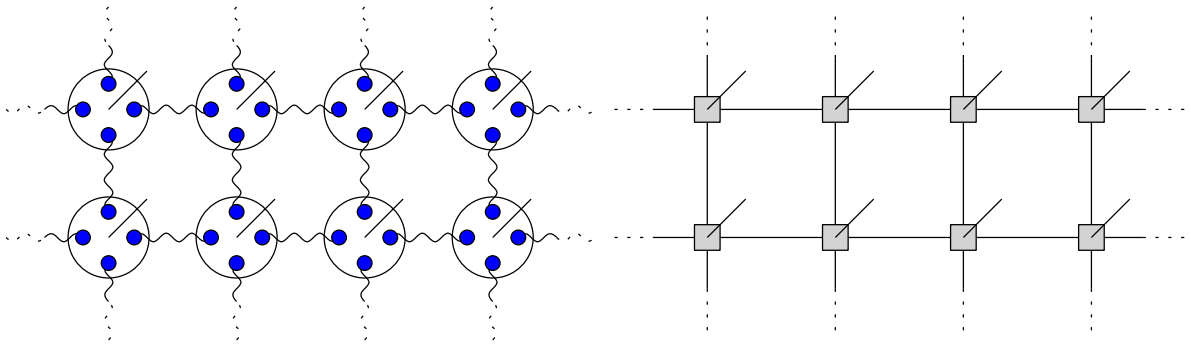

(a) (b)

Figure 1.1: (a) 2 dimensional 2×4 patch of a PEPS lattice, with the physical index sticking out up and to the right. (b) The same patch with more general tensors.

1.4 Matrix product operators

We end this chapter by defining what we mean by matrix product operators (MPOs). A general translation invariant MPO with periodic boundary conditions on N sites is given by

$$\hat{O} = \sum_{\{i\},\{j\}=1}^{d} \mathrm{Tr}\left(B^{i_1 j_1} \dots B^{i_N j_N}\right) |i_1 \dots i_N\rangle \langle j_1 \dots j_N| \tag{1.17}$$

which is graphically depicted as

$\hat{O} =$ 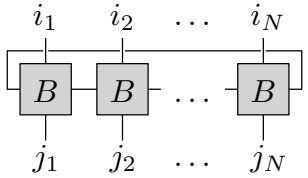

(1.18)

These can be interpreted as a map between two MPS states, but we will use them exclusively on the virtual degrees of freedom of a PEPS,

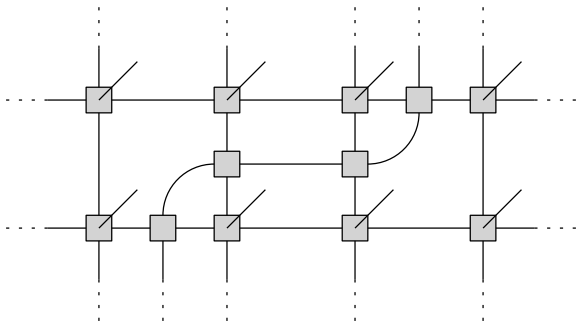

(1.19)

and PEPS tensors that exhibit certain symmetries under these MPO operations can be used to construct topologically ordered PEPS, which is the subject of Chapter 3.

Chapter 2

Conformal Field Theory

In this chapter, we aim to give an brief introduction to 2-dimensional conformal field theory (CFT). It is a vast subject and has been an important tool in theoretical physics during the last decades, with its origins in the description and classification of critical phenomena. It was subsequently developed mainly for its use in string theory, and has been extensively studied in the context of the AdS/CFT-correspondence [3].

The central idea of CFT is invariance under conformal transformations. Since this includes scale invariance, these theories are particularly suited for describing critical phenomena at the fixed point of some RG flow [9, 10], which is the context in which we will be using it. We can situate CFT by looking at the Coleman-Mandula theorem [11], which restricts the possible symmetries we can impose on a QFT. According to this theorem, under the assumption that

1. the theory has a set of Lorentz scalar conserved quantities,
2. the theory has an S-matrix,

the only symmetry we can consistently impose is Poincaré invariance. The two loopholes to this theorem are precisely those that break one of these two assumptions. More specifically, if we allow the conserved quantities to be more general than Lorentz scalars, we arrive at supersymmetry, and if we drop the requirement for the existence of an S-matrix we arrive at CFT. Because we are only interested in describing 2D statistical mechanics models at criticality, we will be restricting ourselves to 2D CFT, which turns out to be rather different from CFT in any other dimension. The main references used for this chapter are [12, 13], and we will be working with a Euclidean metric.

2.1 Classical conformal invariance

We define a conformal transformation as a coordinate transformation which acts on the metric as a Weyl transformation:

$$g_{\mu\nu}(x) \to \Omega(x) g_{\mu\nu}. \tag{2.1}$$

Rotations and translations do not change the metric, and we can interpret them as conformal transformation with $\Omega(x) = 1$. The angle α between two vectors is given by

$$\cos(\alpha) = \frac{g_{\mu\nu} v^\mu w^\nu}{\sqrt{g_{\mu\nu} v^\mu v^\nu} \sqrt{g_{\mu\nu} w^\mu w^\nu}} \tag{2.2}$$

which does not change under a Weyl transformation of the metric. Geometrically then, the conformal transformations correspond to the set of transformations that preserve all angles. Given some action S, the energy momentum tensor is defined as

$$\delta S = \frac{1}{2} \int d^d x \sqrt{g} T^{\mu\nu} \delta g_{\mu\nu}, \tag{2.3}$$

for the variation of S under changes of the metric, and invariance under general coordinate transformations implies conservation of the energy momentum tensor

$$\partial_\mu T^{\mu\nu} = 0. \tag{2.4}$$

The Weyl transformation in infinitesimal form is given by

$$g_{\mu\nu} \to g_{\mu\nu}(x) + \omega(x) g_{\mu\nu}(x), \tag{2.5}$$

and substituting this into eq. 2.3 we find

$$\delta S = \frac{1}{2} \int d^d x \sqrt{g} T^\mu{}_\mu \omega(x). \tag{2.6}$$

Demanding now that the action is invariant under conformal transformations means that we must have $\delta S = 0$, which implies that the energy momentum tensor must be traceless,

$$T^\mu{}_\mu = 0, \tag{2.7}$$

since this has to hold for arbitrary functions $\omega(x)$.

2.1.1 Conformal transformations in 2D

We are not interested in curved space-times, and in 2D Euclidean space we can write the line element as

$$ds^2 = dx^2 + dy^2 = \frac{1}{2} dz d\bar{z}, \tag{2.8}$$

with (following the convention of [13]),

$$z = x - iy, \quad \bar{z} = x + iy. \tag{2.9}$$

The Weyl transformation of the metric implies that the line element should change by a rescaling under a conformal transformation. For an infinitesimal transformation

$$z \to z + \epsilon(z, \bar{z}), \quad \bar{z} \to \bar{z} + \bar{\epsilon}(z, \bar{z}) \tag{2.10}$$

we have to linear order in ϵ and $\bar{\epsilon}$

$$ds^2 \to \frac{1}{2}(1 + \partial_z \epsilon + \partial_{\bar{z}} \bar{\epsilon}) dz d\bar{z} + \frac{1}{2}\partial_z \bar{\epsilon} dz dz + \frac{1}{2}\partial_{\bar{z}} \epsilon d\bar{z} d\bar{z}. \tag{2.11}$$

For a conformal transformation, this means that we should have

$$\partial_{\bar{z}} \epsilon = \partial_z \bar{\epsilon} = 0, \tag{2.12}$$

which means that ϵ is an arbitrary holomorphic function and $\bar{\epsilon}$ and anti-holomorphic function, or non-infinitesimally, that the coordinates z and $\bar{z}$ transform as

$$z \to f(z), \quad \bar{z} \to \bar{f}(\bar{z}) \tag{2.13}$$

with f and $\bar{f}$ arbitrary holomorphic and anti-holomorphic functions respectively. These transformations can be written as generated by differential operators: the generator

$$L_n = -z^{n+1}\partial_z \tag{2.14}$$

generates the transformation

$$z \to z - z^{n+1}, \tag{2.15}$$

and satisfies the commutation relation

$$[L_n, L_m] = (n - m)L_{m+n}. \tag{2.16}$$

This defines the de Witt algebra, and we will later see that its central extension is the celebrated Virasoro algebra [14]. The case for the barred quantities is exactly the same, and furthermore we have

$$[L_n, \bar{L}_m] = 0. \tag{2.17}$$

The global conformal transformations form a subgroup of the local conformal transformations, and its generators are the only ones that are defined on the entire complex plane including ∞, known as the the Riemann sphere. Given the definition of L_n, it is immediately clear that this requires $n \geq -1$ in order for it to be non-singular at $z = 0$. To investigate the behaviour at infinity, it is useful to perform a conformal mapping that

interchanges $z = 0$ and $z = \infty$. Such a transformation is given by $z = 1/w$, and the generator L_n transforms to

$$-z^{n+1}\partial_z \to w^{1-n}\partial_w, \tag{2.18}$$

which is non-singular for $n \leq 1$. Combined with the previous result we have $-1 \leq n \leq 1$, and one can show that we have the following global transformations:

- $i(L_0 + \bar{L}_0)$: generator of global dilatations,
- $-(L_0 - \bar{L}_0)$: generator of global rotations,
- $L_{-1} \pm \bar{L}_{-1}$: generators of global translations,
- $L_1 \pm \bar{L}_1$: generators of special conformal transformations.

There is much more to be said about the group structure of the global conformal transformations, but since it is not relevant for our discussion we will not go into it here.

2.1.2 Scaling dimension and conformal spin

In general, the components of a tensor ϕ of rank n are of the form $\phi_{z\ldots z,\bar{z}\ldots\bar{z}}(z,\bar{z})$, and under a conformal transformation they transform as

$$\phi_{z\ldots z,\bar{z}\ldots\bar{z}}(z,\bar{z}) \to \phi'_{z\ldots z,\bar{z}\ldots\bar{z}}(f(z),\bar{f}(\bar{z})) = \left(\frac{\partial f(z)}{\partial z}\right)^{-p}\left(\frac{\partial \bar{f}(\bar{z})}{\partial \bar{z}}\right)^{-q}\phi_{z\ldots z,\bar{z}\ldots\bar{z}}(z,\bar{z}) \tag{2.19}$$

where p and q are the amount of indices equal to z and $\bar{z}$ respectively. A field that transforms in this way is called a conformal field of weight (p,q). Although we derived this rule for a tensor component, which implies that p and q should be integer, there is a more general version of this statement and we define a *primary* field as a field that transforms as

$$\phi(z,\bar{z}) \to \phi'(f(z),\bar{f}(\bar{z})) = \left(\frac{\partial f(z)}{\partial z}\right)^{-h}\left(\frac{\partial \bar{f}(\bar{z})}{\partial \bar{z}}\right)^{-\bar{h}}\phi(z,\bar{z}), \tag{2.20}$$

where the conformal weight is now $(h,\bar{h})$. The bar on h does not denote complex conjugation, but merely that it is linked to the anti-holomorphic part of the transformation; this notation is unfortunate, but standard. We will later see that $h+\bar{h}$ are the eigenvalues of $L_0 + \bar{L}_0$, which is proportional to dilatation operator and therefore $\Delta = h + \bar{h}$ is called the scaling dimension of the field. Similarly, $h - \bar{h}$ are the eigenvalues of $L_0 - \bar{L}_0$, which is proportional to the rotation operator and $s = h - \bar{h}$ is called the conformal spin.

2.1.3 Conserved current

The fact that the energy momentum tensor is traceless is translated in complex coordinates to

$$T_{z\bar{z}} = T_{\bar{z}z} = 0, \tag{2.21}$$

and the fact that it is conserved implies

$$\partial_{\bar{z}} T_{zz} = \partial_z T_{\bar{z}\bar{z}} = 0, \tag{2.22}$$

which means that T_{zz} and $T_{\bar{z}\bar{z}}$ have to be holomorphic and anti-holomorphic respectively. Noether's theorem implies that the conformal symmetry should come with a conserved current, and it is given by

$$J_z = T_{zz}\epsilon \equiv T(z)\epsilon(z), \quad J_{\bar{z}} = T_{\bar{z}\bar{z}}\bar{\epsilon} \equiv T(\bar{z})\epsilon(\bar{z}) \tag{2.23}$$

where ϵ and $\bar{\epsilon}$ are the infinitesimal changes of the coordinates under a conformal transformation, which we showed to be arbitrary holomorphic and anti-holomorphic respectively. This infinite number of conserved currents is a key difference between 2D CFT and CFT in arbitrary dimensions. Since T_{zz} is holomorphic and $T_{\bar{z}\bar{z}}$ is anti-holomorphic, so are J_z and $J_{\bar{z}}$, this current is manifestly conserved:

$$\partial_{\bar{z}} J_z = \partial_z J_{\bar{z}} = 0. \tag{2.24}$$

2.2 Quantum conformal invariance

As discussed in the previous section, we consider theories defined in 2D Euclidean space. These can be interpreted as 2D statistical mechanics models, but also as 1+1D quantum field theories after a Wick rotation:

$$(x^1, ix^0) \to (x, y), \tag{2.25}$$

which for the metric means

$$\eta_{\mu\nu} \to \delta_{\mu\nu}. \tag{2.26}$$

In a QFT, symmetries are generated by charges, which are the space integrals of the zeroth component of a conserved current:

$$Q = \int dx^1 J^0. \tag{2.27}$$

After a Wick rotation, this becomes

$$Q = \int dx(-iJ_y), \tag{2.28}$$

which gives us an expression for the charge Q in Euclidean space.

2.2.1 Radial quantisation

It will turn out to be convenient to make the space direction finite, by imposing periodic boundary conditions in the x^1 direction. This is similar to regulating a quantum system by putting it in a finite box in space with periodic boundary conditions. We will fix the size of the box to 2π, but because of scale invariance this value is irrelevant. After a Wick rotation, the finite space direction x^1 translates to a finite space direction x, while y is still infinite; this effectively means that we are now studying the theory on a cilinder. In this topology, the charge is given by

$$\frac{1}{2\pi}\int_0^{2\pi} dx(-iJ_y), \tag{2.29}$$

where we normalised to the length of the interval. Introducing again complex coordinates $z = x - iy$ as before, we find $J_2 = -i(J_z - J_{\bar{z}})$, and the charge becomes

$$Q = -\frac{1}{2\pi}\left[\oint dz J_z^{\text{cyl}}(z,\bar{z}) - \oint d\bar{z} J_{\bar{z}}^{\text{cyl}}(z,\bar{z})\right]. \tag{2.30}$$

The integration is along a closed contour that winds around the cylinder, and we chose $\bar{z}$ as integration variable in the second term for convenience, which makes no difference since we only integrate over x, the real part of z. The orientations of these contours is such that

$$\oint dz = \oint d\bar{z} = 2\pi, \tag{2.31}$$

and the superscripts "cyl" remind us that the currents are defined on the cylinder. We now perform a conformal transformation

$$w = e^{ix+y} = e^{iz}, \tag{2.32}$$

which maps the cylinder to the plane. In particular, the surface at the Euclidean time coordinate $y = -\infty$ is mapped to $w = 0$, and the surface at $y = +\infty$ is mapped to the infinite circle at $|w| = \infty$. The integration variables transform as

$$\oint dz = \oint \frac{dw}{iw}, \quad \oint d\bar{z} = \oint \frac{d\bar{w}}{i\bar{w}} \tag{2.33}$$

where these are now contour integrals around the origin and the contours are chosen such that

$$\frac{1}{2\pi i}\oint \frac{dw}{w} = \frac{1}{2\pi i}\oint \frac{d\bar{w}}{\bar{w}} = 1. \tag{2.34}$$

The currents on the cylinder are transformed to the plane by using eq. 2.20, where J_z and $J_{\bar{z}}$ are primary fields with conformal weight $(h = 1, 0)$ and $(0, \bar{h} = 1)$ respectively. We get

$$J_w^{\text{plane}}(w,\bar{w}) = (iw)^{-h} J_z^{\text{cyl}}(z(w), \bar{z}(\bar{w})),$$
$$J_{\bar{w}}^{\text{plane}}(w,\bar{w}) = (-i\bar{w})^{-h} J_{\bar{z}}^{\text{cyl}}(z(w), \bar{z}(\bar{w})),$$

and so the charge becomes

$$Q = -\frac{1}{2\pi}\left[\oint dw(iw)^{h-1}J_w^{\text{plane}}(w,\bar{w}) + \oint d\bar{w}(-i\bar{w})^{\bar{h}-1}J_{\bar{w}}^{\text{plane}}(w,\bar{w})\right]. \tag{2.35}$$

For the current, we obviously have to put $h = \bar{h} = 1$, but we will later re-use this formula for different values of h and $\bar{h}$. The result of the contour integrations depends on the poles inside the contour, and we will see that in a quantum field theory these can arise when considering the product of two operators.

2.2.2 Radial ordering

In order to sensibly discuss products of operators, we first have to make a detour to elaborate on radial ordering. In a classical theory, the ordering of fields or charges in a product is of course irrelevant, but this changes when they are promoted to operators in a quantum theory and we have to be more careful. To see this, we go back to basic 1D quantum mechanics and consider two operators A and B in the Heisenberg picture. The products of these two operators acting at some points (x_a, t_a) and (x_b, t_b) can be written with the Hamiltonian H as

$$A(x_a,t_a)B(x_b,t_b) = e^{iHt_a}A(x_a,0)e^{-iHt_a}e^{iHt_b}B(x_b,0)e^{-iHt_b}. \tag{2.36}$$

After a Wick rotation, we get

$$e^{-iH(t_a-t_b)} \to e^{-H(\tau_a-\tau_b)}, \tag{2.37}$$

which is no longer a bounded operator for $\tau_a < \tau_b$ since the Hamiltonian is usually not bounded from above. This means that expectation values are no longer defined, and we therefore impose time ordering, denoted as

$$T(A(x_a,\tau_a)B(x_b,\tau_b)) = \begin{cases} A(x_a,\tau_a)B(x_b,\tau_b) & \text{for} \quad \tau_a > \tau_b, \\ B(x_b,\tau_b)A(x_a,\tau_a) & \text{for} \quad \tau_a < \tau_b. \end{cases} \tag{2.38}$$

After mapping from the cylinder to the plane, the Euclidean time coordinate becomes the radial coordinate, and time ordering becomes radial ordering:

$$R(A(z_a,\bar{z}_a)B(z_b,\bar{z}_b)) = \begin{cases} A(z_a,\bar{z}_a)B(z_b,\bar{z}_b) & \text{for} \quad |z_a| > |z_b|, \\ B(z_b,\bar{z}_b)A(z_a,\bar{z}_a) & \text{for} \quad |z_a| < |z_b|. \end{cases} \tag{2.39}$$

2.2.3 The generator of conformal transformations

Returning to charge operators, we now consider the generator of the conformal transformations. The conserved current for an infinitesimal transformation is given by $T(z)\epsilon(z)$

and $T(\bar{z})\epsilon(\bar{z})$ for the holomorphic and anti-holomorphic part of the transformation respectively. Ideally, we would write the current on the cylinder first and then perform a conformal transformation to the plane, but as we will later see the energy-momentum tensor is not a conformal field and so it does not transform as eq. 2.20. Instead, we define the charge corresponding to an infinitesimal conformal transformation directly on the plane as

$$Q_\epsilon = \frac{1}{2\pi i}\left[\oint dz\epsilon(z)T(z) + \oint d\bar{z}\epsilon(\bar{z})T(\bar{z})\right] \tag{2.40}$$

Since the holomorphic and anti-holomorphic part of a conformal transformation decouple, we will restrict ourselves to the holomorphic part and omit the anti-holomorphic part of the transformation as well as the anti-holomorphic component of T in the following. We expect Q_ϵ to generate conformal transformations of a conformal field ϕ of the form

$$\phi(w,\bar{w}) \to \phi'(w,\bar{w}) = \left(\frac{\partial f(w)}{\partial w}\right)^h \phi(f(w),\bar{w}) \tag{2.41}$$

with $f(w) = w + \epsilon(w)$. We note that z and w are both coordinates on the complex plane, and no longer have anything to do with complexified cylinder coordinates. Infinitesimally, this transformation is

$$\delta_\epsilon\phi(w,\bar{w}) = h\partial_w\epsilon(w)\phi(w,\bar{w}) + \epsilon(w)\partial_w\phi(w,\bar{w}), \tag{2.42}$$

and the quantum version of this transformation should satisfy

$$\delta_\epsilon\phi(w,\bar{w}) = [Q_\epsilon, \phi(w,\bar{w})]. \tag{2.43}$$

Trying to evaluate this commutator with the above expression for the charge, we get

$$[Q_\epsilon, \phi(w,\bar{w})] = \frac{1}{2\pi i}\oint \left(dz\epsilon(z)\left[T(z)\phi(w,\bar{w}) - \phi(w,\bar{w})T(z)\right]\right., \tag{2.44}$$

but as we just saw, we have to impose radial ordering and therefore the first term is only defined for $|z| > |w|$, whereas the second term requires $|z| < |w|$. Obviously, this can not be satisfied with a single choice of contour, so we will have to redefine Q_ϵ in order for it to be well-defined after quantisation. Classically, Q_ϵ is in fact independent of the contour because the integrand is a holomorphic function, and the Cauchy theorem states that we can freely deform the contour as long as we don't cross any poles of the integrand. The commutator vanishes clasically, but we can write it in such a way that it remains well-defined after quantisation:

$$[Q_\epsilon, \phi(w,\bar{w})] = \frac{1}{2\pi i}\oint_{|z|>|w|} dz\epsilon(z)T(z)\phi(w,\bar{w}) - \frac{1}{2\pi i}\oint_{|z|<|w|} dz\epsilon(z)\phi(w,\bar{w})T(z), \tag{2.45}$$

or, equivalently,

$$[Q_\epsilon, \phi(w,\bar{w})] = \frac{1}{2\pi i}\left[\oint_{|z|>|w|} - \oint_{|z|<|w|}\right] dz\epsilon(z)R(T(z)\phi(w,\bar{w})). \tag{2.46}$$

If we now deform these contours as

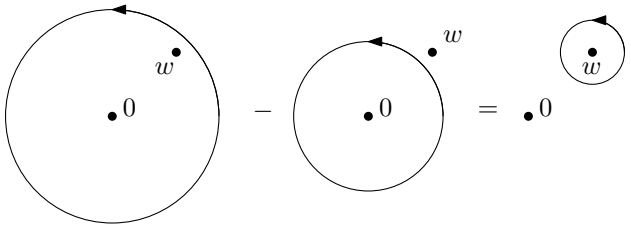

(2.47)

we end up with

$$[Q_\epsilon, \phi(w,\bar{w})] = \frac{1}{2\pi i}\oint dz\epsilon(z)R(T(z)\phi(w,\bar{w})) \tag{2.48}$$

where the integration contour encircles the point w. The integration only makes sense if the radially ordered product is analytic around w, in which case we can expand it as a Laurent series around w:

$$R(T(z)\phi(w,\bar{w})) = \sum_n (z-w)^n O_n(w,\bar{w}), \tag{2.49}$$

where the expansion coefficients O_n are operators. The integration will only produce the required infinitesimal transformation if

$$R(T(z)\phi(w,\bar{w})) = \frac{h}{(z-w)^2}\phi(w,\bar{w}) + \frac{1}{z-w}\partial_w\phi(w,\bar{w}) + \sum_{n=0}^{\infty}(z-w)^n O_n(w,\bar{w}). \tag{2.50}$$

The terms with operators O_n for $n \geq 0$ do not contribute to the integral since they do not contain poles, and therefore they can be anything and are usually not written. The property in eq. 2.50 and its anti-holomorphic counterpart define what we mean by a conformal field ϕ.

2.2.4 Operator Product Expansion

The expression obtained in eq. 2.50 is an example of an Operator Product Expansion (OPE). More generally, this concept states that for all possible local operators in the CFT, we can write the product of two local operators as a (possibly infinite) linear combination of other local operators:

$$\mathcal{O}_i(x)\mathcal{O}_j(y) = \sum_k C_{ij}^k(x-y)\mathcal{O}_k(y) \tag{2.51}$$

where the $C_{ij}^k(x-y)$ are expansion coefficients. The OPE should really be understood in terms of correlation functions, where we calculate the expectation value of operator

products in some state. The behaviour of these correlation functions is singular when the positions x and y coincide, and this behavious is precisely described by the OPE. These OPE's can be used to constrain and solve CFT's, a method known as the conformal bootstrap, which has been used most notably for calculating the critical exponents of the critical three-dimensional Ising model [15].

To illustrate, we give (without proof) the OPE of the holomorphic component of the energy momentum tensor with itself (without the finite terms):

$$T(z)T(w) = \frac{c/2}{(z-w)^4} + \frac{2}{(z-w)^2}T(w) + \frac{1}{z-w}\partial_w T(w). \tag{2.52}$$

From this, we see that $T(z)$ would be a conformal field of weight 2, were it not for the term proportional to c. This term arises due to quantum effects, and is known as the *conformal anomaly*. In a free boson theory for example, c is equal to the number of bosonic degrees of freedom.

2.3 The Virasoro algebra

Considering again the current for conformal symmetry $J_\epsilon(z) = T(z)\epsilon(z)$, we derived that ϵ is an arbitrary holomorphic function. It is therefore natural to expand it in modes, where the mode expansion depends on the surface we work on. Since we required fields and transformations to be continuous on contours around the origin, we can choose $\epsilon(z) = z^{n+1}$, and we expect

$$J^n(z) = T(z)z^{n+1} \tag{2.53}$$

to generate the transformation $z \to z - z^{n+1}$, as was the case for classical CFT. The relation with the operators L_n is given by the normalisation

$$L_n = \frac{1}{2\pi i}\oint dz z^{n+1}T(z), \tag{2.54}$$

where we can verify the normalisation by comparing with the classical case. To do this, we compute the commutator $[L_n, L_m]$. We can do this using contour integration and the OPE expanstion of $T(z)$ with itself, and a straightforward calculation leads to

$$[L_n, L_m] = (n-m)L_{m+n} + \frac{c}{12}n(n^2-1)\delta_{n,-m} \tag{2.55}$$

which is known as the *Virasoro algebra*. The conformal anomaly c appears only on the right hand side of these commutators, and commutes with every element of the algebra. It is the central extension of the de Witt algebra we encountered for classical conformal invariance, and is more commonly known as the *central charge*. The same commutation

relations hold for the anti-holomorphic generators. Notably, the generators of global conformal transformations L_{-1}, L_0, L_1 are unaffected by this central extension. Given this algebra, it is important to find its representations, much like we do for the angular momentum algebra. In this case, we label states by the maximally commuting set of operators J^2 and J_z. Such a set is called a Cartan subalgebra, and for the case of the Virasoro algebra we will choose L_0 and c to label the representations.

2.3.1 Unitarity

Given that this thesis considers non-unitary CFT, a note on unitarity is in order. A representation of the Virasoro algebra is called unitary if all generators L_n are realised as operators acting on a Hilbert space, with the additional constraint that $L_n^\dagger = L_{-n}$. The latter condition enforces the energy momentum tensor to be a Hermitian operator. Non-unitary representations have also been studied in the last decades, in particular in the context of statistical mechanics, which is also the context in which it surfaces in this thesis. These representations still consist of states in a Hilbert space (with positive norm, by definition of a Hilbert space), but the requirement $L_n^\dagger = L_{-n}$ is dropped.

2.3.2 Virasoro representation theory

We define a *highest weight representation* as a representation containing a state with a smallest value of L_0. Not all representations have this property, but it is reasonable to expect this in a physical theory since $L_0 + \bar{L}_0$ is the Hamiltonian, which is usually bounded from below. The terminology "highest weight" for representations containing a state with lowest energy is perhaps unfortunate, but standard. If we have a state which is an eigenvector of L_0

$$L_0 |\psi\rangle = h |\psi\rangle , \tag{2.56}$$

we see that when we act on it with L_n:

$$L_0 L_n |\psi\rangle = (L_n L_0 - n L_n) |\psi\rangle = (h - n) |\psi\rangle , \tag{2.57}$$

the eigenvalue of $|\psi\rangle$ is lowered by n, and L_n with $n > 0$ can be interpreted as a raising[1] operator. If $|h\rangle$ is a highest weight state, then by definition, we have

$$L_n |h\rangle = 0 \text{ for } n > 0. \tag{2.58}$$

Suppose now we have the operator L_0 acting on the heighest weight state $|h\rangle$ creating a state $|h\rangle'$, then we have for operartors L_n with $n > 0$

$$L_n |h\rangle' = L_n L_0 |h\rangle = (L_0 + n) L_n |h\rangle = 0, \tag{2.59}$$

[1] We are really lowering the value of h, so the name is again unfortunate but standard.

which means that L_0 maps highest weight states to highest weight states. For the unitary models, L_0 is Hermitian, and therefore we can diagonalise it on the highest weight states:

$$L_0 |h\rangle = h |h\rangle \tag{2.60}$$

$$L_n |h\rangle = 0 \text{ for } n > 0. \tag{2.61}$$

The other states in the representation are then generated by the negative modes $L_n, n < 0$ acting on the highest weight state; these are called descendant states. For the non-unitary models, L_0 is no longer Hermitian, and we can no longer diagonalise it on the highest weight representations; the best we can do is bring it into Jordan normal form. Assuming we have a Jordan block of rank r and $s \in \{0, \ldots, r-1\}$, one can show that we have [16]

$$L_0 |h; s\rangle = h |h; s\rangle + (1 - \delta_{s,0}) |h; s-1\rangle \tag{2.62}$$

$$L_n |h; s\rangle = 0 \text{ for } n > 0. \tag{2.63}$$

The representation theory for non-unitary CFT is considerably more difficult than the unitary case, but we note that for $s = 0$ we recover an irreducible subrepresentation of the algebra which is identical to the unitary case. The other representations with $s \neq 0$ are called logarithmic partners and a full description of a non-unitary CFT has to include these representations, but we will not need them for our discussion. We end by noting that the discussion is the same for the anti-holomorphic representations, and since the holomorphic and anti-holomorphic parts decouple the combined representations are simply the tensor product of the two.

2.3.3 The vacuum

We define the vacuum by the condition that it has to respect the maximum number of symmetries, or that it has to be annihilated by the maximum number of conserved charges. We would like to impose $L_n |0\rangle = 0 \ \forall n$, but due to the conformal anomaly this is not possible. The maximal number of symmetries we can impose is

$$L_n |0\rangle = 0, \quad for \ n \geq -1, \tag{2.64}$$

which implies that the vacuum is a highest weight state.

2.3.4 States and fields

There is a simple connection between highest weight states and conformal fields, known as the state-operator correspondence. We consider a conformal field $\phi(w, \bar{w})$ with weights

h and $\bar{h}$, and compute the commutator with L_n:

$$[L_n, \phi(w,\bar{w})] = \frac{1}{2\pi i}\oint dz z^{n+1} T(z)\phi(w,\bar{w}) \tag{2.65}$$

$$= h(n+1)w^n\phi(w,\bar{w}) + w^{n+1}\partial_w\phi(w,\bar{w}), \tag{2.66}$$

which vanishes for $w = 0$ and $n > 0$. If we now define

$$|h,\bar{h}\rangle = \phi(0,0)\,|0\rangle\,, \tag{2.67}$$

we see that this is a highest weight state and because

$$[L_0, \phi(0,0)] = h\phi(0,0), \tag{2.68}$$

and the same for the anti-holomorphic sector, the notation is justified. The highest weight states are therefore also called Virasoro primaries, because they can be created by primary fields acting on the vacuum. For the descendant states, we consider the OPE of the energy momentum tensor with the same $\phi(w,\bar{w})$:

$$T(z)\phi(w,\bar{w}) = \sum_{k\geq 0}(z-w)^{k-2}\phi^{-k}(w,\bar{w}) \tag{2.69}$$

and project out a term from this sum by

$$\phi^{-k}(w,\bar{w}) = \frac{1}{2\pi i}\oint dz \frac{1}{(z-w)^{k-1}} T(z)\phi(w,\bar{w}). \tag{2.70}$$

We then find

$$\phi^{-k}(0,0)\,|0\rangle = \frac{1}{2\pi i}\oint dz \frac{1}{z^{k-1}} T(z)\phi(0,0)\,|0\rangle = L_{-k}\phi(0,0)\,|0\rangle\,, \tag{2.71}$$

so that $\phi^{-k}(0,0)$ generates the L_{-k} descendant of $|h,\bar{h}\rangle$.

2.3.5 Minimal models

The class of models that we will be considering are the minimal rational CFTs. These have a finite number of irreducible representations for unitary CFTs[2] where all conformal dimensions and the central charge are rational numbers that can be calculated from consistency conditions [12]. For these models, the Verma modules[3] $V(c,h)$ can be shown to contain null states, which can be quotiented out[4] to arrive at irreducible representation

[2]For the non-unitary CFTs, we get also an infinite number of logarithmic indecomposable representations, but we only consider the non-logarithmic irreducible representations [17, 18].

[3]Subspaces of the Hilbert space generated by a primary and its descendants, closed under the Virasoro algebra therefore forming representations or more correctly, modules

[4]For non-unitary models, this is more subtle; we do not go into details, but refer again to [17, 18].

$M(c,h)$, the building blocks of minimal models. The central charge for such models is given by

$$c = 1 - 6\frac{(p-q)^2}{pq} \tag{2.72}$$

where q and p are coprime integers larger than 1. The conformal dimensions of the irreducible representations are given by

$$h_{r,s} = \frac{(pr-qs)^2 - (p-q)^2}{4pq}, \tag{2.73}$$

with r, s integers such that $1 \leq r \leq q-1$ and $1 \leq s \leq p-1$. We denote the minimal model by $\mathcal{M}(p,q)$. A generic Hilbert space looks like [19]

$$\mathbb{H} = \bigoplus_{h,\bar{h}} M(c,h) \otimes \bar{M}(c,\bar{h}), \tag{2.74}$$

but the particular way of combining the components of a minimal model in the tensor product is not obvious and governed by modular invariance, as we will see later when studying CFT on a torus. An example would be to associate the anti-holomorphic module to the holomorphic module, which are known as the diagonal models:

$$\mathbb{H} = \bigoplus_{r,s} M(c,h_{r,s}) \otimes \bar{M}(c,\bar{h}_{r,s}). \tag{2.75}$$

Examples include the Ising model $\mathcal{M}(4,3)$ and the Yang-Lee edge singularity $\mathcal{M}(2,5)$. For a unitary CFT we should have $|p-q| = 1$ since this guarantees that all conformal weights are positive, and we see that the Ising model is unitary while the Yang-Lee edge singularity is not.

2.4 CFT on a torus

In this final section we want to address which ground states can actually occur in a CFT. Once we know these, we have completely specified the set of states in the theory; they consist of the ground states and all their descendants generated by the Virasoro algebra, minus all the null states. We have seen that on the infinite plane, the holomorphic and anti-holomorphic sectors of a CFT completely decouple and can be studied seperately. This situation is very unphysical however, as it only exists at the fixed point in parameter space (the point where we have conformal invariance) and for the infinite plane geometry. In order to impose physical constraints on the coupling between the holomorphic and anti-holomorphic content of a CFT without leaving the fixed point, we are forced to couple these two sectors through the geometry of the space on which the theory is defined. The infinite plane is topologically equivalent to a sphere, a Riemann surface of genus 0.

We could study the CFT on a surface of arbitrary genus, but in the context of critical phenomena that are often described by a lattice with periodic boundary conditions in both directions, we will consider the torus.

2.4.1 Parametrising the torus

We first describe how we parametrise the torus, which we imagine being constructed by gluing together the two ends of a cylinder. We can then describe the torus as a parallelogram in the complex plane where we identify the opposing edges. This is more general than considering a rectangle, and is due to the fact that we allow ourselves to twist one end of the cylinder before gluing it to the other one. We can choose our coordinates such that one of the edges of the parallelogram is aligned with one of the axes and additionally has unit length. The torus is then fully described by specifying the other edge with a complex number we call τ, as shown in Figure 2.1

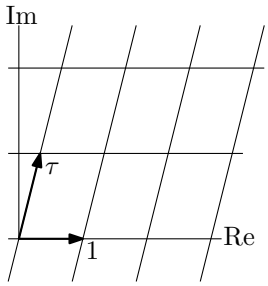

Figure 2.1: The parallelogram is completely parametrised by specifying one point in the complex plane, denoted τ. If we interpret the complex plane modulo the basis vectors 1 and τ this corresponds to a torus.

2.4.2 The partition function

In 1D quantum mechanics, the partition function is given by a Wick rotation of the path integral,

$$Z = \int_{\text{PBC}} \mathcal{D}[q] e^{-S_E(q)} = \operatorname{Tr} e^{-\beta H}, \tag{2.76}$$

where the integration is over all paths $q(y)$, with y the Euclidean time coordinate, that satisfy periodic boundary conditions $q(0) = q(\beta)$. The 2D version of this on the torus is an integration over all field configurations, where we regard the real axis of the parallelogram as the x direction and the imaginary axis as the y direction. For $\operatorname{Re}(\tau) = 0$, i.e. without twisting the torus, we get

$$\int \mathcal{D}\phi e^{-S_E(\phi)} = \operatorname{Tr} e^{-2\pi \operatorname{Im}(\tau) H}. \tag{2.77}$$

The factor 2π appears for consistency with previous conventions. If we now twist the torus, the periodic boundary conditions are shifted in the x direction after going around the torus once. Such a shift is generated by the momentum operator P, and including twists, the partition function becomes

$$Z = \mathrm{Tr}\, e^{-2\pi \mathrm{Im}(\tau) H + 2\pi i \mathrm{Re}(\tau) P}. \tag{2.78}$$

The operators H and P are the time and space translation operators on the cylinder, and they can be derived from the energy-momentum tensor. We have defined the energy-momentum tensor on the plane, but its transformation to the cylinder is not straightforward because it is not a conformal field. The details of the derivation are given in [12,13], and the result is

$$H = L_0 + \bar{L}_0 - \frac{c + \bar{c}}{24}, \tag{2.79}$$

$$P = L_0 - \bar{L}_0 + \frac{c - \bar{c}}{24}. \tag{2.80}$$

We have allowed for different values of the holomorphic and anti-holomorphic central charge, but for sensible theories these are usually equal and we will take them as such from now on. Defining

$$q = e^{2\pi i \tau}, \quad \bar{q} = e^{-2\pi i \bar{\tau}}, \tag{2.81}$$

the partition function can be written as

$$Z = \mathrm{Tr}\, q^{L_0 - c/24} \bar{q}^{\bar{L}_0 - c/24} \tag{2.82}$$

The trace runs over all primary fields and their descendants, and we can write

$$Z = \sum_{h,\bar{h}} M_{h,\bar{h}} \chi_h(q) \chi_{\bar{h}}(\bar{q}), \tag{2.83}$$

where we have defined the *Virasoro characters* as

$$\chi_h(q) = q^{-c/24+h} \sum_{N=0}^{\infty} d_h(N) q^N. \tag{2.84}$$

Here, $d_h(N)$ denotes the degeneracy of the representation at level N. The possible descendants in the characters are constrained by the fact that they should have a positive norm. This condition is expressed by stating that the *Kac determinant* should be positive [12, 13]. This is the determinant of the Gram-matrix, the matrix containing all possible inner products between all descendants at some level N. A discussion falls well beyond the scope of this thesis; we only give the expansion for (a subset of) the characters from the 3-state Potts model $\mathcal{M}(6,5)$ relevant in chapter 5 and the characters of the Yang-Lee edge singularity $\mathcal{M}(5,2)$, taken from table 8.1 in [12].

	$h_{r,s}$	$q^{c/24-h}\chi_{h_{r,s}}(q)$
$\mathcal{M}(6,5)$	$h_{1,1}=0$	$1+q^2+q^3+2q^4+2q^5+4q^6+\ldots$
	$h_{2,1}=2/5$	$1+q+q^2+2q^3+3q^4+4q^5+6q^6+\ldots$
$\mathcal{M}(5,2)$	$h_{1,1}=0$	$1+q^2+q^3+q^4+q^5+2q^6+\ldots$
	$h_{1,2}=-1/5$	$1+q+q^2+q^3+2q^4+2q^5+3q^6+\ldots$

Table 2.1: The low-q expansions of two characters of the 3-state Potts model and the characters of the Yang-Lee edge singularity up to order 6.

2.4.3 Modular invariance

We have defined the torus in terms of two basis vectors 1 and τ spanning a parallelogram in the complex plane, where we identified opposing edges. It is clear that these choices of basis vectors is not unique, and we can construct the same torus by taking for example the basis vectors 1 and $1+\tau$ instead. We have another transformation that leaves the torus invariant, but it is a little more difficult to see. We note that we chose one of the basis vectors along the real axis and rescaled it to 1. This choice is arbitrary, and transforming between these two boils down to replacing τ by $-1/\tau$. These two transformations,

$$T: \quad \tau \to \tau + 1 \tag{2.85}$$

$$S: \quad \tau \to -\frac{1}{\tau} \tag{2.86}$$

generate a group, called the *modular group*. The characters transform in a simple way under T:

$$\chi_h(\tau+1) = e^{2\pi i(h-c/24)}\chi_h(\tau), \tag{2.87}$$

which we can write in matrix form as

$$\chi_{h_i}(\tau+1) = \sum_j T_{ij}\chi_{h_j}(\tau), \tag{2.88}$$

with T a diagonal matrix of phases. The transformation S is much harder to compute, but since it is a basis transformation, we can also write it as

$$\chi_{h_i}\left(-\frac{1}{\tau}\right) = \sum_j S_{ij}\chi_{h_j}(\tau), \tag{2.89}$$

with S a unitary symmetric matrix. In order for the partition function to be invariant under modular transformations, we must have

$$[M,T] = [M,S] = 0, \tag{2.90}$$

with the additional condition that there exists a unique vacuum labelled by 0 so that $M_{00}=1$. This strongly restricts the possible matrices M, and it is this modular invariance

that dictates how the holomorphic and anti-holomorphic sectors of the model couple to each other. The simplest solution is $M = \mathbb{1}$, the so called *diagonal models*, in which case it is easy to show that all the conformal spins $s = h - \bar{h}$ should be integer. This is no longer true for non-diagonal models, which we will encounter in chapter 5 where we do not use periodic boundary conditions but rather *topological conformal defects* that introduce a topological correction to the conformal spin.

Chapter 3

Topological order and Matrix Product Operators

Topological order is a vast subject that has its conception in the study of the experimental observations of superconductivity and the (fractional) quantum Hall effect. It has been rich source of interesting physics for well over 30 years, and it netted its founders Thouless, Haldane and Kosterlitz the Nobel prize in Physics 2016 [20]. In this chapter we will briefly describe some features of topological order in quantum many-body systems relevant to this thesis by considering the simplest model in which it occurs. We will subsequently build up the theory of Projection Matrix Product Operators (PMPO's), which is the tensor network description of topological order, following the exposition of [6].

3.1 The toric code

We will only consider topological order in the context of lattice models. The effective field theories that are the continuum limit of these lattices form the subject of topological quantum field theory (TQFT), but a discussion falls beyond the scope of this thesis. The model we describe here is called the toric code, and it was first introduced by Kitaev in 1997 in the context of fault-tolerant quantum computing [21]. Consider a 2D $N \times N$ lattice, where we take periodic boundary condition in both directions, i.e. we identify the opposing edges. This gives the lattice the topology of a torus, which is where the model gets its name. We now place a spin (or qubit) degree of freedom on each edge (not vertex!) of the lattice, described by the vector operator $\boldsymbol{\sigma}_i$, with its components being the three Pauli matrices. We have the following anticommutation/commutation relations:

$$\{\sigma_i^\alpha, \sigma_i^\beta\} = 2\delta_\beta^\alpha, \quad [\sigma_i^\alpha, \sigma_j^\beta] = 0, \quad (\alpha, \beta = x, y, z), \quad i \neq j. \tag{3.1}$$

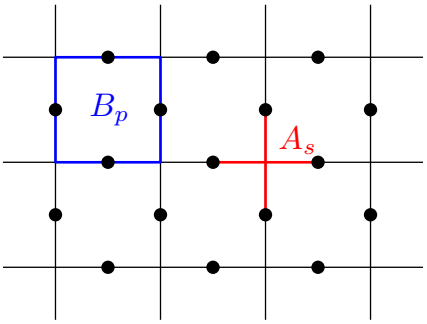

Figure 3.1: The operators A_s and B_p acting on the spins living on the edges of the lattice.

For each of the N^2 vertices s and N^2 faces p, we define the operators

$$A_s = \prod_{j \in s} \sigma_j^x, \quad B_p = \prod_{j \in p} \sigma_j^z, \tag{3.2}$$

where we have used the notation $j \in s$ and $j \in p$ to denote the edges touching the vertex s and the boundary edges of face p respectively. Graphically, these operators are depicted in Figure 3.1. Due to the fact that these operators consist of an even number of anti-Hermitian commuting Pauli matrices, the operators A_s and B_s are Hermitian operators with eigenvalues ± 1. We associate a Hamiltonian to this system of the form

$$H = -\sum_s A_s - \sum_p B_p, \tag{3.3}$$

and the total Hilbert space is 2^{2N^2} dimensional because we have $2N^2$ spins. The set of operators A_s all commute with one another, as do the set of operators B_p. Furthermore, we have that

$$[A_s, B_p] = 0, \quad \forall s, p \tag{3.4}$$

since A_s and B_p have either 0 or 2 edges in common. This means that the combined set of operators can be simultaneously diagonalised, and any eigenstates of the Hamiltonian can be specified by its eigenvalues of the set of operators A_s and B_p. In particular, the ground state is a common eigenstate of all the A_s and B_p with $A_s = B_p = 1$. At first glance, this provides us with $2N^2$ conditions on $2N^2$ degrees of freedom, which uniquely determines the ground state. We note however that because we work on a torus, the identification of the opposing edges leads to the following conditions on the operators A_s and B_p:

$$\prod_s A_s = 1, \quad \prod_p B_p = 1, \tag{3.5}$$

since in each of these products we have counted each link exactly twice and any of the Pauli matrices square to the identity. These two conditions imply that the number of independent operators is really $2N^2 - 2$. This means that for the ground state there are

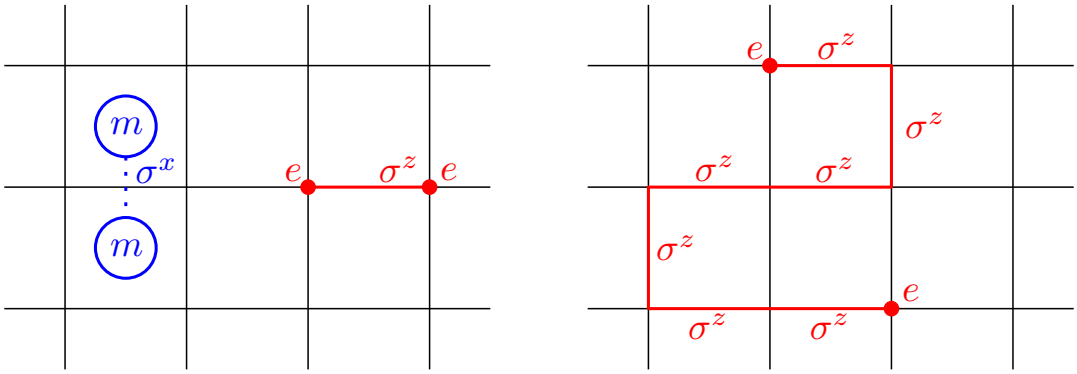

(a) (b)

Figure 3.2: (a) The excitations e and m created in pairs by the operators σ^z and σ^x respectively. (b) A pair of e charges connected by a string of σ^z operators.

two spin degrees of freedom left so that the dimensionality of the ground state manifold is given by

$$2^{2N^2-(2N^2-2)} = 4. \tag{3.6}$$

This degeneracy is simply a consequence the fact that we are working on a non-trivial topology, and this ground state degeneracy turns out to be a general feature of systems exhibiting topological order. We now consider the two types of excitations in this model; we have

1. $A_s = -1$ corresponding to an *electric charge* e living on a vertex of the lattice
2. $B_p = -1$ corresponding to a *magnetic vortex* m living on a face of the lattice (or equivalently a vertex of the dual lattice)

Condition 3.5 implies that both the electric charges e and the magnetic vortices m must always be created in pairs. The creation operators of the charges and the vortices correspond to the local operators σ^z and σ^x respectively, as can be easily seen from Figure 3.2a. If we now consider strings of operators σ^z and σ^x,

$$\prod_i \sigma_i^z, \quad \prod_i \sigma_i^x, \tag{3.7}$$

where the index i runs over the edges of some connected path, we see that these operators create and move excitations along the path. The product of σ^z operators along a path is depicted in Figure 3.2b. Importantly, a closed string of σ^z operators commutes with the Hamiltonian: it creates, moves and annihilates two electric charges. We can see this by noting that for a closed loop, every vertex must have either 0 or 2 σ^z operators acting on it, which means that they commute with all of the A_s operators. The same conclusion

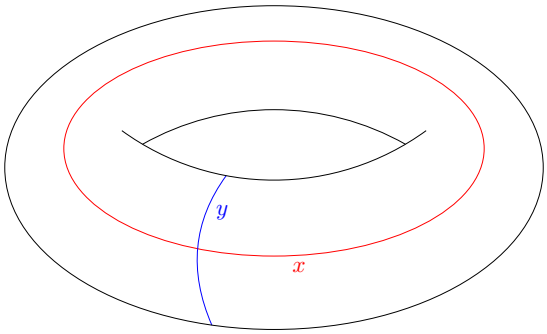

Figure 3.3: Torus with two non-contractible loops in the y and x direction

holds for the magnetic vortices, and we note that any topologically trivial (contractible) loop can be written as a product of the operators A_s, B_p. Considering now again the ground state, with $A_s = B_p = +1$ for all s and p, we see then that these closed loops act as the identity on the ground state, and that by acting with the operators A_s and B_p we can freely deform these loops without changing the energy. The only non trivial closed loop operators are the loops that go around a non-contractible cycle of the torus, shown in Figure 3.3. Assuming we work in the σ^z basis, we have 4 possible configurations:

1. No non-contractible loops of σ^z operators
2. A non-contractible loop of σ^z operators in the x-direction
3. A non-contractible loop of σ^z operators in the y-direction
4. Two non-contractible loop of σ^z operators, one in the x-direction and one in the y-direction.

These four configurations correspond to the 4 degenerate ground states of the model, and they can not be transformed into each other by applying local operators. We note that a closed contractible loop of operators can be deformed to 2 non-contractible loops both in either the x- or y-direction, so it is really the number of non-contractible loops in the x- and y-directions modulo 2 that label the 4 different ground states. The fact that we cannot transform between the different ground states with local operators is also a general feature of topological phases, and it is this robustness against local operations that makes them interesting for storing quantum information [21, 22].

3.1.1 Anyons

We now consider what happens when we take two excitations and rotate them around each other. Due to the fact that the excitations are connected with strings of either σ^z or σ^x, we are really looking at what happens when we braid these strings with each

other. Because the σ^z and σ^x commute with themselves, the charges e and vortices m are bosonic with respect to themselves. If we take a vortex around a charge however, the wave function picks up a minus sign due to the fact that the σ^z and σ^x anticommute on the link where the two strings cross each other. This process is shown graphically in Figure 3.4.

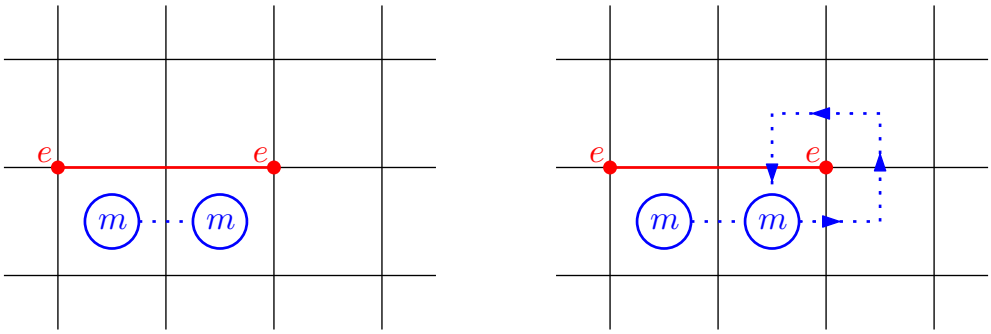

Figure 3.4: The braiding of a vortex m around a charge e results in an overall minus sign for the wave functions.

This result for the mutual statistics is neither bosonic nor fermionic statistics, and we are forced to conclude that the e and m particles are *anyons*; particles that are not restricted to ± 1 under exchange. These exist only in 2D systems because in higher dimensions the rotation of two particles around each other, which corresponds to swapping them twice, can always be deformed to the identity operator. The particles e and m are clearly their own antiparticles since they are always created in pairs, and we can write this in terms of *fusion rules* as

$$\boldsymbol{e} \times \boldsymbol{e} = \mathbf{1}, \quad \boldsymbol{m} \times \boldsymbol{m} = \mathbf{1}, \tag{3.8}$$

where $\mathbf{1}$ denotes the vacuum. We can also construct a non-trivial particle composed of a charge and a vortex, which we will denote as

$$\boldsymbol{e} \times \boldsymbol{m} = \boldsymbol{\psi} \tag{3.9}$$

where ψ has fermionic self-statistics due to the mutual statistics of the charges and vortices. These anyonic excitations are again a general feature of systems exhibiting topological order. To summarise, we have the following general properties for these systems:

1. A ground state with a degeneracy that depends on the topology of the system
2. Different ground state sectors that can not be transformed into one another by local operation
3. Particles with fractional statistics called anyons created an annihilated with string-like operators that can be moved freely through the lattice

3.2 Matrix product operators and fusion categories

In this section, we give a tensor network description of topological order. We will see that given some input fusion category, we can construct a set of MPOs that satisfies this fusion algebra, and that these MPOs can be fused to each other with fusion tensors. From this we construct a PEPS lattice such that these MPOs can be moved freely through the lattice. Finally, we will construct the different topological sectors corresponding to the topological models. To briefly illustrate before delving into the full theory, we get a bit ahead of ourselves and consider again the toric code. The input fusion category is simply the group $\mathbb{Z}_2$ represented by the identity and σ^z, and the MPOs and fusion tensors are

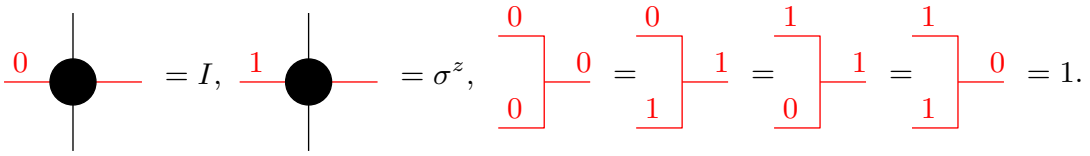

(3.10)

With this, we can construct a four dimensional ground state manifold by considering a second type of algebra and calculating its irreducible representations, which we then identify with the topological sectors of the model. The basis elements of this second type of algebra are given by

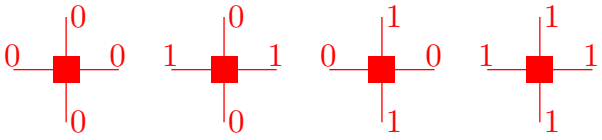

(3.11)

The red tensor can be interpreted as the intersection of two non-contractible loops, and we see that these basis elements correspond to the earlier definition of the degenerate ground states in terms of non-contractible loops in the x- and y-direction. The irreducible representations of this algebra correspond to the topological sectors that we can then identify with the four types of anyonic excitations in the model: 1, e, m and ψ. In the remainder we build up the full theory of PMPOs and see how it can describe a large class of models exhibiting topological order, but it will help to keep the toric code in mind to give a more concrete interpretation to the concepts we will introduce.

3.2.1 Projector Matrix Product Operators

We start by considering the most general form of a translation invariant Matrix Product Operator (MPO), given by

$$P_L = \sum_{\{i\},\{j\}=1}^{D} \operatorname{tr}\left(\Delta B^{i_1 j_1} \dots B^{i_L j_L}\right) |i_1 \dots i_L\rangle \langle j_1 \dots j_L| \,. \tag{3.12}$$

In this expression, for every pair of indices $i, j = 1, 2, \ldots D$, with D the dimension of Hilbert space, B^{ij} is a $\chi \times \chi$ matrix and Δ is a matrix such that changing its point of insertion leaves the MPO unchanged. We now impose that there exists a canonical form of the MPO, where the individual tensors assume a block diagonal structure:

$$B^{ij} = \bigoplus_{a=1}^{\mathcal{N}} B_a^{ij}, \tag{3.13}$$

$$\Delta = \bigoplus_{a=1}^{\mathcal{N}} \Delta_a, \tag{3.14}$$

where both B_a^{ij} and Δ_a are now $\chi_a \times \chi_a$ matrices such that

$$\sum_{a=1}^{\mathcal{N}} \chi_a = \chi \tag{3.15}$$

with $\mathcal{N}$ the number of blocks in the block decomposition of the MPO. In this canonical form, the MPO becomes a sum of MPOs

$$P_L = \sum_{a=1}^{\mathcal{N}} \sum_{\{i\},\{j\}=1}^{D} \operatorname{tr}\left(\Delta_a B_a^{i_1 j_1} \ldots B_a^{i_L j_L}\right) |i_1 \ldots i_L\rangle \langle j_1 \ldots j_L| . \tag{3.16}$$

If we now impose that the Δ_a commute with every B_a^{ij}, we have a sufficient condition for translation invariance of the MPO. The fact that the B_a^{ij} can not be decomposed into smaller blocks implies that the MPOs labelled by a are injective, or equivalently that for every a the matrices $\{B_a^{ij}\} := \{B_a^{ij} : i, j = 1, 2, \ldots, D\}$ span the entire space of $\chi_a \times \chi_a$ matrices. This then implies that Δ_a has to be proportional to the identity on the space of $\chi_a \times \chi_a$ matrices,

$$\Delta_a = w_a \mathbb{1}_{\chi_a}, \tag{3.17}$$

with w_a some complex number associated to the block labelled by a, which we will henceforth refer to as *weights*. We finally arrive at the following form for the MPO:

$$P_L = \sum_{a=1}^{\mathcal{N}} w_a \sum_{\{i\},\{j\}=1}^{D} \operatorname{tr}\left(B_a^{i_1 j_1} \ldots B_a^{i_L j_L}\right) |i_1 \ldots i_L\rangle \langle j_1 \ldots j_L| \tag{3.18}$$

$$= \sum_{a=1}^{\mathcal{N}} w_a O_a^L. \tag{3.19}$$

We now require the MPO constructed in the previous section to be a projector,

$$P_L^2 = \sum_{a,b=1}^{\mathcal{N}} w_a w_b O_a^L O_b^L = \sum_{a=1}^{\mathcal{N}} w_a O_a^L = P_L. \tag{3.20}$$

Since this has to hold for every L (and in particular, for $L \to \infty$), the fundamental theorem for injective MPS [23] (which generalises to MPOs by grouping the indices i, j into one index) implies that the matrices B_a that build up P_L and P_L^2 are the same. This then leads to the following relationship for the injective MPOs that build up the projector [6, 24]:

$$O_a^L O_b^L = \sum_{c=1}^{\mathcal{N}} N_{ab}^c O_c^L. \tag{3.21}$$

From this, we can derive the following condition on the weights,

$$\begin{aligned} &\sum_{a,b=1}^{\mathcal{N}} w_a w_b O_a^L O_b^L = \sum_{a,b,c=1}^{\mathcal{N}} w_a w_b N_{ab}^c O_c^L = \sum_{c=1}^{\mathcal{N}} w_c O_c^L \\ \Rightarrow &\sum_{a,b=1}^{\mathcal{N}} w_a w_b N_{ab}^c = w_c. \end{aligned} \tag{3.22}$$

The fact that eq. 3.21 has to hold for every length L restricts the rank three tensor N_{ab}^c to integer values, from which it follows that the MPOs O_a form a fusion ring [24]. The objects N_{ab}^c are known as fusion rules or fusion multiplicities. For the purpose of this thesis, it suffices to restrict to the case where the fusion multiplicities are either 0 or 1. This will significantly simplify the notation, but it should be stressed that the framework in this chapter was developed in [6] for fusion multiplicities greater than unity.

3.2.2 Fusion tensors

From the theory of MPS representations [25] and eq. 3.21, it follows that there exist matrices called *fusion tensors*:

$$X_{ab}^c : \mathbb{C}^{\chi_a} \times \mathbb{C}^{\chi_b} \to \mathbb{C}^{\chi_c}, \tag{3.23}$$

with left inverses X_{ab}^{d+} such that

$$X_{ab}^{d+} X_{ab}^c = \delta_{dc} \mathbb{1}_{\chi_c}, \tag{3.24}$$

so that, on the level of the individual matrices B_a that constitute O_a^L, we have

$$X_{ab}^{c+} \left(\sum_{j=1}^{D} B_a^{ij} \otimes B_b^{jk} \right) X_{ab}^c = B_c^{ik}. \tag{3.25}$$

As noted in [6],

$$X_{ab}^{d+} \left(\sum_{j=1}^{D} B_a^{ij} \otimes B_b^{jk} \right) X_{ab}^c \tag{3.26}$$

can be non-zero for $c \neq d$, which has no influence on the MPO when closed by tracing, but prevents us from writing

$$\sum_{c=1}^{\mathcal{N}} X_{ab}^{c} B_{c}^{ik} X_{ab}^{c+} = \sum_{j=1}^{D} B_{a}^{ij} \otimes B_{b}^{jk}. \tag{3.27}$$

For the remainder of this thesis, we will assume that 3.26 is zero for $c \neq d$, and we note that we can rewrite 3.27 as

$$\left(\sum_{j=1}^{D} B_{a}^{ij} \otimes B_{b}^{jk} \right) X_{ab}^{c} = X_{ab}^{c} B_{c}^{ik}, \tag{3.28}$$

$$B_{c}^{ik} X_{ab}^{c+} = X_{ab}^{c+} \left(\sum_{j=1}^{D} B_{a}^{ij} \otimes B_{b}^{jk} \right). \tag{3.29}$$

These latter two equations will be referred to from now on as the *zipper condition*. We are now at a point where we can introduce the graphical language for the (P)MPOs and the fusion tensors that will be used extensively in this thesis. The diagrams that we use are shown in Figure 3.5. The matrices building up the MPOs are represented by black circles, where the red line carries the label a of the block the MPO O_a belongs to and represents the matrix indices, while the black lines carry the indices i and j. The matrices building up the PMPO are represented in a similar way but with a square instead of a circle, indicating that they are weighted sums of the matrices building up the MPOs. The fusion tensors are shown satisfying the zipper condition, where we only have one unlabeled type of fusion tensor specified by its virtual index labels, in contrast to the more general setting of [6] with fusion multiplicities greater than one. We will see that for our purposes the fusion tensor and its inverse will in fact be the same tensor and therefore the diagrams can simply be flipped, but this is certainly not true in general.

3.2.3 Hermiticity of the PMPO

We now require the projector P_L to be Hermitian for all L. This condition enforces unitarity of the resulting theory, and we will see in the next chapter that we have to weaken this constraint in order to describe non-unitary fusion categories. We find that

$$P_L = P_L^{\dagger}$$
$$\sum_{a=1}^{\mathcal{N}} w_a O_a^L = \sum_{a=1}^{\mathcal{N}} \bar{w}_a O_a^{L\dagger}$$

implies that for every label a there exists some label a^* such that

$$\bar{w}_a = w_{a^*}, \tag{3.30}$$

$$\left(O_a^L\right)^{\dagger} = O_{a^*}^L, \tag{3.31}$$

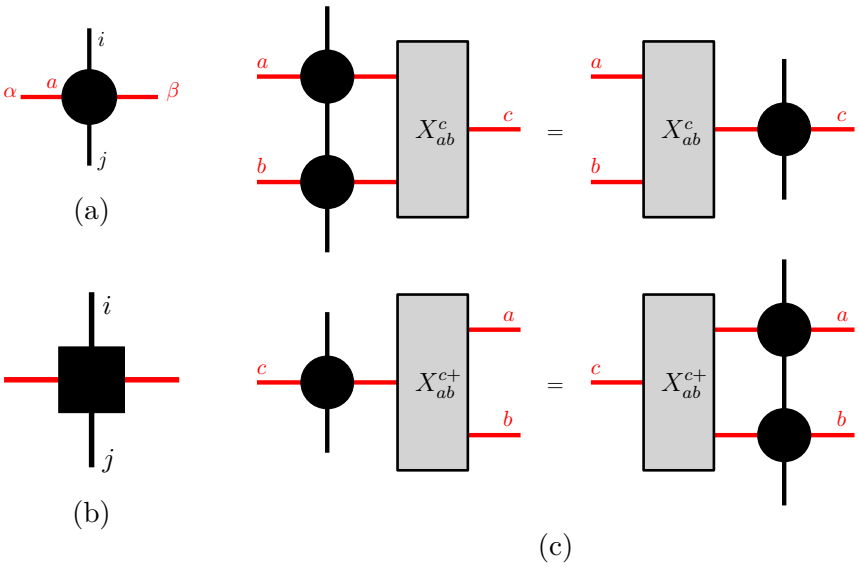

Figure 3.5: Diagrammatic convention for (a) the MPOs, (b) PMPOs and (c) the fusion tensors satisfying the zipper conditions.

where the bar denotes complex conjugation and the dagger is defined with respect to the physical indices. We now again invoke the fundamental theorem of MPS to state that the tensors $\bar{B}^{ji}_a$ and $B^{ij}_{a^*}$, the building blocks of $O^{L\dagger}_a$ and $O^L_{a^*}$ respectively, are related by a gauge transformation

$$B^{ij}_a = \bar{Z}^{-1}_a \bar{B}^{ji}_{a^*} \bar{Z}_a, \tag{3.32}$$

which applied twice yields

$$B^{ij}_a = \bar{Z}^{-1}_a Z^{-1}_{a^*} B^{ij}_a Z_{a^*} \bar{Z}_a. \tag{3.33}$$

From the injectivity of $\{B^{ij}_a\}$ we see that $Z_{a^*}\bar{Z}_a$ has to be proportional to the identity, or more precisely

$$Z_{a^*}\bar{Z}_a = \bar{Z}_a Z_{a^*} = \gamma_a \mathbb{1}, \tag{3.34}$$

with γ_a some complex number for which $\gamma_a = \bar{\gamma}_{a^*}$. For $a = a^*$ we can at most absorb the absolute value of γ_a in the definition of the gauge matrices, and the remaining signs $\chi_a = \text{sign}(\gamma_a)$, for each label a, are discrete invariants of the PMPO.

3.2.4 The pentagon equation

The multiplication of two MPOs is associative,

$$\left(O^L_a O^L_b\right) O^L_c = O^L_a \left(O^L_b O^L_c\right), \tag{3.35}$$

which implies that on the level of the tensors B that build up these MPOs we have two options:

1. We fuse B_a^{ij} and B_b^{jk} to B_e^{ik}, which we then fuse with B_c^{kl} to obtain B_d^{il}
2. We fuse B_b^{jk} and B_c^{kl} to B_f^{jl}, which we then fuse with B_a^{ij} to obtain B_d^{il}

These two options are shown graphically in Figure 3.6 on the left and right hand side respectively.

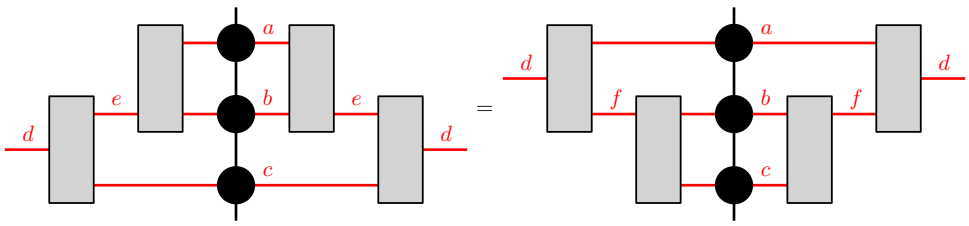

Figure 3.6: Two equivalent ways of fusing three MPOs. We have omitted the labels on the fusion tensors to simplify notation, as they are completely determined by their labels and the orientation in the diagram.

For PMPOs satisfying the zipper conditions, we can write down the following identity

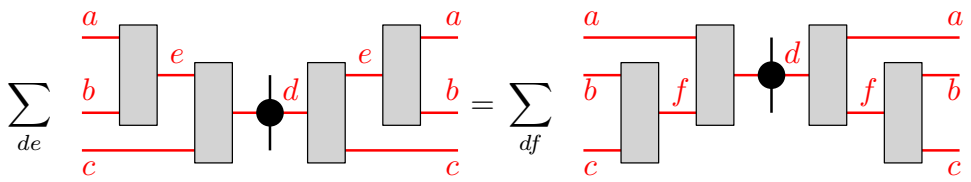

(3.36)

We act on both sides with fusion tensors to obtain

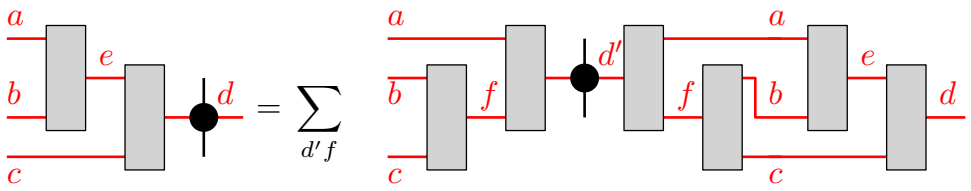

(3.37)

The injectivity of the B tensors that build up the MPO implies that, when interpreted as a map from the virtual to the physical indices, these maps have an inverse. Acting with this inverse on both sides of the previous equation, we find

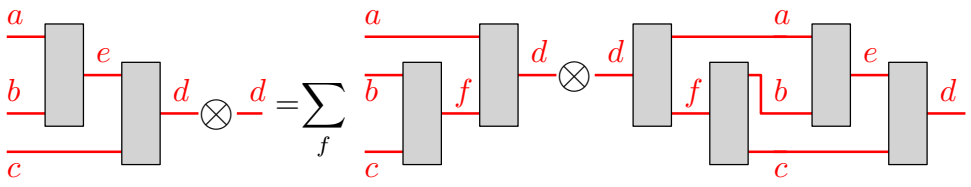

(3.38)

This equation implies that there exists a linear transformation between the two different ways of fusing three MPOs. We denote the second factor of the tensor product on the right hand side as

$$\left(F_d^{abc}\right)_e^f := F_{def}^{abc}, \tag{3.39}$$

a matrix from label e to label f. With this object, which we will call the *F-symbol* of the theory, we are able to transform between the two ways to fuse three particles, a process we will call an *F-move*. We can now make the connection with fusion category theory [26,27]: it is well known that the F-symbols have to satisfy a consistency condition called the pentagon equation. This equation arises from the different paths of F-moves one can make when fusing 4 labels to a single label, as illustrated in Figure 3.7.

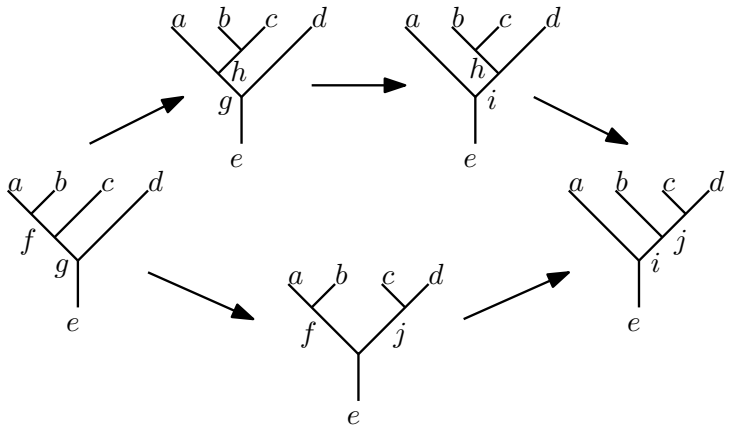

Figure 3.7: Schematic representation of the two paths that lead to the pentagon equation.

Written down explicitly, the pentagon equation reads

$$\sum_h F^{abc}_{gfh} F^{ahd}_{egi} F^{bcd}_{ihj} = F^{fcd}_{egj} F^{abj}_{efi}. \tag{3.40}$$

A theorem called the *Mac Lane coherence theorem* states that the pentagon equation can be used as the defining equation for the F-symbols, in that it suffices (although this is very non-trivial in practice) to find the solutions to this equation to completely determine the F-symbols, given some input fusion rules N^c_{ab}. The F-symbols we obtain this way then automatically satisfy all other possible consistency conditions [26–28], although it is not guaranteed that every set of fusion rules leads to a pentagon equation with solutions, in which case the fusion category is not consistent. We conclude by remarking that there exists another theorem by the name of *Ocneanu rigidity* [27, 29], which says that the algebraic data $(N^c_{ab}, F^{abc}_{def}, \chi_a)$ we have derived from the Hermitian PMPO is in many cases robust. This means that any small deformation of the F-symbols that satisfies the pentagon equation can be absorbed in the gauge freedom of the fusion tensors,

$$F^{abc}_{def} \to \frac{f(a,b,e)f(e,c,d)}{f(a,f,d)f(b,c,f)} F^{abc}_{def}, \tag{3.41}$$

and therefore the PMPOs that satisfy the zipper condition fall into discrete families. We end this section by mentioning that the sign χ_a is strongly related to the Frobenius-Schur indicator in category theory, but a discussion falls beyond the scope of this thesis.

3.3 MPO-injective PEPS

It was shown in [30,31] that topologically ordered systems (or at least, a subset of them) can be described by PEPS that exhibit a type of symmetry on the virtual level. This class of PEPS was termed MPO-injective PEPS, due to the fact that these symmetries manifest themselves as MPOs on the virtual level that can be moved freely through the PEPS lattice. This formalism is a generalisation of G-injectivity [32], and it was shown that all string-net models [33] can be described in terms of MPO-injective PEPS [31]. In this section we will impose the additional requirements on the PMPOs for them to be usable for the construction of PEPS that satisfy the axioms of MPO-injectivity listed in [31].

3.3.1 Zipper, unitarity and pivotal structure

We impose three requirements on the PMPOs in order to be able to construct MPO-injective PEPS. The first of these is the zipper condition we have already encountered and assumed to be valid in order to be able to derive the F-symbols. The second property we impose is that there exists a gauge on the internal MPO indices such that the fusion tensors X^c_{ab} are isometries,

$$X^{c+}_{ab} = (X^c_{ab})^\dagger \tag{3.42}$$

and the gauge matrices Z_a are unitary. This requirement restricts the formalism to unitary fusion categories (UFC), and we will see in the next chapter that we will have to modify this condition to describe non-unitary fusion categories (nUFC). We now introduce a new graphical notation for the gauge matrices illustrating that they transform between a label a and its dual a^* as discussed in Section 3.2.3:

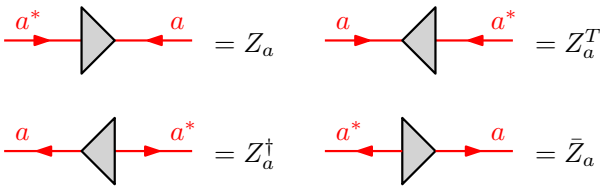

(3.43)

The final requirement is that the fusion tensors satisfy the so-called *pivotal property*:

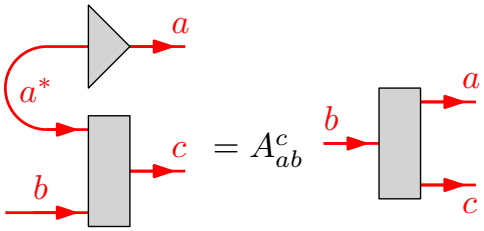

(3.44)

Where the numbers A^c_{ab} satisfy

$$|A^c_{ab}|^2 = \frac{w_c}{w_b} \tag{3.45}$$

This property has a deep connection with the pivotal scructure in category theory, and it is known [27, 29] that every UFC admits a pivotal structure, while for nUFC this is conjectured in [29]. The left hand side of eq. 3.45 is real and positive, which implies that all the weights must have the same phase. Combining eq. 3.30 and 3.22 leads to the conclusion that all w_a must be positive. We will see that eq. 3.45 is modified for nUFCs, and that negative weights will be allowed.

3.3.2 Right- and left-handed MPOs

We need one additional ingredient for defining the MPO-injective PEPS, which is the notion of left- and right-handed MPOs, necessary for the consistent virtual symmetry of arbitrary branching structures. The right-handed MPOs are defined as the original MPOs we used to construct the PMPO,

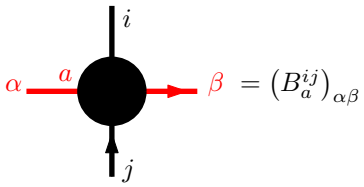

(3.46)

while we define a left-handed type as the Hermitian conjugate on the physical indices of the right-handed type,

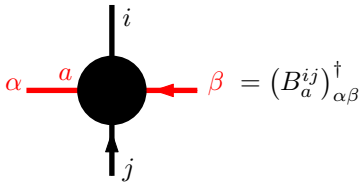

(3.47)

Using eq. 3.32, and the fact that the gauge matrices are unitary, we can write the following graphical relation between the right- and left-handed MPOs:

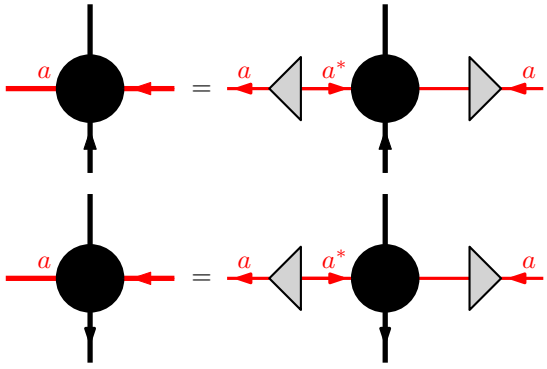

(3.48)

We have added the arrow to the physical indices merely to keep track of the handedness of the MPOs, as we will be rotating them to construct PEPS on arbitrary lattices.

3.3.3 MPO-injective PEPS

We now have everything we need to construct an MPO-injective PEPS. We will work on a square lattice, but the construction can be done for arbitrary lattices. We begin by assigning an orientation to every edge in the lattice. We then place a closed PMPO loop around every vertex, where we choose (for now) the orientation of the internal (red) indices to be counter-clockwise. We choose right- and left-handed MPOs according to the edge and internal index orientation, as illustrated in Figure 3.8a.

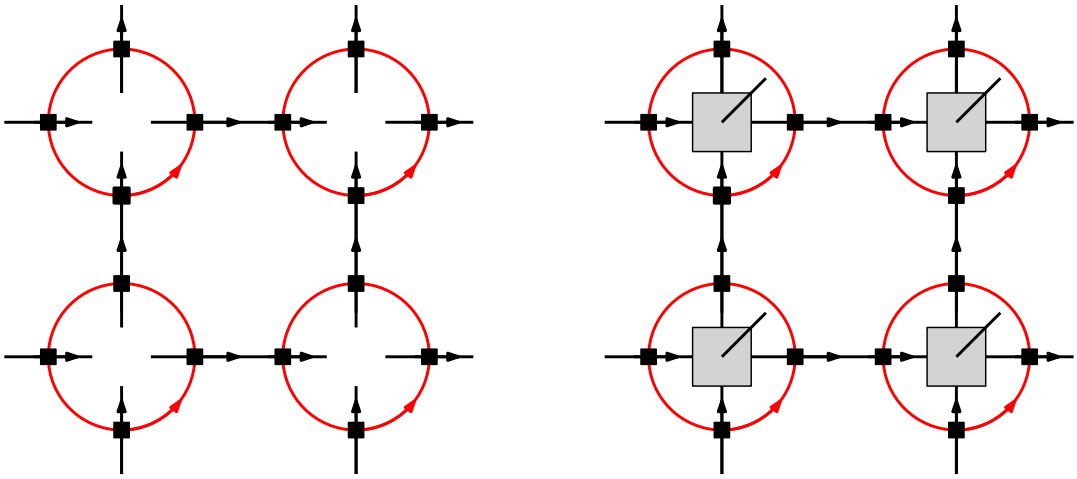

(a) (b)

Figure 3.8: (a) 2 by 2 square lattice on which the above described procedure has been applied. (b) The same lattice completed with a tensor A.

Changing the orientation of any of the virtual indices to clockwise amounts to taking the Hermitian conjugate due to the relation between the right- and left-handed MPOs, and since we assumed the PMPO to be Hermitian the orientations of the internal indices are arbitrary. The PMPO rings are connected to each other by placing a maximally entangled qudit pair on all edges of the lattice (which just amounts to connecting the black lines in Figure 3.8a). To obtain a PEPS similar to those we have described in Chapter 1, we can place a tensor

$$A = \sum_{i=1}^{d} \sum_{\alpha}^{D} A^{i}_{\alpha_1\alpha_2\alpha_3\alpha_4} |i\rangle \langle \alpha_1\alpha_2\alpha_3\alpha_4| \tag{3.49}$$

at every vertex acting as an injective map from $\mathbb{C}^{D^4}$ to $\mathbb{C}^d$, which requires $d > D^4$. The resulting PEPS tensor is shown in Figure 3.8b and satisfies the MPO injectivity axioms defined in [31], but there it was also argued that all topological properties are captured by the structure on the virtual level, and therefore we will not be using the tensor A but rather the more general picture of Figure 3.8a.

3.3.4 Pulling through equation

A key property that allows the MPO-injective PEPS to describe topological order is the existence of MPO-symmetries on the virtual level that can be pulled freely through the lattice. These MPOs are the same MPOs that build up the PMPOs, and for each label a we have the following identity:

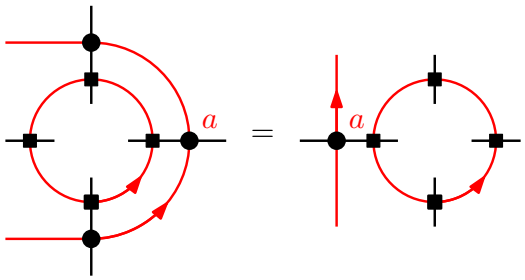

(3.50)

where we have not assigned an orientation to the external (black) MPO indices, indicating that this property is valid independently of these orientations. To prove this, we write the PMPO as the weighted sum of the constituent MPOs, and we use eq. 3.26 with the zipper condition to write the left hand side of eq. 3.50 as

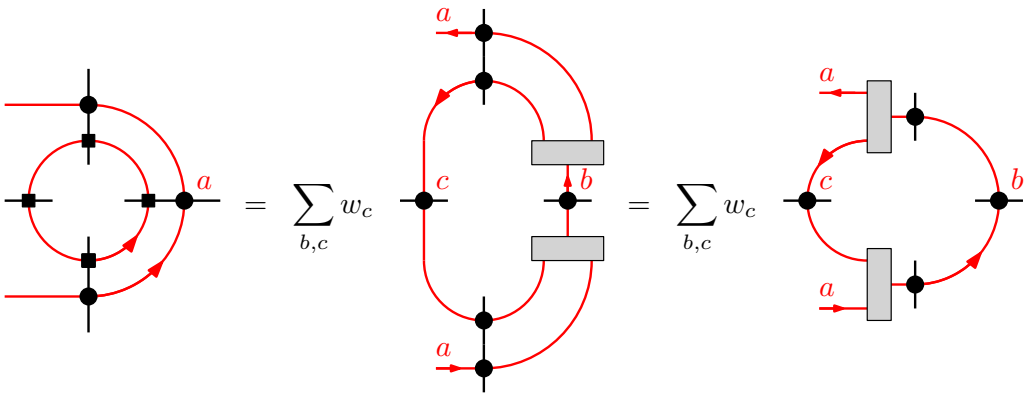

(3.51)

where we can then use the pivotal property, the fact that $|A^c_{ab}|^2 = \frac{w_c}{w_b}$ and once again eq. 3.26 to write

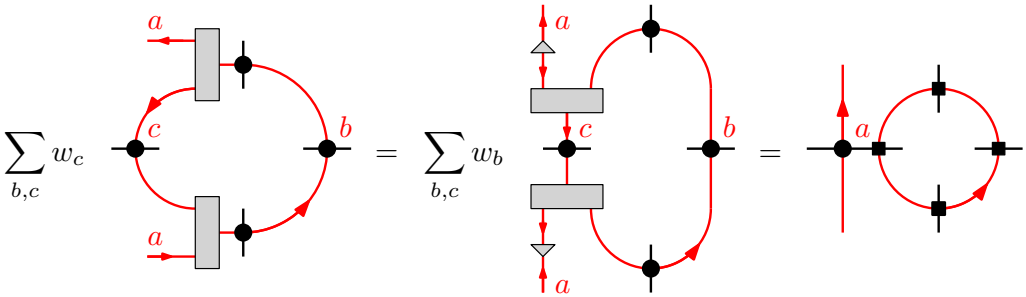

(3.52)

which proves the pulling through property. Variations of eq. 3.50 with different internal orientations of the MPO and PMPO indices, as well as the case where the MPO connects to two PMPO tensors on both sides of the equation have completely analogous proofs.

3.4 The anyon ansatz

A key feature of MPO-injective PEPS is that they can exhibit degenerate ground states on non-trivial manifolds [31] (i.e. cylinder, torus, ...), a hallmark of topological order. It was shown in [6, 31] that the ground state PEPS tensor has to have a support space corresponding to the support of the following tensors,

$A_{abcd} =$ 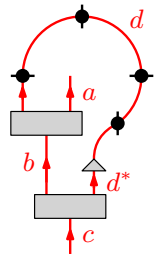

(3.53)

if we interpret them as a matrix from the outer to the inner indices. The derivation of this tensor as presented in [6, 31] is beyond the scope of this thesis, but the models we will be considering allow for various simplifications, and a proof is given in Appendix A.1. These tensors form a $\mathcal{C}^*$ algebra as proven in [6] by using F-moves and the pivotal property,

$$A_{hegf}A_{abcd} = \delta_{ga}\sum_{ij}\Omega^{hjci}_{hegf,abcd}A_{hjci} \tag{3.54}$$

$$A^{\dagger}_{abcd} = \sum_{e}\Theta^{e}_{abcd}A_{cead^*} \tag{3.55}$$

and we give an alternative proof for eq. 3.54 without the need for a pivotal structure in Appendix A.2. We can identify the topological ground state sectors with the irreducible representations of the algebra spanned by the tensors A_{abcd}, or more specifically that for every sector i there exists an minimal central idempotent, which we refer to as the anyon ansatz, of the form

$$\mathcal{P}_i = \sum_{abd} c^{i}_{abd}A_{abad}, \tag{3.56}$$

$$\mathcal{P}_i\mathcal{P}_j = \delta_{ij}\mathcal{P}_i, \quad \mathcal{P}_i^{\dagger} = \mathcal{P}_i.$$

to which we associate a topological sector. The algebra formed by the matrices A_{abcd} is an example of what is known in the mathematical literature as Ocneanu's *tube algebra* [34, 35]. We will be denoting the minimal central idempotents graphically as

$\mathcal{P}_i =$ 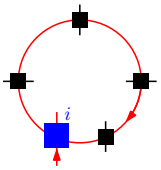

(3.57)

where in this case the black blocks represent the sum in eq. 3.56.

3.4.1 Topological spin

Imagine that we have some region of the PEPS in the topological sector defined by $\mathcal{P}_i$. This region has one internal MPO-index at its boundary that connects to the blue tensor in 3.57 when acted upon with $\mathcal{P}_i$, and doing so leaves this region unchanged since $\mathcal{P}_i$ is a projector on the topological sector it defines. If we now rotate this region one full turn, while leaving the surrounding PEPS unchanged, $\mathcal{P}_i$ is transformed to

$\mathcal{P}_{i,2\pi} =$ 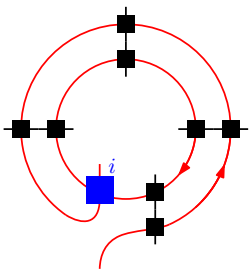

(3.58)

due to the fact that we can not freely move the blue tensor in 3.57. We can interpret this as $\mathcal{P}_i$ acting on a matrix [1]

$\mathcal{R}_{2\pi} =$ 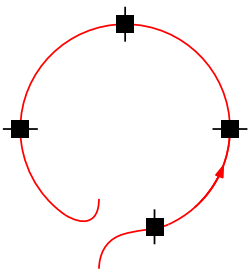

(3.59)

It is proven in [6] that the matrix $\mathcal{R}_{2\pi}$ is unitary and that its left eigenvectors correspond to the central idempotents $\mathcal{P}_i$:

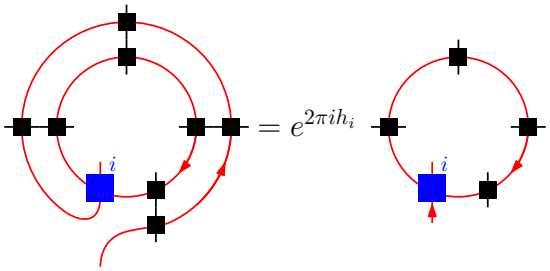

(3.60)

where the eigenvalues of $\mathcal{R}_{2\pi}$ are pure phases due to its unitarity, and we identify h_i as the topological spin associated to $\mathcal{P}_i$. We note that the blocks in the graphical notation for $\mathcal{R}_{2\pi}$ represent the unweighed sum over all MPO labels, and simply calculating the eigenvalues of this matrix gives all the possible topological spins in the theory; if we want to assign them to a specific topological sector, we have to perform the calculation in 3.60.

[1] This matrix will correspond to the Dehn twist on a torus in Chapter 5

3.5 Fibonacci fusion category

We now turn to the simplest fusion category with multiple fusion channels (unlike e.g. the group Z_2 for the toric code) to illustrate the concepts introduced so far, and we will see in the next chapter that this category also allows us to construct an equally simple nUFC. The unitary category we consider here is the Fibonacci fusion category, which is defined by specifying that there are two labels, $\mathbf{1}$ and $\boldsymbol{\tau}$, obeying the following fusion rules:

$$\mathbf{1} \times \mathbf{1} = \mathbf{1}, \quad \boldsymbol{\tau} \times \mathbf{1} = \mathbf{1} \times \boldsymbol{\tau} = \boldsymbol{\tau}, \quad \boldsymbol{\tau} \times \boldsymbol{\tau} = \mathbf{1} + \boldsymbol{\tau}. \tag{3.61}$$

It can be shown that $\boldsymbol{\tau} \times \boldsymbol{\tau} = \mathbf{1} + a\boldsymbol{\tau}$ only yields consistent solutions to the pentagon equation for $a = 0$ and $a = 1$ [36], so that this is the unique fusion category of this type. Given these fusion rules we have

$$N_{11}^{1} = N_{\tau 1}^{\tau} = N_{1\tau}^{\tau} = N_{\tau\tau}^{1} = N_{\tau\tau}^{\tau} = 1 \tag{3.62}$$

and 0 for the other components, leading to the following set of equations for the weights:

$$\begin{cases} w_1 = w_1^2 + w_\tau^2, \\ w_\tau = 2w_1 w_\tau + w_\tau^2. \end{cases} \tag{3.63}$$

which can easily be solved to yield

$$w_1 = \frac{1}{1+\phi^2} \equiv \frac{d_1}{d_1^2 + d_\tau^2}, \quad w_\tau = \frac{\phi}{1+\phi^2} \equiv \frac{d_\tau}{d_1^2 + d_\tau^2}, \tag{3.64}$$

where we have introduced the golden ratio ϕ, the positive root of

$$\phi = \phi^2 - 1, \tag{3.65}$$

and $d_1 = 1, d_\tau = \phi$ are known as the quantum dimensions in string-net models. The F-symbols can be obtained from the pentagon equation, and they are given by [6, 33, 37]

$$F_{def}^{abc} = \delta_{ab}^{e} \delta_{cd}^{e} \delta_{ad}^{f} \delta_{bc}^{f} F_{def}^{abc}, \tag{3.66}$$

with

$$\begin{cases} \delta_{ij}^{k} = 1 & \text{if } N_{ij}^{k} \neq, 0 \\ \delta_{ij}^{k} = 0 & \text{if } N_{ij}^{k} = 0. \end{cases} \tag{3.67}$$

The non-trivial components of F are given by the following matrix:

$$F_{\tau ef,\mathrm{Fib}}^{\tau\tau\tau} = \frac{1}{\phi} \begin{pmatrix} 1 & c^{-1}\sqrt{\phi} \\ c\sqrt{\phi} & -1 \end{pmatrix} = \frac{1}{\phi} \begin{pmatrix} 1 & \sqrt{\phi} \\ \sqrt{\phi} & -1 \end{pmatrix} \tag{3.68}$$

where $c \in \mathbb{C}$ is the gauge freedom we have in the F-symbols [38] and subsequently put $c = 1$ which brings us in the symmetrical gauge.

3.5.1 MPOs and fusion tensors

The Fibonacci fusion category is already well understood in terms of string-net models as introduced by Levin and Wen in [33], and the explicit expressions of the MPOs and fusion tensors was given in [6, 31, 39]. We will use the convention of [39], which is also the convention used in the strange correlator of [40] and Chapter 5. The right- and left-handed MPO tensors are given by

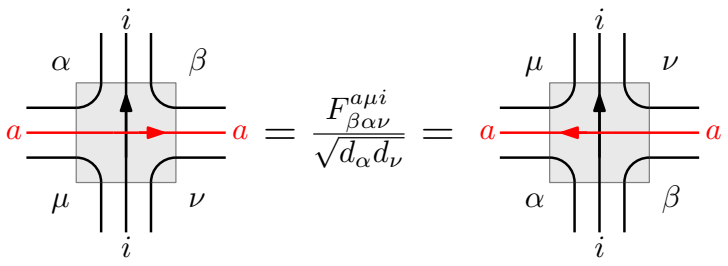

(3.69)

where the 4 sets of three indices should be grouped into 4 regular indices to correspond to the definition of MPOs we gave previously. The right-handed MPO on the right hand side is simply the Hermitian conjugate on the external indices of the MPO of the left-handed MPO on the left hand side, and we used that for the Fibonacci fusion category the F-symbols are real. These MPOs consist of a two-dimensional block labelled by $a = 1$ and a three-dimensional block labelled by $a = \tau$, and due to the fact that the F-symbols have to satisfy 3.66, we have the following possible values for some internal index b:

$$\text{1-block}: \begin{cases} 111 \to b = 1 \\ \tau 1 \tau \to b = 2 \end{cases}, \quad \tau\text{-block}: \begin{cases} 1\tau\tau \to b = 3 \\ \tau\tau 1 \to b = 4 \\ \tau\tau\tau \to b = 5 \end{cases}. \tag{3.70}$$

The same conventions hold for the external MPO indices. We will be freely switching between the string-net and grouped indices, and the transformations are given in eq. 3.70. The fusion tensors are given by

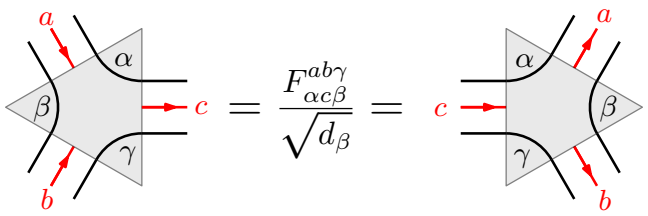

(3.71)

We take the convention that for every closed loop with some Greek index α we multiply by a factor of d_α, in line with [39] but in contrast to [6] where these factors of quantum dimensions were included in the MPOs themselves. We will discuss this convention, that we will call the *closed loop convention*, as well as the factors of quantum dimensions appearing in eq. 3.69 and 3.71 in more detail in the next chapter.

3.5.2 Central idempotents

An algorithm to find the central idempotents of the anyon ansatz algebra is presented in [6]. We will not elaborate on the details and merely give the results for the Fibonacci fusion category. There are 7 non-zero basis elements

$$A_{1111}, A_{\tau\tau\tau 1}, A_{1\tau 1\tau}, A_{1\tau\tau\tau}, A_{\tau 1\tau\tau}, A_{\tau\tau 1\tau}, A_{\tau\tau\tau\tau} \tag{3.72}$$

so we expect the algebra to be 7-dimensional. The central idempotents are found to be

$$\mathcal{P}_1 = \frac{1}{\sqrt{5}}\left[\frac{1}{\phi}A_{1111} + \sqrt{\phi}A_{1\tau 1\tau}\right], \tag{3.73}$$

$$\mathcal{P}_2 = \frac{1}{\sqrt{5}}\left[\frac{1}{\phi}A_{\tau\tau\tau 1} + \frac{1}{\sqrt{\phi}}e^{-\frac{4\pi i}{5}}A_{\tau 1\tau\tau} + e^{\frac{3\pi i}{5}}A_{\tau\tau\tau\tau}\right],$$

$$\mathcal{P}_3 = \frac{1}{\sqrt{5}}\left[\frac{1}{\phi}A_{\tau\tau\tau 1} + \frac{1}{\sqrt{\phi}}e^{\frac{4\pi i}{5}}A_{\tau 1\tau\tau} + e^{-\frac{3\pi i}{5}}A_{\tau\tau\tau\tau}\right],$$

$$\mathcal{P}_4 = \frac{1}{\sqrt{5}}\left[\phi A_{1111} + A_{\tau\tau\tau 1} - \sqrt{\phi}A_{1\tau 1\tau} + \sqrt{\phi}A_{\tau 1\tau\tau} + \frac{1}{\phi}A_{\tau\tau\tau\tau}\right].$$

The central idempotents $\mathcal{P}_1, \mathcal{P}_2, \mathcal{P}_3$ are one-dimensional, in that they can not be decomposed further into irreducible non-central idempotents. The idempotent $\mathcal{P}_4$ however is two-dimensional, and it can be written as $\mathcal{P}_4 = \mathcal{P}_{4,1} + \mathcal{P}_{4,\tau}$ with $\mathcal{P}_{4,1}$ and $\mathcal{P}_{4,\tau}$ two non-central idempotents given by

$$\mathcal{P}_{4,1} = \frac{1}{\sqrt{5}}\left[\phi A_{1111} - \sqrt{\phi}A_{1\tau 1\tau}\right], \tag{3.74}$$

$$\mathcal{P}_{4,\tau} = \frac{1}{\sqrt{5}}\left[A_{\tau\tau\tau 1} + \sqrt{\phi}A_{\tau 1\tau\tau} + \frac{1}{\phi}A_{\tau\tau\tau\tau}\right]. \tag{3.75}$$

A d-dimensional idempotent projects onto a d^2 dimensional subspace, so that we have $1^2 + 1^2 + 1^2 + 2^2 = 7$, which is indeed the dimension of the algebra. We conclude by giving the topological spins associated to these idempotents calculated with eq. 3.60:

$$h_1 = 0, \quad h_2 = -\frac{2}{5}, \quad h_2 = \frac{2}{5}, \quad h_2 = 0. \tag{3.76}$$

These topological sectors can be identified with the *quantum double* [21] of the Fibonacci category [41]. This is a general feature for modular categories [42, 43], and this will turn out to be relevant in the CFT continuum limit of these models where we identify the idempotents with the product of 2 characters.

Chapter 4

Non-unitary fusion categories

The central question of this thesis is whether the formalism described in the previous chapter can be extended to include non-unitary fusion categories. These nUFCs are intimately related to non-unitary CFT [1], and one such connection is made in the next chapter by the use of a strange correlator [40]. Besides from their theoretical interest, non-unitary CFTs find application in the description of critical points in certain statistical mechanics models, with one prominent example being percolation described by a CFT with vanishing central charge [44, 45]. We discuss two applications of nUFCs in the next chapter.

4.1 Yang-Lee fusion category

We will use the simplest nUFC as a proxy for verifying the MPO formalism for these types of categories. It is known as the Yang-Lee fusion category, and its CFT counterpart, known as the *Yang-Lee edge singularity*, appears in the 2D classical Ising model with complex magnetic field [12]. This CFT is well studied, and we will be able to use the CFT literature for verifying the predictions made by the MPO formalism. it should be stressed that all results have been obtained by using the Yang-Lee fusion category as an example, and that the proposed modifications have only been validated for this simple category, but are expected to be valid for a broader range of nUFCs.

4.1.1 Weights and F-symbols

As mentioned in the description of the Fibonacci fusion category, it has an equally simple non-unitary counterpart that we will use to investigate the PMPO description for nUFCs. The fusion rules for this category are identical to those of the Fibonacci category, but

[1] Also called logarithmic CFT in some contexts.

both the pentagon equation and the equation that determines the weights admit a second solution that will give us non-unitary F-symbols and one negative weight. In more abstract terms, the Fibonacci category is one of two models described by the integer subset of the quantum deformed group $\mathrm{su}(2)_k$. The F-symbols for the $\mathrm{su}(2)_k$ theory are calculated in [46] as generalisations of the Wigner-6j symbols and are given for $\mathrm{su}(2)_3$ by [37]

$$F^{\tau\tau\tau}_{\tau ef} = \begin{pmatrix} \frac{1}{q^{-1}+1+q} & \frac{1}{\sqrt{q^{-1}+1+q}} \\ \frac{1}{\sqrt{q^{-1}+1+q}} & \frac{q^{-1}-1+q}{q^{-1}+q} \end{pmatrix}, \tag{4.1}$$

where $q = e^{\frac{2\pi i}{5}}$ and $q = e^{\frac{4\pi i}{5}}$, both roots of $q^5 = 1$, correspond to the Fibonacci and Yang-Lee fusion category respectively. For the Fibonacci case, this result corresponds to the symmetric F-symbol we used in the previous chapter where it was given in terms of the golden ratio ϕ. Similarly, we can express the Yang-Lee F-symbol as

$$F^{\tau\tau\tau}_{\tau ef,\mathrm{YL}} = \begin{pmatrix} -\phi & i\sqrt{\phi} \\ i\sqrt{\phi} & \phi \end{pmatrix} \tag{4.2}$$

and we see that going from the Fibonacci to the Yang-Lee F-symbol comes down to the transformation

$$\phi \to -\frac{1}{\phi} \equiv \phi', \tag{4.3}$$

where ϕ' is also a root of eq. 3.65. Both in transforming between the two values for q and as in eq. 4.3 we go from one root of an algebraic equation to another. This process is known as *Galois conjugation* [37, 38], and we say that the Fibonacci and Yang-Lee fusion categories are Galois conjugates of one another. The Yang-Lee F-symbol is still symmetric, but it is no longer unitary,

$$\left(F^{\tau\tau\tau}_{\tau ef,\mathrm{YL}}\right)^\dagger F^{\tau\tau\tau}_{\tau ef,\mathrm{YL}} \neq \mathbb{1}, \tag{4.4}$$

which is why we refer to it as a non-unitary fusion category. The equation that defines the weights, eq. 3.30, also admits another solution that also can be written in terms of ϕ':

$$w_1 = \frac{1}{1+\phi'^2}, \quad w_\tau = \frac{\phi'}{1+\phi'^2}, \tag{4.5}$$

where w_τ is negative, also an indicator of nUFCs. If we define the right-handed MPOs in the same way as for the Fibonacci case, but with the Yang-Lee F-symbol, we find that they still satisfy the algebra on the level of the MPOs:

$$O_1 O_1 = O_1, \quad O_1 O_\tau = O_\tau O_1 = O_\tau, \quad O_\tau O_\tau = O_1 + O_\tau, \tag{4.6}$$

which is ultimately due to the fact that ϕ and ϕ' have the same algebraic properties. This is certainly reassuring in our attempt to describe a nUFC in the PMPO formalism. In

the previous chapter, we already hinted to the modifications that will need to be made to accommodate these non-unitary theories, and these modifications are the subject of the following sections.

4.1.2 Hermiticity of the PMPO

In the previous chapter we derived that imposing the PMPO to be Hermitian implied the existence of a gauge transformation between an MPO tensor $\bar{B}_a^{ji}$ and its Hermitian conjugate $B_{a^*}^{ij}$, written down explicitly in eq. 3.32. We will now show that this is no longer true for the Yang-Lee category. Two MPOs A and B are equivalent up to a gauge transformation on the virtual indices if and only if the transfer matrix

$$E(A,A) = \sum_{ij} A^{ij}\bar{A}^{ij} = \quad , \tag{4.7}$$

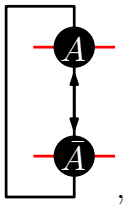

where the bar denotes complex conjugation, and the mixed transfer matrix

$$E(A,B) = \sum_{ij} A^{ij}\bar{B}^{ij} = \tag{4.8}$$

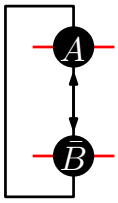

have the same eigenvalues [23]. The black arrows here do not have the interpretation of indicating handedness of the MPO (for this, an arrow on the internal MPO index would also be required), but merely indicate that we are using 1 MPO type (for our purpose, the right-handed Yang-Lee MPO tensor) and we have rotated one of them 180°. We have verified that the eigenvalues of the regular and the mixed transfer matrices are indeed equal for the Fibonacci MPO tensors, but not for the Yang-Lee MPO tensors, from which we conclude that we can not demand the PMPO to be Hermitian.

4.1.3 Symmetric PMPOs

In the previous chapter we used the Hermiticity of the PMPO to derive the existence of left- and right-handed MPOs. For the Fibonacci model, taking the Hermitian conjugate simply amounts to taking the transpose due to the fact that for this model all the F-symbols are real. Inspired by this, we require the PMPO to be symmetric instead of Hermitian:

$$(P_L)^T = P_L \tag{4.9}$$

which for each label a requires the existence of a label a^* such that

$$w_a = w_{a^*},$$
$$\left(O_a^L\right)^T = O_a^L.$$

This now implies that the tensors building up $\left(O_a^L\right)^T$ and O_a^L are related by a gauge transformation Z_a, which for the Yang-Lee category turns out to be the same as the gauge transformation for the Fibonacci category.

4.1.4 MPO-injective PEPS

We thus propose the following form for the left-handed MPOs; given that the right-handed MPOs are still given by

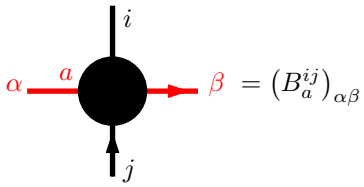

$= \left(B_a^{ij}\right)_{\alpha\beta}$, (4.10)

we now define the left-handed types to be the transpose on the physical indices of the right-handed type,

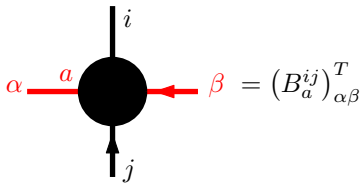

$= \left(B_a^{ij}\right)^T_{\alpha\beta}$. (4.11)

Equipped with this new notion of right- and left-handed MPOs, and the gauge transformation Z_a between them, we can investigate the other assumptions needed to construct MPO-injective PEPS. The first of these was that the zipper condition holds, which is still the case for the Yang-Lee category since the zipper equation for string-net models is really the pentagon equation in disguise. The second assumption, that there exists a gauge on the internal MPO indices such that the fusion tensors are isometries, has to be dropped and eq. 3.42 has to be replaced by

$$X_{ab}^{c+} = \left(X_{ab}^c\right)^T, \tag{4.12}$$

and in this gauge the gauge matrices are now orthogonal instead of unitary. The final property we need is the pivotal structure; we find that the Yang-Lee fusion tensors do indeed satisfy the pivotal property with the gauge matrices proposed above, with the change that eq. 3.45 has to be modified to

$$\left(A_{ab}^c\right)^2 = \frac{w_c}{w_b} \tag{4.13}$$

As already noted, these gauge matrices are the same for both the Fibonacci and Yang-Lee models, and in the convention of eq. 3.70, these gauge matrices are given by

$$Z_1 = \begin{pmatrix} 1 & 0 \\ 0 & 1 \end{pmatrix}, \quad Z_\tau = \begin{pmatrix} 0 & 1 & 0 \\ 1 & 0 & 0 \\ 0 & 0 & 1 \end{pmatrix} \tag{4.14}$$

which graphically amounts to switching the outer 2 lines, which can also be seen in (3.69). With this we have all the elements to prove the pulling through property just like we did for the unitary case. We note that the pulling through equation always must involve both types of MPOs, for example in

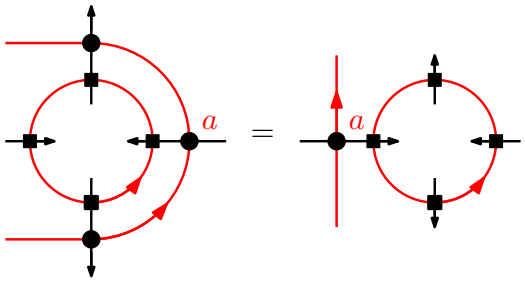

(4.15)

we have 3(4) right(left)-handed MPOs on the left hand side, and 2(3) right(left)-handed MPOs on the right hand side. We have verified this and all possible variations of this equation, which indicates that the new relation we proposed between the right- and left-handed MPOs is indeed correct.

4.1.5 Central Idempotents

Just like the for the unitary categories, the ground state tensors are still given by the support of the tensors A_{abcd} as defined in the previous chapters. These tensors still form an algebra for the Yang-Lee category, but it is no longer closed under Hermitian conjugation which means that it is no longer a $\mathcal{C}^*$ algebra. We can however still look for the irreducible representations of this algebra, i.e. the central idempotents, and associate topological sectors to these central idempotents.

For the Fibonacci case, these were given in eq. 3.73, and these were found using the algorithm described in [6]. We could use the same algorithm to find the central idempotents of the Yang-Lee model, but given its similarity to the Fibonacci model, we can guess that the structure of the central idempotents for the Yang-Lee model will be very similar. By using the structure factors of the algebra, we have an expression for any possible product of tensors A_{abcd} as a sum of the tensors A_{abcd} themselves. To illustrate, we write the Yang-Lee central idempotent $\mathcal{P}_1$ as

$$\mathcal{P}_1 = aA_{1111} + bA_{1\tau 1\tau} \tag{4.16}$$

We find the following expressions for A_{1111} and $A_{1\tau1\tau}$:

$$\begin{aligned}(A_{1111})^2 &= A_{1111},\\ (A_{1\tau1\tau})^2 &= (\phi'-1)\,A_{1111} + \frac{1}{\sqrt{\phi'}}A_{1\tau1\tau},\\ A_{1111}A_{1\tau1\tau} &= A_{1\tau1\tau}A_{1111} = A_{1\tau1\tau}.\end{aligned}$$

Requiring $\mathcal{P}_1^2 = \mathcal{P}_1$ and using the expressions above we find the following set of equations for a and b:

$$\begin{cases} a = a^2 + (\phi'-1)b \\ b = \dfrac{1}{\sqrt{\phi'}}b^2 + 2ab \end{cases} \tag{4.17}$$

which can easily be solved. For the other central idempotents, simply requiring them to be idempotent gives multiple solutions for the coefficients, and we have to include the condition that they are central to arrive at a unique solution. Doing so for the all central idempotents, we find

$$\mathcal{P}_1 = -\frac{1}{\sqrt{5}}\left[\frac{1}{\phi'}A_{1111} + \sqrt{\phi'}A_{1\tau1\tau}\right], \tag{4.18}$$

$$\mathcal{P}_2 = -\frac{1}{\sqrt{5}}\left[\frac{1}{\phi'}A_{\tau\tau\tau1} + \frac{1}{\sqrt{\phi'}}e^{-\frac{2\pi i}{5}}A_{\tau1\tau\tau} + e^{-\frac{\pi i}{5}}A_{\tau\tau\tau\tau}\right],$$

$$\mathcal{P}_3 = -\frac{1}{\sqrt{5}}\left[\frac{1}{\phi'}A_{\tau\tau\tau1} + \frac{1}{\sqrt{\phi'}}e^{\frac{2\pi i}{5}}A_{\tau1\tau\tau} + e^{\frac{\pi i}{5}}A_{\tau\tau\tau\tau}\right],$$

$$\mathcal{P}_4 = -\frac{1}{\sqrt{5}}\left[\phi'A_{1111} + A_{\tau\tau\tau1} - \sqrt{\phi'}A_{1\tau1\tau} + \sqrt{\phi'}A_{\tau1\tau\tau} + \frac{1}{\phi'}A_{\tau\tau\tau\tau}\right].$$

We again have 3 one-dimensional idempotents and 1 two-dimensional idempotent, corresponding to the 7-dimensional algebra. The topological spins associated to these idempotents are given by

$$h_1 = 0, \quad h_2 = -\frac{1}{5}, \quad h_2 = \frac{1}{5}, \quad h_2 = 0, \tag{4.19}$$

and we see that these results are consistent with the CFT literature [47], and this will also become evident in Chapter 5.

4.2 Mixing Fibonacci and Yang-Lee

We have obtained the Yang-Lee model by taking the Fibonacci model and replacing $\phi \to \phi'$ which gives us the Yang-Lee weights and the Yang-Lee MPOs as defined above. One could wonder if the pairing of the weights with the MPOs is unique, or in other

words, if the labelling of the weights by either "Fibonacci" or "Yang-Lee" is justified. After all, as long as the MPOs represent the fusion algebra and the weights satisfy eq. 3.30, the PMPO we construct with them will be a projector. We can not impose this PMPO to be Hermitian if we use the Yang-Lee MPOs, but this does not matter as we can simply replace it by the requirement to be symmetric since in the Fibonacci model this is equal to demanding Hermiticity due to the reality of the Fibonacci MPO tensors.

We would like to verify if, for example, the Fibonacci MPOs and the Yang-Lee weights can be used to build an MPO-injective PEPS. This mixing of the Fibonacci and Yang-Lee categories leads to a slight complication however: we are working in the string-net picture, with the closed loop convention. It is not immediately clear which fusion category's quantum dimensions we should be multiplying with in order for everything to be consistent. We therefore first investigate if we can find an alternative to this convention, and we will see that we can get rid of it altogether by a redefinition of the left-handed MPOs.

4.2.1 Closed loop convention

From a tensor network point of view, the need to artificially add a factor d_a for every closed loop seems somewhat unsatisfactory. In fact, the reason that the zipper condition holds is that for our string-net models it corresponds precisely to the pentagon equation, i.e.

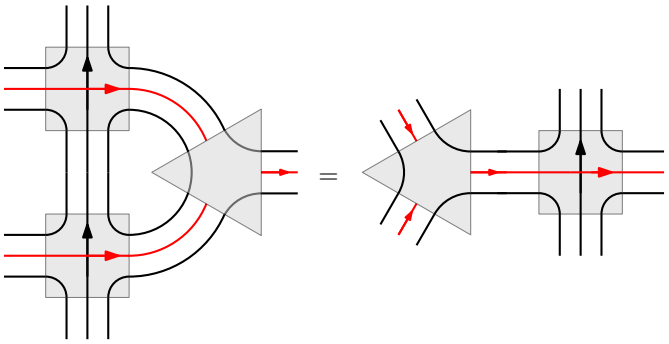

(4.20)

is really just eq. 3.40, with the loop on the left hand side being the summation index. We therefore know that, if we just use the F-symbols to define the MPOs and fusion tensors,

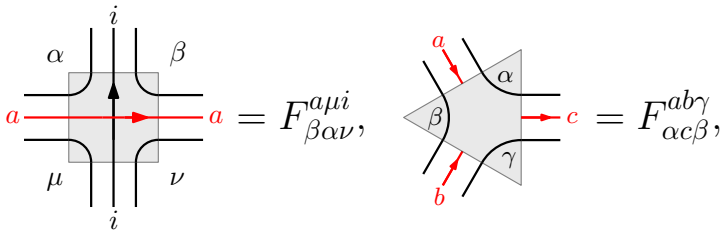

(4.21)

without the extra factors of quantum dimensions as in eqs. 3.69 and 3.71, these satisfy the zipper conditions, and consequently the MPOs also represent the fusion algebra. The question we now want to ask is if we can use the MPOs and fusion tensors defined in this way to build an MPO injective PEPS. For this we need the pivotal property to hold, and we find that it can only be satisfied for the fusion tensors in eq. 4.21 if the gauge matrices are of the form

$$Z_1 = \begin{pmatrix} 1 & 0 \\ 0 & 1 \end{pmatrix}, \quad Z_\tau = \begin{pmatrix} 0 & 1/\sqrt{d_\tau} & 0 \\ \sqrt{d_\tau} & 0 & 0 \\ 0 & 0 & 1 \end{pmatrix}. \tag{4.22}$$

The gauge matrix Z_τ is no longer unitary/orthonormal, nor are the fusion tensors isometries/symmetric for the UFC/nUFC case respectively, but if we ignore this and use it to define a left-handed MPO, we find again that all the possible pulling through equations are satisfied. The PMPO is no longer symmetric with these right-handed MPOs, which ultimately explains why the right- and left-handed MPOs are no longer connected by a true gauge transformation. We note that we still use Z_a and $(Z_a)^T$ to define the left-handed MPO, but that $(Z_a)^T \neq (Z_a)^{-1}$, so we are abusing the term "gauge matrix" and we will simply call them transformation matrices.

We conclude then that when we drop the convention of multiplying by quantum dimensions for closed loops, the quantum dimensions sneak their way into the transformation matrices, or equivalently in the definition of the left-handed MPOs. We have verified that these left-handed MPOs also satisfy the fusion algebra, which no longer trivially follows from the algebra of the right-handed MPOs due to the fact that these two are no longer related by a gauge transformation.

4.2.2 Pulling through equation

In the previous section we have compensated for the lack of loop counting by including the quantum dimensions in the gauge matrices. This change in transformation matrices was imposed by requiring that the pivotal property holds for the new fusion tensors without quantum dimensions in their definition. In proving the pulling through property, we used that the matrices A^C_{ab} satisfy eq. 4.13, which gives us a connection between the fusion tensors and the weights. One could wonder however whether eq. 4.13 can be modified by changing the transformation matrices, just as we accommodated for the lack of loop

counting in the previous section. To verify this, we look at

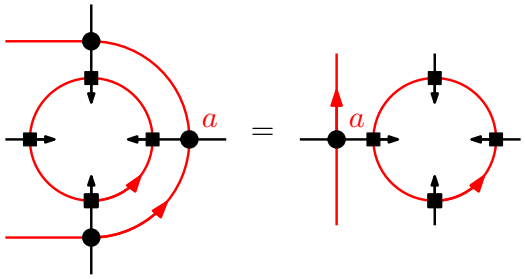

(4.23)

This is one of many pulling through equations, but its proof is independent of the handedness of the MPOs, and so it should hold for all of them. The advantage of this particular choice is that this is a linear equation in the left-handed MPO, and assuming that we know the right-handed MPO we can solve for the left-handed MPO and ultimately the transformation matrices. We find

1. For the Fibonacci weights and Fibonacci MPOs, we find the left-handed Fibonacci MPO tensor as defined above

2. For the Yang-Lee weights and Yang-Lee MPOs, we find the left-handed Yang-Lee MPO tensor as defined above

3. For the Yang-Lee weights and the Fibonacci MPOs, this equation has no solutions for the left-handed MPO

4. For the Fibonacci weights and the Yang-Lee MPOs, this equation has no solutions for the left-handed MPO

We conclude that the pulling through equation excludes the mixing of the Fibonacci and Yang-Lee models, and that the names "Fibonacci/Yang-Lee weights" are indeed justified. It is remarkable that solving eq. 4.23 yields the exact left-handed tensor as we have been using it. This implies that we can really use the pulling through equation to define the left-handed MPO tensor, without requiring any Hermiticity or symmetry of the PMPO.

We end this section by noting that although the inclusion of quantum dimensions in the definitions of the MPOs and fusion tensors may seem cumbersome and the loop counting convention unnatural, it allows for a more symmetrical definition of the right- and left-handed MPO tensors related by a true gauge transformation. The description without loop counting is further complicated due to the need to define more types of fusion tensors depending on the input MPOs, again due to the lack of gauge transformation between right- and left-handed MPOs. In practical implementations it is therefore often easier to just use the loop counting convention; nevertheless, it is satisfying to know that at least for our purposes, we can get rid of this convention.

4.3 Other non-unitary fusion categories

As already mentioned, the results in this chapter were obtained solely by looking at the Yang-Lee fusion category. The main conclusion from this chapter is that, due to the reality of the F-symbols of the Fibonacci category we can replace the Hermiticity requirement of the PMPO by the requirement to be symmetric. The fact that this modification then also describes the Yang-Lee category is due to the fact that they are both solutions to the same pentagon equation and therefore have near identical algebraic properties.

In [6], the PMPO formalism is also applied for the Ising fusion category. This category has three labels, $\mathbf{1}, \boldsymbol{\psi}, \boldsymbol{\sigma}$, and is defined by the fusion rules

$$\begin{aligned} &\mathbf{1} \times \mathbf{1} = \mathbf{1}, \quad \mathbf{1} \times \boldsymbol{\psi} = \boldsymbol{\psi}, \quad \mathbf{1} \times \boldsymbol{\sigma} = \boldsymbol{\sigma}, \\ &\boldsymbol{\psi} \times \boldsymbol{\psi} = \mathbf{1}, \quad \boldsymbol{\sigma} \times \boldsymbol{\psi} = \boldsymbol{\sigma}, \quad \boldsymbol{\sigma} \times \boldsymbol{\sigma} = \mathbf{1} + \boldsymbol{\psi}. \end{aligned} \tag{4.24}$$

There are two unitary solutions to the pentagon equation characterised by their Frobenius-Schur indicator [22], and the choice in [6] corresponds to $\xi = +1$. Using an unpublished algoritm based on Gröbner basises [48], we can calculate all the solutions to the pentagon equation, unitary or not. We find that for the Ising category there are 4 solutions in total including the 2 unitary solutions described above, and 2 non-unitary solutions. The F-symbols corresponding to these non-unitary solutions are not invertible however, and therefore these do not describe a valid non-unitary solution.

The story is similar for other fusion categories. It seems then that non-unitary solutions to the pentagon equation with invertible F-symbols are quite scarce, and we have not found any examples besides the Yang-Lee category with which we can verify our results.

Chapter 5

Strange correlators

In this chapter we will apply our results for the Yang-Lee fusion category to the strange correlator construction of [40, 49]. We will first give a very superficial overview of the strange correlator method for mapping a topological PEPS wave function to a classical partition function. Consequently, we will describe and extend the results for the Fibonacci category in [40] for describing the so called *hard hexagon* model to the Yang-Lee category. Finally, we speculate that the hard square model, for which there is numerical evidence [50] that there exists a critical point at negative fugacity in the Yang-Lee universality class, can be described by a strange correlator using a Yang-Lee PEPS.

5.1 PEPS to classical partition functions

The idea of a strange correlator is that, given some wave function, we can act on the physical indices with a product state yielding a classical partition function. This idea was first introduced in [51] for symmetry protected topological order (SPT) states and extended in [40] to long-range entangled string-net wave functions. It is argued in [40] that the resulting partition function has to be either critical/gapless or symmetry broken. In some cases, the continuum limit of these critical partition functions is described by a CFT, and the properties of topological conformal defects have been shown to be very similar to those of virtual MPO symmetries and topological sectors [52, 53]. With this method we therefore have an explicit tensor network representation of these topological conformal defects and we are able to numerically calculate the conformal spectra in the presence of these topological conformal defects [54].

5.2 The hard hexagon model

The statistical model we consider here is the hard hexagon model. This model is defined on a hexagonal lattice of which the faces can be either occupied or not occupied by a particle with the restriction that no two adjacent faces can be occupied. This model was first introduced and analytically solved by Baxter [55] in 1980, who found that it was related to the Rogers-Ramanujan identities. The partition function of this model is given by

$$\mathcal{Z}(z) = \sum_n z^n g(n, N) = 1 + Nz + \frac{1}{2}N(N-7)z^2 + \dots \tag{5.1}$$

where

$$z = \exp\left(\frac{\mu}{kT}\right) \tag{5.2}$$

is the fugacity given some chemical potential μ and $g(n, N)$ gives the number of ways to place n particles on N hexagons such that no 2 particles are adjacent. The energy of all the allowed configurations is the same so that the only important thermodynamic control variable is the fugacity z. We define the function κ by

$$\kappa(z) = \lim_{N\to\infty} \mathcal{Z}(z)^{1/N} = 1 + z - 3z^2 + \dots \tag{5.3}$$

such that $\log(\kappa)$ is the free energy per site. The mean density is then given by

$$\rho = z\frac{d}{dz}\log\kappa(z) = z - 7z^2 + 58z^3 - 519z^4 + 4856z^5 + \dots \tag{5.4}$$

There are 3 different ways to maximally fill the lattice with hard hexagons that define 3 sub-lattices, corresponding local densities labelled ρ_1, ρ_2 and ρ_3. When the fugacity z is large, the system approximates one of the 3 maximal packings and the local densities differ, but when it is below a certain critical point the three local densities are the same. Baxter used the Rogers-Ramanujan identities to write an exact expression for κ as a function of z, and found that the critical point is given by

$$z_c = \frac{11 + 5\sqrt{5}}{2} = \phi^5 \tag{5.5}$$

where ϕ is again the golden ratio.

5.2.1 Fibonacci string-net

In Chapter 3, we derived the PEPS wave function for topological models where we represented the individual PEPS tensors as a closed loop of PMPOs. In this section, we use a different definition for the PEPS tensor used in [39], but we will show later that these

two are completely equivalent. We define 2 types of Fibonacci string-net PEPS tensors on a hexagonal lattice as

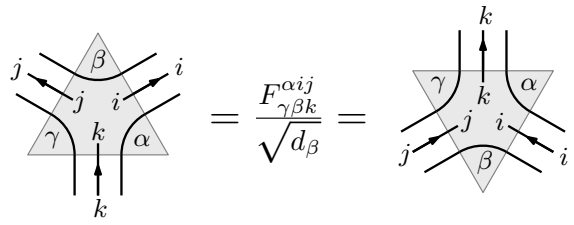

(5.6)

where the physical indices correspond to i, j, k and the F symbols are the ones defined in Chapter 3. Together these 2 trivalent tensors can be used to build up a hexagonal lattice. Note that these are very similar to the fusion tensors defined in Chapter 3, and that the pulling through equation for these PEPS tensors is again really the pentagon equation. To obtain the partition function for the hard hexagon model, we now project the physical i, j, k indices onto the τ label by taking the overlap of the PEPS with a suitable product state. The result is a number, given by the contraction of the PEPS tensor network while summing over all possible loop configurations. Given the fusion rules of the Fibonacci category and because we projected all the physical indices to the τ label, we see that this implies that no two adjacent loops can have value 1. If we now interpret the loops as the faces of the hard hexagon model, a 1 loop as a particle and the τ loop as an empty face, we see that we have constructed the partition function of the hard hexagon model where the sum over all loop configurations is precisely the sum over all valid hard hexagon configurations. As already mentioned, it was shown in [40] that this partition function is either critical or symmetry broken; we will find that it is critical, which means that the fugacity assigned to a 1 loop in this strange correlator construction of the partition function corresponds to the critical fugacity. Explicitly evaluating the possible tensors, we get

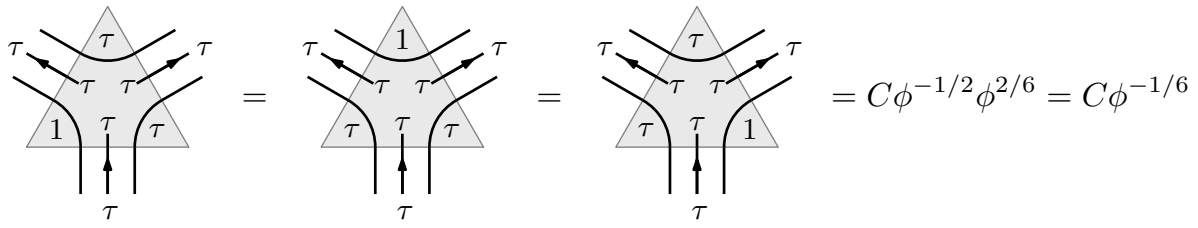

(5.7)

for tensors surrounding a face containing a particle, and

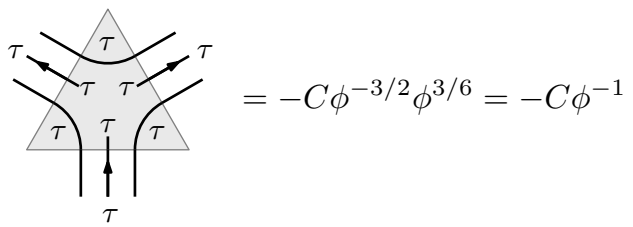

(5.8)

for tensors that do not. We have already included the closed loop convention in the tensors themselves by multiplying by a factor of $\phi^{1/6}$ for every $1/6^{\text{th}}$ of a τ valued loop. The second type of tensors, the right hand side of eq. 5.6, are the same. The multiplication by a constant C preserves the pulling through property, and we can fix it by requiring that an empty lattice configuration has a contribution of 1 to the partition function; we find $C = \phi$ so that the tensor A_τ in eq. 5.8 is equal to -1. The positivity of the Boltzmann weights is guaranteed by the fact that in any valid hard hexagon configuration, the negative tensors must always come in pairs. For the tensors T_1 in eq. 5.7 we get $A_1 = \phi^{5/6}$, and noting that every occupied face is surrounded by 6 such tensors, we find for the critical fugacity

$$z_c = (A_1)^6 = \phi^5 \tag{5.9}$$

which corresponds to the result obtained by Baxter [55] by vastly more complicated methods. It is remarkable that this simple ansatz gives the correct critical fugacity, and it is not unreasonable to hope that this strange correlator mapping of topological PEPS to partition functions will provide new insights in certain statistical mechanics models.

To make the connection with results from CFT, we consider again eq. 2.78 for the partition function on a torus, following [19]. Assuming equal holomorphic and anti-holomorphic central charges, we find

$$\begin{aligned} Z &= \operatorname{Tr} \mathrm{e}^{-2\pi \mathrm{Im}(\tau) H + 2\pi i \mathrm{Re}(\tau) P} \\ &= \operatorname{Tr} \mathrm{e}^{-2\pi \mathrm{Im}(\tau)(L_0 + \bar{L}_0 - \frac{c}{12}) + 2\pi i \mathrm{Re}(\tau)(L_0 - \bar{L}_0)} \\ &= \sum_\alpha \mathrm{e}^{-2\pi \mathrm{Im}(\tau)\left(h_\alpha + \bar{h}_\alpha - \frac{c}{12}\right) + 2\pi i \mathrm{Re}(\tau)(h_\alpha - \bar{h}_\alpha)} \\ &= \sum_\alpha \mathrm{e}^{-2\pi \mathrm{Im}(\tau)\left(\Delta_\alpha - \frac{c}{12}\right) + 2\pi i \mathrm{Re}(\tau) s_\alpha} \end{aligned} \tag{5.10}$$

where we have used $\Delta_\alpha = h_\alpha + \bar{h}_\alpha$ and $s_\alpha = h_\alpha - \bar{h}_\alpha$ for the scaling dimensions and the conformal spin respectively, and the sum runs over all the primaries and their descendants. It was shown in [54, 56] that this partition function can be written on a lattice as

$$Z = \operatorname{Tr}(M^{L_x}), \tag{5.11}$$

with M the column-to-column transfer matrix where we neglected effects of finite-size scaling

$$M \approx \mathrm{e}^{aL_y} \sum_\alpha \mathrm{e}^{-\frac{2\pi}{L_y}\left(\Delta_\alpha - \frac{c}{12}\right)} |\alpha\rangle \langle\alpha| , \tag{5.12}$$

where L_x and L_y are the number of lattice sites in the x and y direction respectively, and a is a non-universal contribution corresponding to the free energy per site. We could extract the free energy by varying L_x and L_y while keeping their ratio fixed, and subsequently

rescale M such that the free energy factor disappears, but we will see that we can use a different approach. The partition function defined in terms of the transfer matrix M in eq. 5.11 has periodic boundary conditions without twisting of the torus, but the complete partition function in eq. 5.10 also includes twisted boundary conditions. The one-site shifts are generated by the momentum operator P, given in the lattice description by

$$T_1 = \mathrm{e}^{\frac{2\pi i}{L_y}P}. \tag{5.13}$$

Assuming translation invariance, this shift operator commutes with M, and its eigenvalues $\mathrm{e}^{\frac{2\pi i}{L_y}p_\alpha}$ are good quantum numbers. Because we have $P = L_0 + \bar{L}_0$, these momentum quantum numbers correspond to the conformal spin s_α. This means that in the lattice description, we can obtain the scaling dimensions and the conformal spins by diagonalising the matrices M_α and T. There is a short-cut to obtain both by diagonalising the product $T \cdot M$ instead, which has the eigenvalues

$$\lambda_\alpha = \mathrm{e}^{-\frac{2\pi}{L_y}\left(\Delta_\alpha - \frac{c}{12}\right) + \frac{2\pi i}{L_y}s_\alpha} \tag{5.14}$$

so that the modulus gives the scaling dimensions and the phase yields the conformal spin. In the above derivation, we assumed periodic boundary conditions, which corresponds to the case of no conformal defects. This means that we have

$$(T_1)^{L_y} = \mathbb{1} \tag{5.15}$$

so that the momenta (or conformal spins) have to be integers. We can also however consider the following object:

$T_a =$ 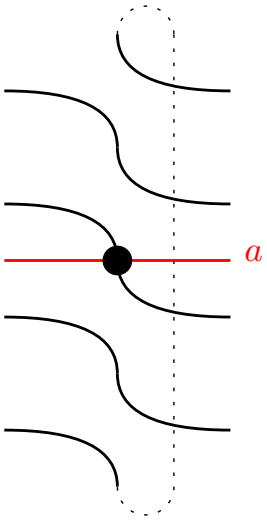

(5.16)

where we have inserted a defect of type a (much like in Appendix A.1), and the twisting action of T introduces an MPO tensor with label a where the lines cross. We define the *Dehn twist* operator D_a as

$$D_a \equiv (T_a)^{L_y} \tag{5.17}$$

which corresponds to cutting the torus into a cylinder, twisting one of its ends and gluing it back together. We already encountered this operator as the matrix that contains information on the topological spin, and its effect is to introduce topological corrections to the conformal spin. For the hard hexagon model, we can either insert a 1 (which corresponds to no defect) or a τ defect. The spectra are shown in 5.1 for the 1 and τ defect respectively, and the eigenvalues have been labelled by projecting the transfer matrices onto the different topological sectors given by the central idempotents and labelling them by their topological spins. The spectra are consistent with a subset of the minimal model $\mathcal{M}(6,5)$ with central charge $4/5$, called the 3-state Potts model, corresponding to the trivial defect partition function $Z_{1|1}$ and the τ defect partition function $Z_{1|9}$ in [40, 57].

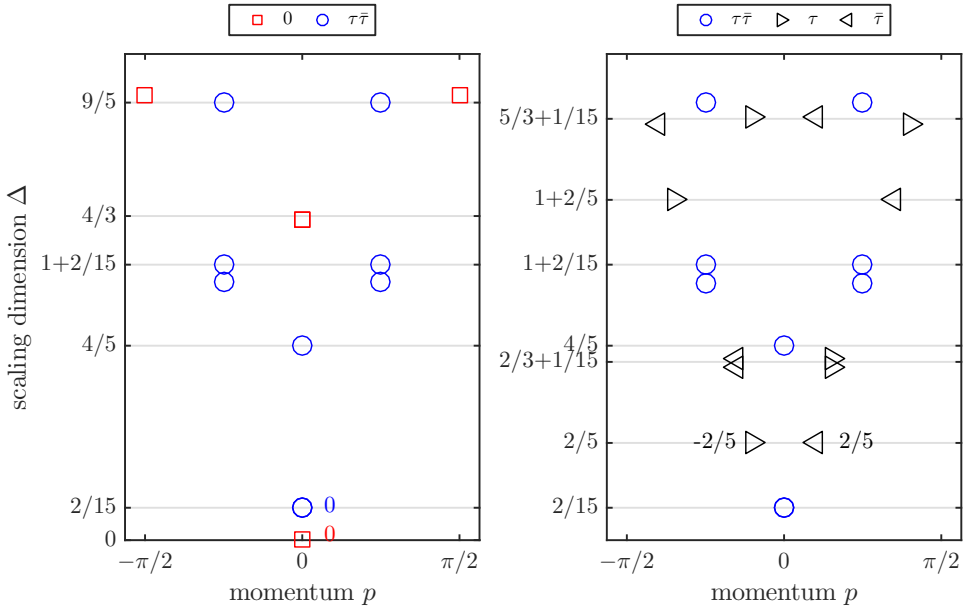

Figure 5.1: The Fibonacci spectra calculated by diagonalising $T \cdot M$ extrapolated from $L = 18, 21, 24$, without and with the presence of a τ defect on the left and right respectively [40]. The different topological sectors have been labelled by different symbols shown above the plots.

5.2.2 Yang-Lee string-net

In 1967 Gaunt [58] obtained a numerical value for the hard hexagon critical fugacity by using a series expansion for the local densities. He found

$$z_c = 11.05 \pm 0.15, \tag{5.18}$$

but observed that the function $\kappa(z)$ appeared to have another singularity at

$$z_{NP} = -0.0900 \pm 0.0003, \tag{5.19}$$

where the subscript NP indicates non-physical since a negative fugacity implies a complex chemical potential. Speculating that these two numbers are the roots of some simple quadratic equation, he formed their sum and product, yielding

$$\begin{aligned} z_c + z_{NP} &= 10.96 \pm 0.15 \\ z_c z_{NP} &= -0.995 \pm 0.014. \end{aligned} \tag{5.20}$$

He then guessed that these numbers might be exactly 11 and -1, which was shown by Baxter [55] to be exactly right. This means that $z_{NP} = -1/z_c$ is another critical fugacity [59], albeit non-physical. Looking at the exact expression we found for the fugacity z_c, we have

$$z_{NP} = -\frac{1}{\phi^5} \tag{5.21}$$

which corresponds precisely to the Galois conjugation of $\phi \to -1/\phi$. This result is precisely what we obtain if we apply the strange correlator formalism of the previous section to the Yang-Lee PEPS tensors instead of the Fibonacci PEPS tensors, using the same product state. We can again calculate the spectra for this partition function, shown in Figure 5.2. We find that the no-defect spectrum is consistent with the non-unitary

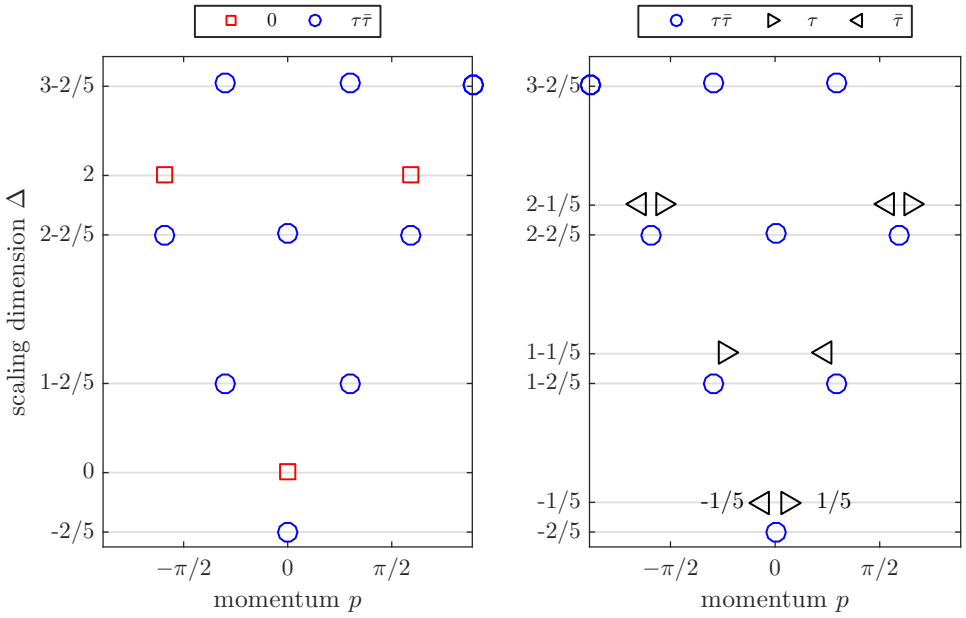

Figure 5.2: The Yang-Lee spectra calculated by diagonalising $T \cdot M$ for $L_y = 18$, without and with the presence of a τ defect on the left and right respectively. The different topological sectors have been labelled by different symbols shown above the plots, and the conformal spins $-1/5$ and $1/5$ are denoted next to their respective primaries.

minimal model $\mathcal{M}(5,2)$ with central charge $-22/5$, which we already encountered in

chapter 2, and this agrees with the results in [37]. The no-defect partition function is diagonal in the Virasoro characters and can be written as

$$Z_1 = |\chi_0(q)|^2 + |\chi_{-\frac{1}{5}}(q)|^2 \tag{5.22}$$

containing two primary fields usually labeled I and ϵ with conformal weights

$$I = (0,0)\,, \quad \epsilon = \left(-\frac{1}{5}, -\frac{1}{5}\right). \tag{5.23}$$

The partition function with a τ defect is not diagonal and is given by

$$Z_\tau = \chi_0(q)\chi_{-\frac{1}{5}}(\bar{q}) + \chi_{-\frac{1}{5}}(q)\chi_0(\bar{q}) + |\chi_{-\frac{1}{5}}(q)|^2, \tag{5.24}$$

which corresponds to the three primary fields found in [47] with conformal weights

$$\left(0, -\frac{1}{5}\right), \quad \left(-\frac{1}{5}, 0\right), \quad \left(-\frac{1}{5}, -\frac{1}{5}\right). \tag{5.25}$$

More details on the relation between the anyon ansatz algebra elements A_{abcd} and the Virasoro characters are given in Appendix B.1. In particular, we obtain the following relations:

$$A_{1111} \to |\chi_0(q)|^2 + |\chi_{-\frac{1}{5}}(q)|^2 = Z_1, \tag{5.26}$$

$$A_{\tau\tau\tau 1} \to \chi_0(q)\chi_{-\frac{1}{5}}(\bar{q}) + \chi_{-\frac{1}{5}}(q)\chi_0(\bar{q}) + |\chi_{-\frac{1}{5}}(q)|^2 = Z_\tau, \tag{5.27}$$

$$A_{1\tau 1\tau} \to \sqrt{\phi'}|\chi_0(q)|^2 - \phi'^{-3/2}|\chi_{-\frac{1}{5}}(q)|^2, \tag{5.28}$$

$$A_{\tau 1\tau\tau} \to \frac{1}{\sqrt{\phi'}}\left[e^{\frac{2\pi i}{5}}\chi_0(q)\chi_{-\frac{1}{5}}(\bar{q}) + e^{-\frac{2\pi i}{5}}\chi_{-\frac{1}{5}}(q)\chi_0(\bar{q}) + |\chi_{-\frac{1}{5}}(q)|^2\right], \tag{5.29}$$

$$A_{\tau\tau\tau\tau} \to e^{\frac{\pi i}{5}}\chi_0(q)\chi_{-\frac{1}{5}}(\bar{q}) + e^{-\frac{\pi i}{5}}\chi_{-\frac{1}{5}}(q)\chi_0(\bar{q}) + \frac{1}{\phi'^2}|\chi_{-\frac{1}{5}}(q)|^2. \tag{5.30}$$

From this we infer that A_{1111} and $A_{\tau\tau\tau 1}$ correspond to the no-defect and τ defect partition functions respectively, while the other 3 elements give different combinations of Virasoro characters that correspond to defects on the other non-contractible loop of the torus, which are usually not studied in the CFT literature [47].

5.3 Hard square model

The hard hexagon model can be interpreted as a square lattice with 2 types of diagonal interaction L and M [55], where we take $L = 0$ and $M = \infty$. The closely related

hard square model is obtained by setting $L = M = 0$, such that there are no diagonal interactions and the model can be formulated by stating that an occupied square forces the neighbouring squares with which it shares an edge to be empty. Unlike the hard hexagon model, the hard square model has not yielded to exact solution and is widely believed to be non-integrable [60]. Various numerical methods have been employed to obtain the critical fugacities for this model [61, 62], and investigations along the negative fugacity axis have yielded [50, 63]

$$z_c = -0.11933888188(1). \tag{5.31}$$

In [63] it is also found that the central charge and the dominant scaling dimension are

$$c = -4.399996(8), \quad \Delta = -0.3999996(7), \tag{5.32}$$

which strongly implies that this model lies in the Yang-Lee edge singularity universality class which has

$$c = \frac{22}{5}, \quad \Delta = -\frac{2}{5}. \tag{5.33}$$

It is therefore natural to wonder whether we can use the Yang-Lee topological PEPS description and map it to the hard square partition function at criticality using a strange correlator.

We first consider again the hard hexagon model. We used the topological PEPS on a hexagonal lattice as defined in eq. 5.6, but as we mentioned this PEPS is different from the one we used in Chapter 3, where we considered the following object instead:

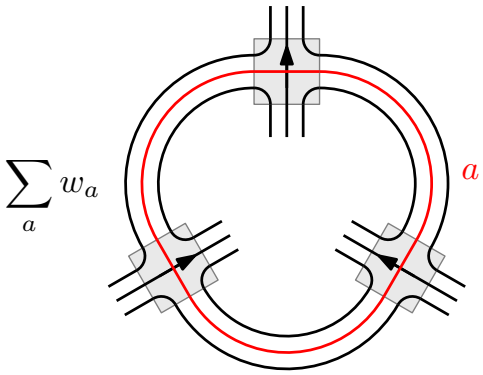

(5.34)

If we now fix the physical indices of this tensor to τ and interpret this as a matrix from the inner to the outer PMPO indices, we find that this matrix is rank 1 and its column space is given precisely by the tensor in eq. 5.6, showing that these two PEPS tensors are completely equivalent. The advantage of the PMPO definition is that the generalisation to any coordination number is straightforward, and in particular for coordination number

4 we have the following tensor:

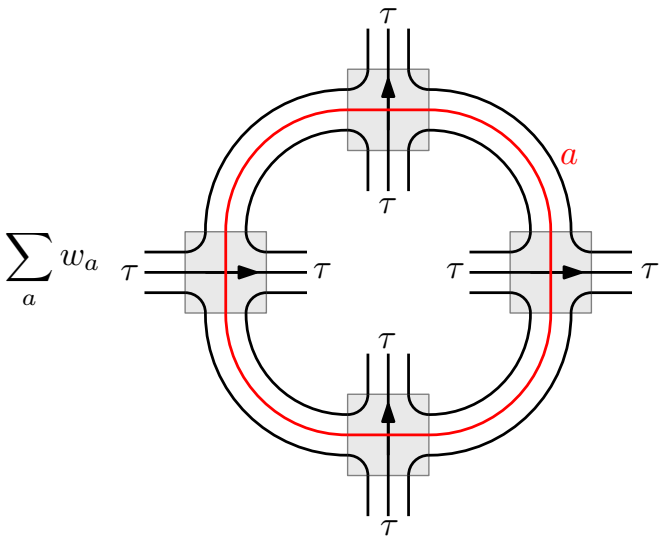

(5.35)

If we consider a square lattice with these tensors as building blocks, we see that the hard square condition is enforced in the same way as for the hard hexagon model. When interpreted as a matrix, this tensor is now rank 2 meaning that we have two degrees of freedom with which we can tune this tensor to obtain a partition function that assigns a Boltzman weight of z to every 1-valued loop. We have verified that the tensor in eq. 5.35 is completely equivalent to

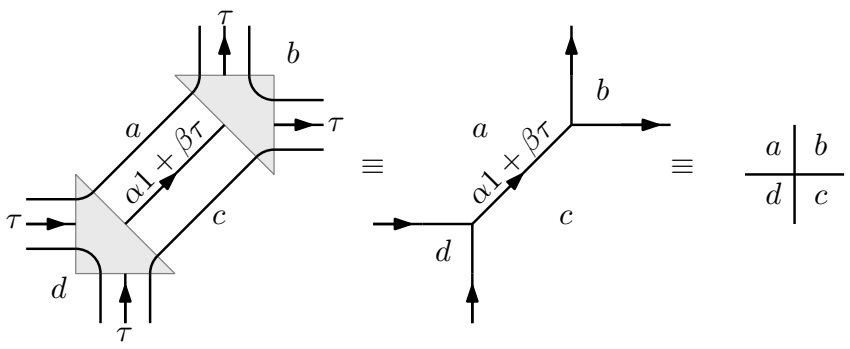

(5.36)

where α and β parametrise the two degrees of freedom of the 2 dimensional column space of the tensor in eq. 5.35 by fixing the physical index to $\alpha 1 + \beta\tau$, and the trivalent tensors are the same as the ones for the hard hexagon model defined in eq. 5.6. The variables a, b, c, d label the loops, and we also introduced two levels of notational simplification that we will use for the remainder of this chapter. We can construct a square lattice with this tensor by using a *truncated square* tiling, which is built out of octagons and squares which we both interpret as faces of the hard square lattice. A unit cell for this lattice

looks like

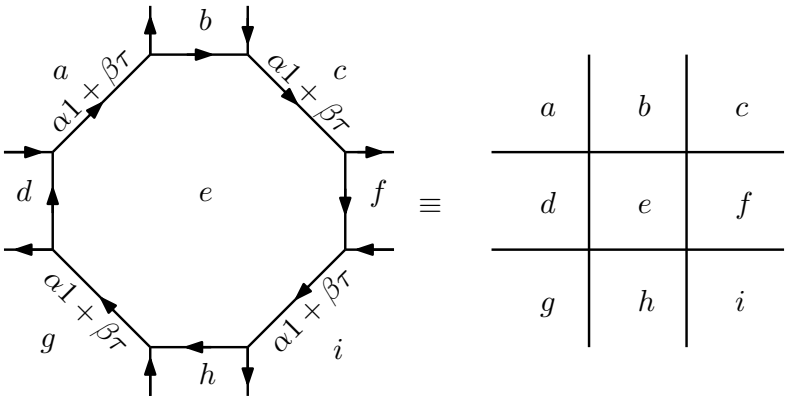

(5.37)

which is obtained by rotating and gluing together the tensors from eq. 5.36 and the variables $a, b, c, d, e, f, g, h, i$ label the loops. Because the unit cell tensor is built out of 4 copies of the same tensor, we can split it into smaller unit cell tensors and write the condition that every 1-valued loop should be weighed with a factor z on the level of these tensors as

$$\begin{array}{|c|c|}\hline \tau & \tau \\ \hline \tau & \tau \\ \hline \end{array} = 1, \quad \begin{array}{|c|c|}\hline 1 & \tau \\ \hline \tau & 1 \\ \hline \end{array} = \begin{array}{|c|c|}\hline \tau & 1 \\ \hline 1 & \tau \\ \hline \end{array} = z^{1/2},$$

$$\begin{array}{|c|c|}\hline \tau & \tau \\ \hline 1 & \tau \\ \hline \end{array} = \begin{array}{|c|c|}\hline 1 & \tau \\ \hline \tau & \tau \\ \hline \end{array} = \begin{array}{|c|c|}\hline \tau & 1 \\ \hline \tau & \tau \\ \hline \end{array} = \begin{array}{|c|c|}\hline \tau & \tau \\ \hline \tau & 1 \\ \hline \end{array} = z^{1/4} \tag{5.38}$$

which is a set of 7 algebraic equations for the three variables z, α, β, where the solution for z would yield the critical fugacity for the hard square model. Unfortunately, this set of equations has no solution. In the above construction we took the overlap of the Yang-Lee PEPS on a truncated square lattice with a product state that fixes the vertical and horizontal indices to τ to enforce the hard square condition, and the diagonal indices to $\alpha 1 + \beta\tau$ to obtain the correct Boltzmann weight. We showed that this does not yield the hard square partition function at criticality, but we can try to take the overlap of the PEPS with other states than the one we used. One possibility is allowing for the diagonal physical indices to be fixed to different values and taking a bigger unit cell tensor, i.e.

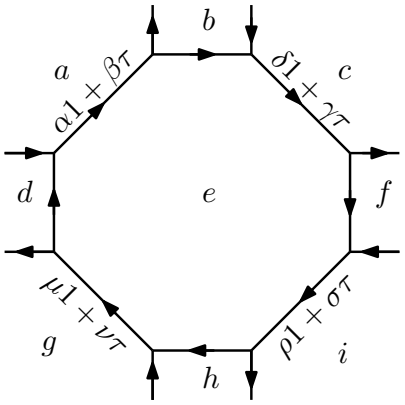

(5.39)

but this means that we can not impose the conditions of counting 1-valued loops on the level of the individual tensors, and we have to consider the entire unit cell tensor instead. The additional freedom we gain by using more parameters is compensated by the fact that the amount of conditions also increases due to the larger amount of possible hard square configurations on this unit cell tensor compared to eq. 5.38, and we again find that this set of equations has no solution. We can guess that this will be a general trend, and that the increased amount of parameters by increasing the unit cell size will be compensated by an increase in the amount of conditions that have to be satisfied, leading to contradictions. We can however try something more general than a product state, and place a tensor $A_{\alpha\beta\gamma\delta}$ at the center of the octagon with 4 indices corresponding to the 4 diagonal physical indices of the unit cell:

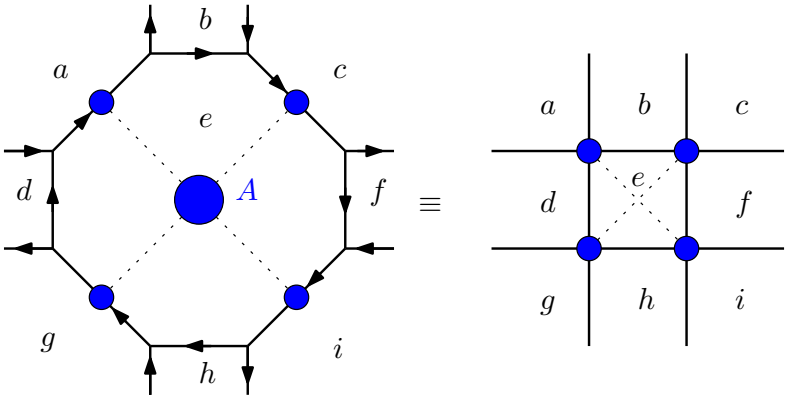

(5.40)

We could consider a general tensor A and write out all the valid hard square configurations of this unit cell to obtain the correct counting of the 1-valued loops, but given that there is some symmetry in these configurations we can be a bit more clever. We know that if we have one possible configuration, its image under the elements of the dihedral group D_4 [1] must also be an allowed configuration with the same Boltzmann weight assigned to it. This means that the tensor $A_{\alpha\beta\gamma\delta}$ should be invariant under D_4, and we can introduce a new tensor A_i with 6 degrees of freedom in which this invariance is manifest:

$$\begin{cases} A_1 \equiv A_{\tau\tau\tau\tau} \\ A_2 \equiv A_{1\tau\tau\tau} + A_{\tau 1\tau\tau} + A_{\tau\tau 1\tau} + A_{\tau\tau\tau 1} \\ A_3 \equiv A_{11\tau\tau} + A_{\tau 11\tau} + A_{\tau\tau 11} + A_{1\tau\tau 1} \\ A_4 \equiv A_{1\tau 1\tau} + A_{\tau 1\tau 1} \\ A_5 \equiv A_{111\tau} + A_{11\tau 1} + A_{1\tau 11} + A_{\tau 111} \\ A_6 \equiv A_{1111} \end{cases} \tag{5.41}$$

[1] D_4 is the symmetry group of the square consisting of 4 rotations (including the identity), 2 reflections along perpendicular bisectors and 2 reflections along the diagonal bisectors.

This means that we effectively have 6 degrees of freedom to tune the tensor A_i such that all hard square configurations will be given the correct Boltzmann weight. We find 19 remaining possible configurations that can not be transformed into each other under D_4, which implies that there are 19 conditions on the 6 degrees of freedom of A_i and the 1 fugacity parameter z. These configurations are given in Appendix B.2 together with their appropriate Boltzmann weight. We end up with an equation of the form

$$M \cdot A = Z \tag{5.42}$$

where M is a 19×6 matrix containing the unit cell tensor evaluated at every allowed configuration for the 6 elements of A_i, A is a 6×1 vector containing the 6 degrees of freedom of A_i, and Z is a 19×1 vector containing the appropriate Boltzmann weights (powers of the fugacity z) for each of the 19 allowed configurations. This looks like a standard problem in linear algebra, but the catch is that we do not know the vector Z, only that it is parametrized by 1 variable z. It is however fairly straightforward to check whether Z is in the image of M: we calculate a basis for this 6-dimensional column space by computing the row reduced echelon form of M^T. We can then try to write Z as a linear combination of these basis vectors, which very straightforwardly leads to a consistency condition on the coefficients and z due to the orthogonality of these basis vectors. Unfortunately, we find that the vector Z is not in the column space of M, which implies that we can not write the hard square partition function in this way. We should note that we have really only put tensors A_i on a checkerboard sublattice of the original lattice, as shown in Figure 5.3a; placing a tensor on every octagon of the lattice as in Figure 5.3b significantly complicates the conditions we have to impose on this tensor, and we have not yet found a way to do this.

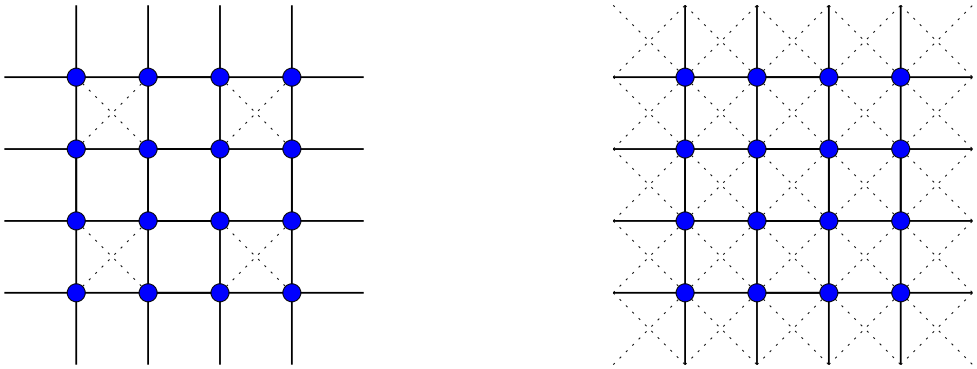

(a) (b)

Figure 5.3: The checkerboard configuration that we have been able to implement (a), and the full configuration for which it is unclear how to impose the conditions of the correct Boltzmann weights (b).

The difficulties in trying to write the hard square partition function as a strange correlator can be traced back to the fact that this model is believed to be not integrable, and we should therefore not expect to find an analytical expression for the critical fugacity in this way. One approach we can take is to calculate the value of z for which the vector Z is closest to the column space of M. We can then keep increasing the size of the unit cell tensor and perform such a fit for z at every step, and we might expect this value for z to grow closer to the exact critical fugacity. We have performed this procedure for the unit cell in 5.36, which yields a promising value of

$$z_c = -0.08073292780, \tag{5.43}$$

which is pretty close to the value $z_c = -0.11933888188(1)$ as calculated in [50]. Doing the same for the bigger unit cell however, we find

$$z_c = -0.00004828549551, \tag{5.44}$$

which is orders of magnitude worse. This is most likely due to the fact that this configuration breaks translation invariance due to its checkerboard-like structure. We expect to find some checkerboard structure in the hard square configuration but only at large enough occupation number, and the low value for z_c at criticality seems to indicate that this is not the case.

Conclusion and outlook

The main objective of this thesis was to verify whether the PMPO formalism for topological order could be extended to include non-unitary fusion categories. We used the Yang-Lee fusion category as a probe for these categories, and found that with some modifications based on the very similar Fibonacci category the PMPO formalism is indeed still valid. Based on the fact that we have the unitary and non-unitary version of the same category in the PMPO formalism, we make some remarks on the quantum dimensions of the theory and their relation to the MPOs. We also find indication that the notion of left and right MPOs arising from some constraint on the PMPO can be made more general by defining the relation between these two types via the pulling-through equation.

We verified our results for the Yang-Lee category by constructing the topological sectors associated to the doubled Yang-Lee model and more importantly, by mapping the Yang-Lee topological PEPS to the hard hexagon model using a strange correlator. We find a negative critical fugacity for this model that corresponds to the literature, but since it is non-physical it is mainly of theoretical interest. We find that at this critical fugacity the model is described by the Yang-Lee edge singularity CFT in the continuum limit by putting the lattice on a cylinder to calculate the partition function. We make the connection to recent work on topological conformal defects and in particular, we recover the correct CFT Virasoro primaries for both the no-defect and the τ defect spectra. Notably, we find all Virasoro primaries in the hard hexagon model at negative critical fugacity, in contrast to the Fibonacci case where we only recover a subset of the 3-state Potts CFT. This allows us to provide a mapping between the tube algebra elements of the topological model and the Virasoro characters, which might prove useful in further understanding the connection between topological and conformal field theory defects.

We also used the Yang-Lee topological PEPS to attempt to describe the non-integrable hard square model, given that it is known that there exists a critical point in the Yang-Lee universality class. We explored several options, one of which lead to a promising approximation of the correct critical fugacity, but more work should be done to make these

methods more rigorous and yield better approximations, which could provide a very concrete interpretation of integrable versus non-integrable models in statistical physics.

It is clear that the results for the Yang-Lee fusion category should be investigated for other non-unitary fusion categories to see if generalisations to the non-unitary PMPO formalism should be made. The modifications we made to accomodate for the Yang-Lee category were based on the similar algebraic properties between it and its unitary counterpart, which are ultimately inherited from the pentagon equation. The relation between other non-unitary categories and their unitary counterparts is similar, and we therefore expect that the modified PMPO formalism is general. We mentioned that these non-unitary fusion categories with invertible F-symbols seem to be quite scarce, but it is hard to imagine that these do not exist and we expect to find these solutions given that we have an algorithm to explicitly solve the pentagon equation [48].

The fact that we managed to map a tensor network to a non-unitary CFT opens the door to studying these CFTs using tensor networks. As we mentioned at the start of chapter 4, percolation is described by a non-unitary CFT. The study of percolation has already yielded new understanding and techniques not only in physics but also in materials science, complex networks, epidemics and many more. There remain a large amount of open problems in this field, and we hope that tensor networks can once more prove their usefulness by making progress on some of these issues.

Appendix A

The anyon ansatz

A.1 Ground state support

We begin by assuming that we work in a string-net model where $a^* = a$, such that we have [6]

$$N_{ab}^{c} = N_{ca}^{b} = N_{bc}^{a} \tag{A.1}$$

and that the weights are given by

$$w_a = \frac{d_a}{\mathcal{D}^2}, \quad \mathcal{D}^2 = \sum_a d_a^2. \tag{A.2}$$

It is proven in [27] and mentioned in Appendix A of [6] that the quantum dimensions satisfy the following equation:

$$d_a d_b = \sum_c N_{ab}^{c} d_c, \tag{A.3}$$

which can be rewritten in terms of the weights assuming that the trivial element has quantum dimension $d_1 = 1$ as

$$w_a w_b = w_1 \sum_c N_{ab}^{c} w_c. \tag{A.4}$$

We now prove the following identity:

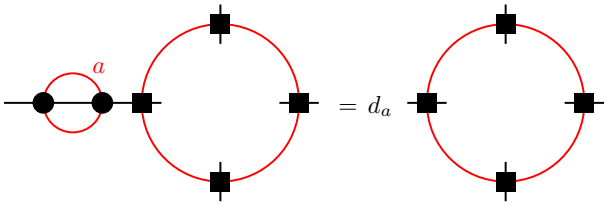

(A.5)

To do this, we first use the pulling through property to write this as

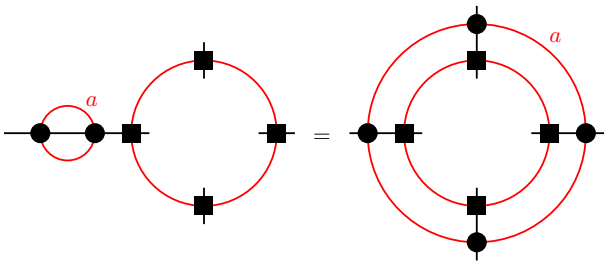

(A.6)

which we then write as

$$O_a P_L = O_a \sum_b w_b O_b = \sum_{b,c} N_{ab}^c w_b O_c = \frac{1}{w_1} w_1 \sum_{b,c} N_{ca}^b w_b O_c. \tag{A.7}$$

where we have used A.1, and we now use A.4 to find

$$\frac{w_a}{w_1} \sum_c w_c O_c = d_a P_L \tag{A.8}$$

which is what we set out to prove. We now consider an MPO-injective PEPS of arbitrary size on a cylinder with a general boundary condition tensor A:

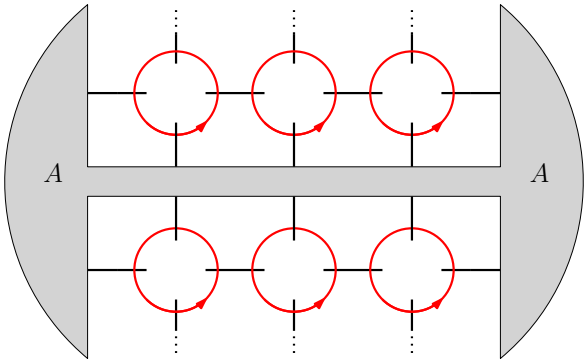

where the dots indicate periodic boundary conditions, and we have omitted the black boxes where the unlabelled red lines cross the black lines since we implicitly assume these are PMPOs. We now impose that locally this PEPS looks the same everywhere, which requires the boundary tensor where the two edges meet to have the property that it can be moved through the PEPS. We know that the tensors that can be moved freely through the lattice are precisely the MPO tensors, and so we get some linear combination of

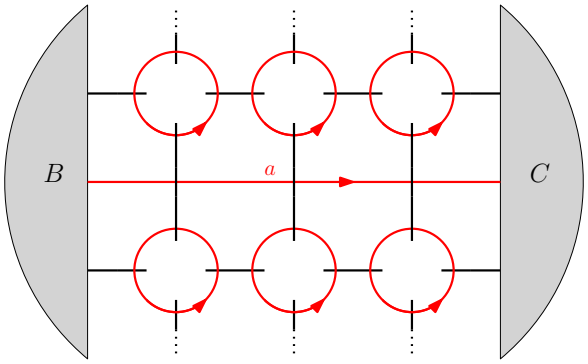

where we now have $A = \sum B \otimes C$, and we assume there are MPO tensors where the labelled red line crosses the black lines. We now use eq. A.5 to see that this is proportional to

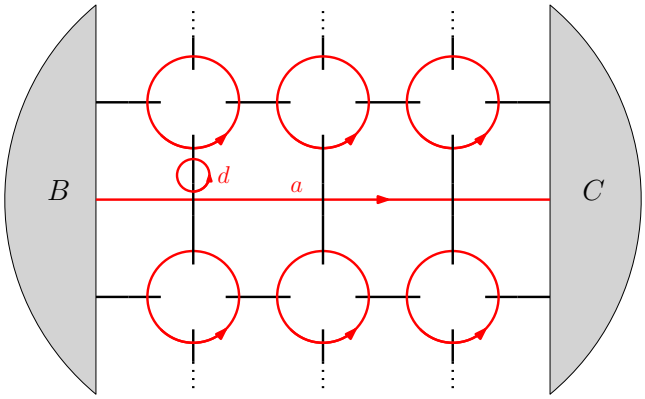

and we use the pulling through property to move this loop to the edge of the PEPS

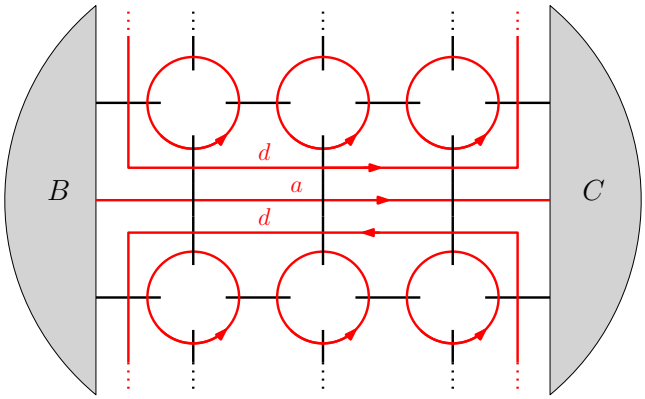

Using the zipper condition, we finally arrive at (summing over b and c)

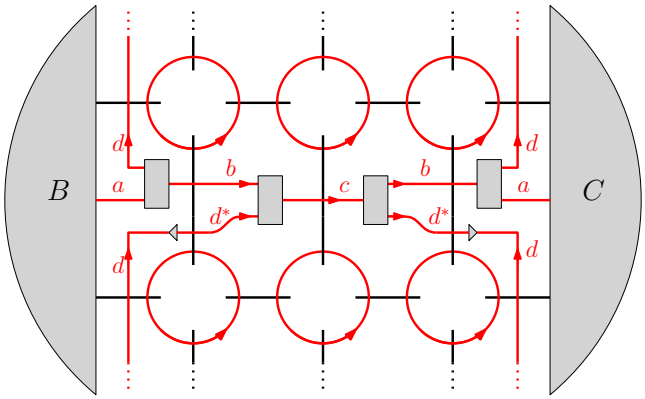

Here we recognise the tensor A_{abcd}, with the left tensor being the Hermitian transpose of the tensor on the right. We conclude that whatever the ground state PEPS tensor is, it must be supported by the tensors A_{abcd} when interpreted as matrices from the outer to the inner indices.

A.2 Closure of the algebra

The ground state support tensors A_{abcd} as derived in the previous section are proven to form an algebra in [6]. The proof requires the pivotal property for the fusion category, one of the assumptions needed for MPO-injective PEPS. Because of this property, we can write

$A_{abcd} =$ 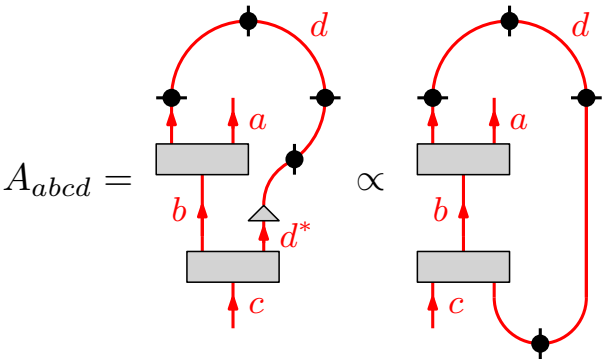

(A.9)

The right hand side of this equation can be used as an alternative definition of the tensors A_{abcd}, since the derivation above can yield both the left and right hand side of this equation. The benefit of using the right hand side is that we can prove it forms an algebra without the use of the pivotal property, and it is therefore more general in some sense; we don't need a pivotal structure in the fusion category. To do this, we first write

$A_{abcd}A_{efah} =$ 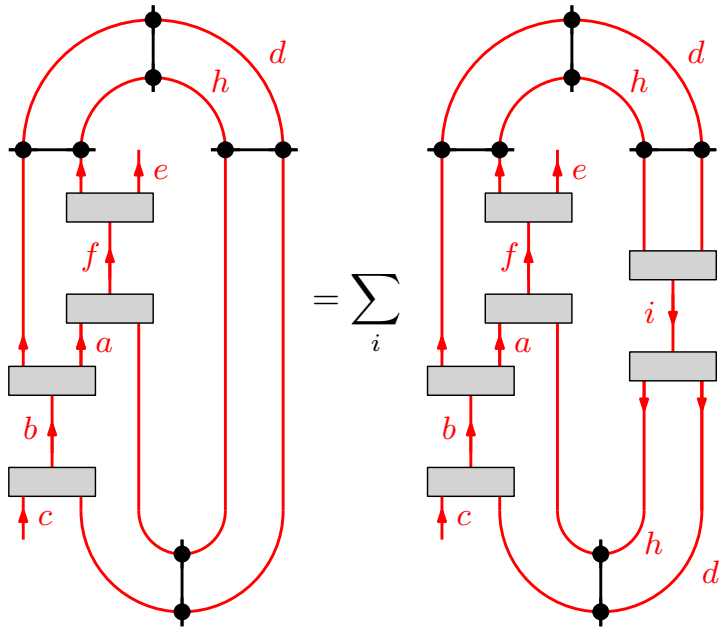

and then use the zipper condition to arrive at

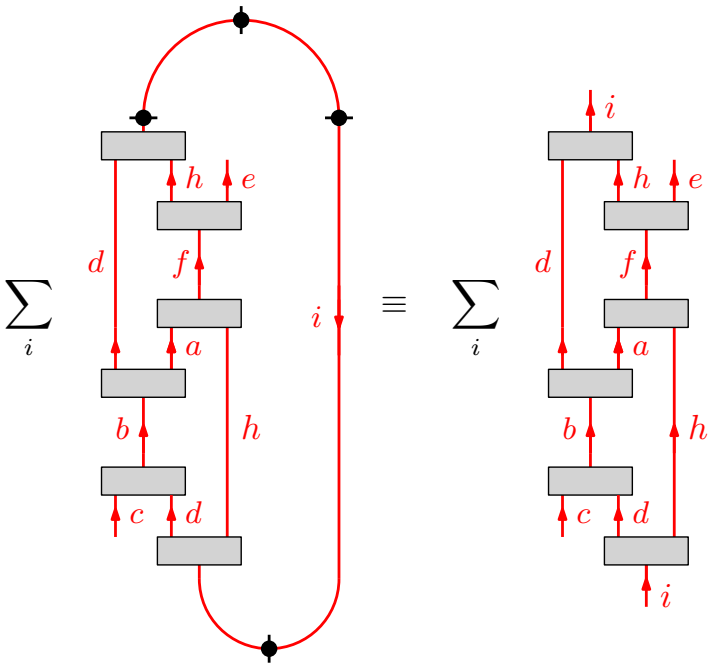

We will be omitting the MPOs for notational simplicity since they are not involved in the proof. We also take all the red arrows to be pointing upwards. Through repeated use of the zipper condition and F-moves we write

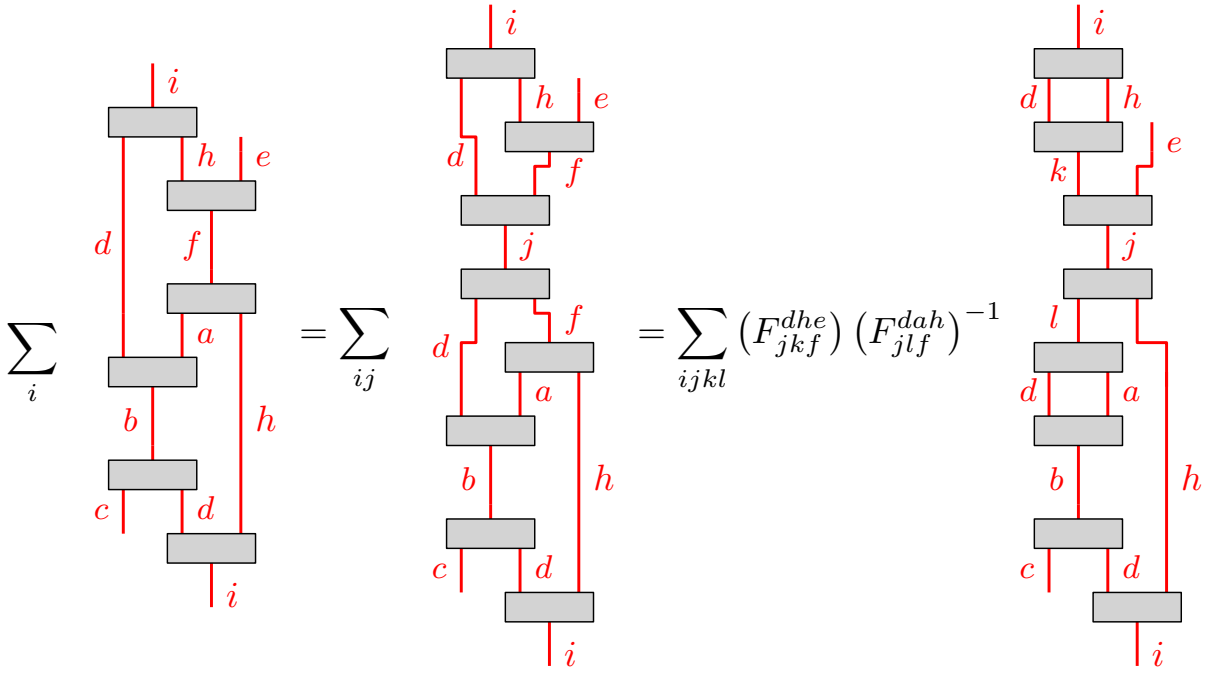

$$= \sum_{ij} \left(F^{dhe}_{jif}\right) \left(F^{dah}_{jbf}\right)^{-1}$$

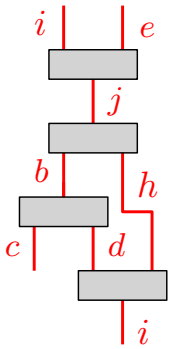

$$= \sum_{ij} \left(F^{dhe}_{jif}\right) \left(F^{dah}_{jbf}\right)^{-1} \left(F^{cdh}_{jbi}\right)$$

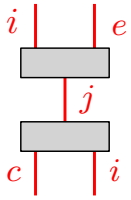

where the tensor on the right hand side is equal to A_{ejci}, which proves that the algebra is closed under multiplication. We have avoided using the pivotal property, which hints towards the fact that the pivotal property is really a consequence of the structure of the F-symbols, also pointed out in [6]. However, the pivotal property does hold for all the fusion categories (be it unitary or non-unitary) described in this thesis, and therefore this section mainly serves as an alternative proof to the one provided in the appendix of [6].

Appendix B

Strange correlator

B.1 Anyon ansatz and Virasoro characters

In this section we elaborate on the connection between the Yang-Lee anyon ansatz algebra elements A_{abcd} and the Yang-Lee CFT $\mathcal{M}(5,2)$. To reiterate, we have the following central idempotents identifying the topological sectors of the doubled Yang-Lee model:

$$\mathcal{P}_1 = -\frac{1}{\sqrt{5}}\left[\frac{1}{\phi'}A_{1111} + \sqrt{\phi'}A_{1\tau1\tau}\right], \tag{B.1}$$

$$\mathcal{P}_2 = -\frac{1}{\sqrt{5}}\left[\frac{1}{\phi'}A_{\tau\tau\tau1} + \frac{1}{\sqrt{\phi'}}e^{-\frac{2\pi i}{5}}A_{\tau1\tau\tau} + e^{-\frac{\pi i}{5}}A_{\tau\tau\tau\tau}\right],$$

$$\mathcal{P}_3 = -\frac{1}{\sqrt{5}}\left[\frac{1}{\phi'}A_{\tau\tau\tau1} + \frac{1}{\sqrt{\phi'}}e^{\frac{2\pi i}{5}}A_{\tau1\tau\tau} + e^{\frac{\pi i}{5}}A_{\tau\tau\tau\tau}\right],$$

$$\mathcal{P}_4 = -\frac{1}{\sqrt{5}}\left[\phi' A_{1111} + A_{\tau\tau\tau1} - \sqrt{\phi'}A_{1\tau1\tau} + \sqrt{\phi'}A_{\tau1\tau\tau} + \frac{1}{\phi'}A_{\tau\tau\tau\tau}\right].$$

where $\mathcal{P}_4$ is a two-dimensional central idempotent that can be written as the sum of two non-central idempotents

$$\mathcal{P}_{4,1} = -\frac{1}{\sqrt{5}}\left[\phi' A_{1111} - \sqrt{\phi'}A_{1\tau1\tau}\right], \tag{B.2}$$

$$\mathcal{P}_{4,\tau} = -\frac{1}{\sqrt{5}}\left[A_{\tau\tau\tau1} + \sqrt{\phi'}A_{\tau1\tau\tau} + \frac{1}{\phi'}A_{\tau\tau\tau\tau}\right]. \tag{B.3}$$

We see that when there is no conformal defect, we can only project with $\mathcal{P}_1$ and $\mathcal{P}_{4,1}$. From the no-defect spectrum in Figure 5.2, we make the identifications

$$\mathcal{P}_1 \to \chi_0(q)\chi_0(\bar{q}) \equiv |\chi_0(q)|^2, \tag{B.4}$$

$$\mathcal{P}_{4,1} \to \chi_{-\frac{1}{5}}(q)\chi_{-\frac{1}{5}}(\bar{q}) \equiv |\chi_{-\frac{1}{5}}(q)|^2, \tag{B.5}$$

which is consistent with the topological spins we derived for these topological sectors. When we insert a τ defect, we can only project onto $\mathcal{P}_2$, $\mathcal{P}_3$ and $\mathcal{P}_{4,\tau}$. From the τ defect spectrum in Figure 5.2, we make the identifications

$$\mathcal{P}_2 \to \chi_0(q)\chi_{-\frac{1}{5}}(\bar{q}), \tag{B.6}$$

$$\mathcal{P}_3 \to \chi_{-\frac{1}{5}}(q)\chi_0(\bar{q}), \tag{B.7}$$

$$\mathcal{P}_{4,\tau} \to \chi_{-\frac{1}{5}}(q)\chi_{-\frac{1}{5}}(\bar{q}) \equiv |\chi_{-\frac{1}{5}}(q)|^2, \tag{B.8}$$

which is again consistent with the topological spins of these topological sectors. Looking at the low-q expansions of the characters, we see that the spectrum in Figure 5.2 has the correct degeneracies. Given this identification of idempotents with Virasoro characters, we can write the idempotents in terms of the tube algebra elements A_{abcd} and invert these relations to obtain

$$A_{1111} \to |\chi_0(q)|^2 + |\chi_{-\frac{1}{5}}(q)|^2 = Z_1, \tag{B.9}$$

$$A_{\tau\tau\tau 1} \to \chi_0(q)\chi_{-\frac{1}{5}}(\bar{q}) + \chi_{-\frac{1}{5}}(q)\chi_0(\bar{q}) + |\chi_{-\frac{1}{5}}(q)|^2 = Z_\tau, \tag{B.10}$$

$$A_{1\tau 1\tau} \to \sqrt{\phi'}|\chi_0(q)|^2 - \phi'^{-3/2}|\chi_{-\frac{1}{5}}(q)|^2, \tag{B.11}$$

$$A_{\tau 1\tau\tau} \to \frac{1}{\sqrt{\phi'}}\left[e^{\frac{2\pi i}{5}}\chi_0(q)\chi_{-\frac{1}{5}}(\bar{q}) + e^{-\frac{2\pi i}{5}}\chi_{-\frac{1}{5}}(q)\chi_0(\bar{q}) + |\chi_{-\frac{1}{5}}(q)|^2\right], \tag{B.12}$$

$$A_{\tau\tau\tau\tau} \to e^{\frac{\pi i}{5}}\chi_0(q)\chi_{-\frac{1}{5}}(\bar{q}) + e^{-\frac{\pi i}{5}}\chi_{-\frac{1}{5}}(q)\chi_0(\bar{q}) + \frac{1}{\phi'^2}|\chi_{-\frac{1}{5}}(q)|^2, \tag{B.13}$$

which are discussed in the main text.

B.2 Hard square configurations

In this appendix we give all the hard square configurations and their associated Boltzmann weights for the unit cell tensor where we place a D_4 invariant tensor in the middle. As mentioned in the main text, there are 19 such configurations that can not be transformed into one another under D_4, and we take the convention that a τ-valued loop is depicted as a blank space so we only have to show the 1-valued loops.

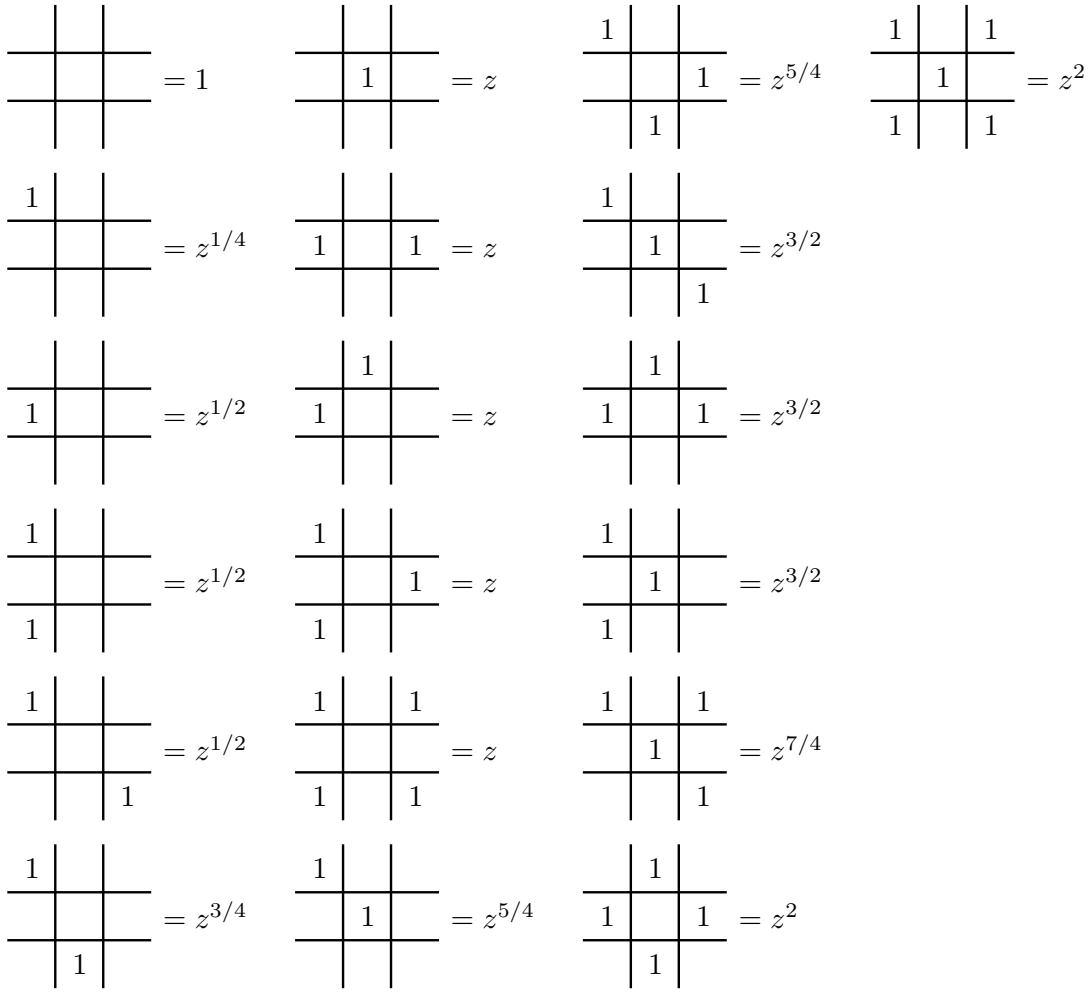

(B.14)

Bibliography

[1] Roman Orus. A practical introduction to tensor networks: Matrix product states and projected entangled pair states. *Annals of Physics*, 349:117 – 158, 2014.

[2] F. Verstraete, V. Murg, and J.I. Cirac. Matrix product states, projected entangled pair states, and variational renormalization group methods for quantum spin systems. *Advances in Physics*, 57(2):143–224, 2008, https://doi.org/10.1080/14789940801912366.

[3] Juan Maldacena. The large-n limit of superconformal field theories and supergravity. *International Journal of Theoretical Physics*, 38(4):1113–1133, Apr 1999.

[4] Shinsei Ryu and Tadashi Takayanagi. Holographic derivation of entanglement entropy from the anti–de sitter space/conformal field theory correspondence. *Phys. Rev. Lett.*, 96:181602, May 2006.

[5] Alexei Kitaev and John Preskill. Topological entanglement entropy. *Phys. Rev. Lett.*, 96:110404, Mar 2006.

[6] N. Bultinck, M. Mariën, D.J. Williamson, M.B. Şahinoğlu, J. Haegeman, and F. Verstraete. Anyons and matrix product operator algebras. *Annals of Physics*, 378:183 – 233, 2017.

[7] Steven R. White. Density matrix formulation for quantum renormalization groups. *Phys. Rev. Lett.*, 69:2863–2866, Nov 1992.

[8] M. B. Hastings. Entropy and entanglement in quantum ground states. *Phys. Rev. B*, 76:035114, Jul 2007.

[9] Kenneth G. Wilson. Renormalization group and critical phenomena. i. renormalization group and the kadanoff scaling picture. *Phys. Rev. B*, 4:3174–3183, Nov 1971.

[10] Kenneth G. Wilson. Renormalization group and critical phenomena. ii. phase-space cell analysis of critical behavior. *Phys. Rev. B*, 4:3184–3205, Nov 1971.

[11] Sidney Coleman and Jeffrey Mandula. All possible symmetries of the S matrix. *Phys. Rev.*, 159:1251–1256, Jul 1967.

[12] P. Francesco, P. Mathieu, and D. Sénéchal. *Conformal Field Theory*, chapter 7, pages 219–220. Springer-Verlag New York, 1997.

[13] A. N. Schellekens. Introduction to conformal field theory. *Fortsch. Phys.*, 44:605–705, 1996.

[14] M. A. Virasoro. Subsidiary conditions and ghosts in dual-resonance models. *Phys. Rev. D*, 1:2933–2936, May 1970.

[15] Sheer El-Showk, Miguel F. Paulos, David Poland, Slava Rychkov, David Simmons-Duffin, and Alessandro Vichi. Solving the 3d ising model with the conformal bootstrap. *Phys. Rev. D*, 86:025022, Jul 2012.

[16] V. Gurarie. Logarithmic operators in conformal field theory. *Nuclear Physics B*, 410(3):535 – 549, 1993.

[17] E. Tartaglia. *Rational and Logarithmic Minimal Models and their Generalisations*. PhD thesis, University of Melbourne, 2016.

[18] Paul A Pearce, Elena Tartaglia, and Romain Couvreur. Kac boundary conditions of the logarithmic minimal models. *Journal of Statistical Mechanics: Theory and Experiment*, 2015(1):P01018, 2015.

[19] Matthias Bal. *Real-space renormalization group methods in the age of tensor network states*. PhD thesis, Ghent University, 2018.

[20] The nobel prize in physics 2016. `https://www.nobelprize.org/nobel_prizes/physics/laureates/2016/`. Consulted on May 9, 2018.

[21] A.Yu. Kitaev. Fault-tolerant quantum computation by anyons. *Annals of Physics*, 303(1):2 – 30, 2003.

[22] Jiannis K. Pachos. *Introduction to Topological Quantum Computation*, pages 55–76. Cambridge University Press, 2012.

[23] Jutho Haegeman and Frank Verstraete. Diagonalizing transfer matrices and matrix product operators: A medley of exact and computational methods. *Annual Review of Condensed Matter Physics*, 8(1):355–406, 2017.

[24] M. Mariën. *The entanglement structure of topological quantum phases*. PhD thesis, Ghent University, 2016.

[25] D. Perez-Garcia, F. Verstraete, M. M. Wolf, and J. I. Cirac. Matrix product state representations. *Quantum Info. Comput.*, 7(5):401–430, July 2007.

[26] J. Preskill. Lecture notes on topological quantum computation. `http://www.theory.caltech.edu/~preskill/ph219/topological.pdf`, 2004.

[27] Alexei Kitaev. Anyons in an exactly solved model and beyond. *Annals of Physics*, 321(1):2 – 111, 2006. January Special Issue.

[28] S. Mac Lane. *Categories for the Working Mathematician*. Springer Science, 1971.

[29] S. Etingof, D Nikshych, and V. Ostrik. On fusion categories, 2002, arXiv:math/0203060.

[30] Oliver Buerschaper. Twisted injectivity in projected entangled pair states and the classification of quantum phases. *Annals of Physics*, 351:447 – 476, 2014.

[31] Mehmet Burak Şahinoğlu, Dominic Williamson, Nick Bultinck, Michael Mariën, Jutho Haegeman, Norbert Schuch, and Frank Verstraete. Characterizing topological order with matrix product operators, 2014, arXiv:1409.2150.

[32] Norbert Schuch, Ignacio Cirac, and David Prez-Garca. "PEPS as ground states: Degeneracy and topology". *Annals of Physics*, 325(10):2153 – 2192, 2010.

[33] Michael A. Levin and Xiao-Gang Wen. String-net condensation: A physical mechanism for topological phases. *Phys. Rev. B*, 71:045110, Jan 2005.

[34] D. Evans and Y. Kawahigashi. On Ocneanu's theory of asymptotic inclusions for subfactors, topological quantum field theories and quantum doubles. *International Journal of Mathematics*, 06(02):205–228, 1995, https://www.worldscientific.com/doi/pdf/10.1142/S0129167X95000468.

[35] Y. Hu, N. Geer, and Y. Wu. Full dyon excitation spectrum in generalized Levin-Wen models, 2015, arXiv:1502.03433.

[36] Viktor Ostrik. Fusion categories of rank 2, 2002, arXiv:math/0203255.

[37] E Ardonne, J Gukelberger, A W W Ludwig, S Trebst, and M Troyer. Microscopic models of interacting Yang-Lee anyons. *New Journal of Physics*, 13(4):045006, 2011.

[38] M. H. Freedman, J. Gukelberger, M. B. Hastings, S. Trebst, M. Troyer, and Z. Wang. Galois conjugates of topological phases. *Phys. Rev. B*, 85:045414, Jan 2012.

[39] Dominic J. Williamson, Nick Bultinck, and Frank Verstraete. Symmetry-enriched topological order in tensor networks: Defects, gauging and anyon condensation, 2017, arXiv:1711.07982.

[40] Matthias Bal, Dominic J. Williamson, Robijn Vanhove, Nick Bultinck, Jutho Haegeman, and Frank Verstraete. Mapping topological to conformal field theories through strange correlators, 2018, arXiv:1801.05959.

[41] Tian Lan and Xiao-Gang Wen. Topological quasiparticles and the holographic bulk-edge relation in $(2+1)$-dimensional string-net models. *Phys. Rev. B*, 90:115119, Sep 2014.

[42] V.G. Turaev and O.Y. Viro. State sum invariants of 3-manifolds and quantum 6j-symbols. *Topology*, 31(4):865 – 902, 1992.

[43] N. Yu. Reshetikhin and V. G. Turaev. Ribbon graphs and their invariants derived from quantum groups. *Comm. Math. Phys.*, 127(1):1–26, 1990.

[44] J. L. Cardy. Critical percolation in finite geometries. *Journal of Physics A: Mathematical and General*, 25(4):L201, 1992.

[45] P. Mathieu and D. Ridout. From percolation to logarithmic conformal field theory. *Physics Letters B*, 657(1):120 – 129, 2007.

[46] A.N. Kirillov and N.Y. Reshetikhin. Representations of the algebra $U_q(sl(2))$, q-orthonormal polynomials and invariants of links. In *Infinite dimensional Lie algebras and groups, Proceedings of the conference held at CIRM, Luminy, Marseille*, page 285, 1988.

[47] Chi-Ming Chang, Ying-Hsuan Lin, Shu-Heng Shao, Yifan Wang, and Xi Yin. Topological defect lines and renormalization group flows in two dimensions, 2018, arXiv:1802.04445.

[48] F. Verstraete. Algorithm for all explicit solutions of the pentagon equation using Gröbner basises. In preparation.

[49] Thomas Scaffidi and Zohar Ringel. Wave functions of symmetry-protected topological phases from conformal field theories. *Phys. Rev. B*, 93:115105, Mar 2016.

[50] Synge T. Transfer-matrix study of negative-fugacity singularity of hard-core lattice gas. *International Journal of Modern Physics C*, 10(04):517–529, 1999, https://www.worldscientific.com/doi/pdf/10.1142/S0129183199000401.

[51] Yi-Zhuang You, Zhen Bi, Alex Rasmussen, Kevin Slagle, and Cenke Xu. Wave function and strange correlator of short-range entangled states. *Phys. Rev. Lett.*, 112:247202, Jun 2014.

[52] Giovanni Felder, Jürg Fröhlich, Jürgen Fuchs, and Christoph Schweigert. Conformal boundary conditions and three-dimensional topological field theory. *Phys. Rev. Lett.*, 84:1659–1662, Feb 2000.

[53] Jürg Fröhlich, Jürgen Fuchs, Ingo Runkel, and Christoph Schweigert. Kramers-wannier duality from conformal defects. *Phys. Rev. Lett.*, 93:070601, Aug 2004.

[54] Markus Hauru, Glen Evenbly, Wen Wei Ho, Davide Gaiotto, and Guifre Vidal. Topological conformal defects with tensor networks. *Phys. Rev. B*, 94:115125, Sep 2016.

[55] R J Baxter. Hard hexagons: exact solution. *Journal of Physics A: Mathematical and General*, 13(3):L61, 1980.

[56] John L. Cardy. Operator content of two-dimensional conformally invariant theories. *Nuclear Physics B*, 270:186 – 204, 1986.

[57] V.B. Petkova and J.-B. Zuber. Generalised twisted partition functions. *Physics Letters B*, 504(1):157 – 164, 2001.

[58] David S. Gaunt. Hardsphere lattice gases, plane-triangular and three-dimensional lattices. *The Journal of Chemical Physics*, 46(8):3237–3259, 1967, https://doi.org/10.1063/1.1841195.

[59] M Assis, J L Jacobsen, I Jensen, J-M Maillard, and B M McCoy. The hard hexagon partition function for complex fugacity. *Journal of Physics A: Mathematical and Theoretical*, 46(44):445202, 2013.

[60] M Assis, J L Jacobsen, I Jensen, J-M Maillard, and B M McCoy. Integrability versus non-integrability: hard hexagons and hard squares compared. *Journal of Physics A: Mathematical and Theoretical*, 47(44):445001, 2014.

[61] L. K. Runnels. Hard-square lattice gas. *Phys. Rev. Lett.*, 15:581–584, Oct 1965.

[62] Dipanjan Mandal, Trisha Nath, and R Rajesh. Estimating the critical parameters of the hard square lattice gas model. *Journal of Statistical Mechanics: Theory and Experiment*, 2017(4):043201, 2017.

[63] D W Wood, R W Turnbull, and J K Ball. Algebraic approximations to the locus of partition function zeros. *Journal of Physics A: Mathematical and General*, 20(11):3495, 1987.